UNIVERSITÉ DU QUÉBEC À MONTRÉAL

EFFET DE L'ASSOMBRISSEMENT PLANÉTAIRE SUR LA CROISSANCE DES ARBRES

THÈSE

PRÉSENTÉE

COMME EXIGENCE PARTIELLE

DU DOCTORAT EN BIOLOGIE

PAR

LIONEL HUMBERT

DÉCEMBRE 2011

REMERCIEMENTS

Je tiens à remercier en premier lieu Frank Berninger d'avoir accepté d'être le directeur de cette thèse et de m'avoir laissé autant de libertés. Mes remerciements vont conjointement et tout particulièrement à Fernando Valladares et Dan Kneeshaw pour leur soutien et leur enthousiasme qui m'ont permis de mener à bien ce projet. Je voudrais également remercier Christian Messier, notre cher ex-Directeur du C.E.F. pour son écoute et son soutien lors des étapes cruciales de cette thèse. J'aimerais aussi le remercier pour son investissement dans cette magnifique structure qu'est le C.E.F., sans qui les travaux présentés ici n'auraient probablement pu aboutir. Je tiens donc à remercier Luc Lauzon, Danielle Charon, Daniel Lessieur et Melanie Desrocher pour leur accueil au sein du centre, ainsi qu'Alain Leduc l'autre adorateur du saint nectar de 9h et Herve Bescond pour nos rechutes de 13h. Merci à Paul Sheppard de l'Université d'Arizona pour m'avoir accueilli à Tucson et permis d'écrire les dernières lignes de cette thèse sous une chaleur accablante tout en me faisant économiser des tonnes de CO_2 et privant ainsi les Mesquites, Palo verdes et Saguaros d'un peu de leurs nutriments. Je tiens particulièrement à remercier Henrik et sa famille, ainsi que Dominique et Geneviève pour nos discussions autour de diner et petits plaisirs brassés. Et un grand merci à Gab, Claudia, Florent, Matt, Dominic Senecal, Caroline, Leila, Sophie, Marie-Claude, Adi, Astrid, Philippe Tremblay, Karine et Karine et Karine (elles se reconnaitront), Eric, Yassin, Frank et tous mes amis pour leur soutien.

Merci enfin à mes parents, grands parents, à ma petite sœur Emeline et ma chère et tendre qui m'ont permis d'être comme en France à chacune de leurs visites et de grosses bises à ma petite filleule Ninon, à mon petit filleul Noé, à leurs parents et à toute ma famille.

"En terme de préhistoire, on parle de l'âge de pierre, de l'âge du fer, de l'âge du bronze. En survolant toute l'histoire de l'humanité, ne devrait-on pas parler de l'âge du bois, du charbon, du pétrole ou de l'atome ?"

Roger Molinier, 1991

tiré de L'Écologie à la croisée des chemins

TABLE DES MATIÈRES

LISTE DES FIGURES

LISTE DES TABLEAUX

RÉSUMÉ

L'utilisation des combustibles fossiles, en plus d'augmenter la concentration du CO_2 mondial, abaisse la lumière directe que l'on reçoit du soleil en la diffractant. Cet "assombrissement global" peut, contrairement au CO_2, diminuer la croissance des arbres car il diminue la lumière donc la photosynthèse est moins importante. L'"assombrissement global", dans le cadre de l'analyse de cernes, présente un atout par rapport à évaluer seulement l'effet du CO_2 comme changement global. On peut théoriquement déduire son effet sur les cernes en observant l'évolution de la relation entre les cernes et la lumière. Cela est possible car la lumière arrivant à la surface du globe suit un cycle déterminé de 11 ans. Ce cycle, le cycle solaire, est bien connu et nous savons qu'il exerce un effet sur les cernes depuis les travaux de Douglass au début du siècle passé. L'étude de l'effet de l'"assombrissement global" sur les cernes est donc un sujet de choix si l'on veut examiner une variable qui peut induire un changement lent sur le long terme, ou une tendance. Mais les méthodes traditionnelles d'analyse des cernes de croissance sont mal adaptées à la recherche de telles tendances. Au cours de cette thèse nous avons testé des méthodes statistiques modernes pour l'analyse de l'effet de la lumière en lien avec l'"assombrissement global" sur les cernes de croissance des arbres. Ces méthodes ont ensuite été utilisées pour détecter les tendances environnementales dans les cernes. Ainsi, l'utilisation d'une méthode aveugle de séparation des signaux sources, l'analyse en composants indépendants (ICA), évite certaines suppositions et permet d'éliminer les effets des perturbations sur la croissance.

Le premier chapitre de cette thèse décrit en détail cette méthode et la teste sur des données simulées de cernes de croissance d'arbres. On retrouve donc la composante climatique de la croissance isolée, telle que décrite dans le model linéaire agrégé classique.

Le second chapitre applique cette méthode différemment. En effet, nous avons voulu tester la capacité de l'ICA à trouver des perturbations. On a donc ré-analysé des données dendroécologiques provenant de publications traitant d'épidemies d'insectes. Nos résultats montrent que l'ICA est capable de detecter les perturbations dans les cernes de croissance déjà identifiées et que cette méthode peut permettre l'analyse des perturbations lorsqu'il est difficile de mettre en œuvre les méthodes traditionnelles avec les données disponibles.

Ensuite, dans le chapitre III, nous utilisons l'ICA dans une analyse de gradients climatiques pour voir si la température, les précipitations et la lumière ont un effet sur les cernes. Nos résultats montrent que la corrélation entre la lumière et les cernes augmente progressivement au cours du temps. Cette augmentation semble être en relation avec le niveau de pollution atmosphérique. Elle est plus forte au Népal où la proximité de l'Inde apporte de nombreux polluants, un peu moins forte en Argentine et non présente en Sibérie où la pollution est majoritairement hivernale (donc durant la saison sans croissance arborescente). Le niveau de pollution semble donc influencer la relation entre les cernes et la lumière. On peut ainsi supposer que la lumière diffuse produite par la pollution influence positivement la croissance, en contraste avec notre supposition originale.

Au chapitre IV, nous voulions vérifier si le niveau de pollution influençait effectivement l'effet de la lumière sur la croissance des arbres au niveau mondial. Nous avons comparé les données d'un réseau mondial de 183 stations de mesures de la pollution atmosphérique avec l'effet du cycle solaire sur les cernes de 841 sites forestiers à proximité de ces stations. Les résultats montrent que pour les sites forestiers provenant des écosystèmes méditérranéens et altitudinaux la pollution augmente l'effet de la lumière diffuse sur la croissance depuis 1960.

Dans le chapitre V j'utilise la réaction des arbres lors des deux plus importantes éruptions volcaniques du siècle dernier pour voir si la lumière diffuse augmente bien la croissance des arbres et que cet effet n'est pas du à la baisse concomitante de la température. Ces deux éruptions sont d'intensité égale, mais au cours de l'une d'elles un événement climatique (El Niño) a masqué son effet de refroidissement. L'analyse de 210 sites forestiers sélectionnés de façon aléatoire dans le monde entier, nous indique que c'est bien la lumière diffuse qui influence la croissance et non pas la baisse de température qui lui est associée.

Au cours de cette thèse nous avons montré que la lumière modifiée par l'"assombrissement global", c'est-à-dire une baisse de la lumière directe au profit de la lumière diffuse, augmente la croissance des arbres. Ce phénomène est surtout présent pour les écosystèmes qui sont limités en eau. Cet effet de la lumière diffuse pourrait rendre difficile l'identification d'un effet de la fertilisation due au CO_2.

Mots-clés : dendro-chronologie, dendro-climatologie, pollution atmosphérique

INTRODUCTION

Depuis la conférence de Rio en 1992, puis celle de Kyoto en 1997 (Houghton, Callander et Varney, 1992 ; United Nations, 1997), l'accent a été mis sur la réduction des émissions de gaz à effet de serre. Cet effet de serre est naturellement lié à la présence de vapeur d'eau pour 75% et de certains gaz. Or, la concentration atmosphérique du dioxyde de carbone (CO_2) et du méthane (CH_4) a été fortement influencée par les activités humaines (Figure 0.1 tirée de Solomon *et al.*, 2007). Les émissions de CO_2 sont le résultat direct de l'utilisation de combustibles fossiles comme source d'énergie. Mais en plus de libérer du CO_2, leur combustion produit un grand nombre de particules qui changent d'autres caractéristiques de l'atmosphère. Notamment, les propriétés optiques de l'atmosphère sont affectées par les particules en suspension qui vont diffracter, absorber et réflechir la lumière.

Les arbres, par une réaction physico-chimique, la photosynthèse (Figure 0.2), vont subir ces changements et utiliser des éléments qui sont dans l'atmosphère et/ou qui peuvent y être modifiés. La modification de la composition et du comportement de l'atmosphère, vont de plus participer à son réchauffement, au refroidissement de surface et à la formation des nuages. Sachant que les principaux éléments de cette réaction physico-chimique sont : le CO_2, la lumière, l'eau et que tout dépend de la température ambiante, il est probable que la croissance des arbres soit affectée par l'utilisation des combustibles fossiles.

Il est connu depuis les années 1920/1930 qu'une augmentation de la concentration atmosphérique du CO_2 stimulait la croissance des plantes (Hoover, Johnston et Brackett, 1933 ; Thomas et Hill, 1949), mais l'effet de l'augmentation du CO_2 sur la croissance des arbres est depuis sujet à controverse. LaMarche *et al.* (1984) ont conclu que l'augmentation de la croissance des arbres dans les années 80 était plus élevée que celle estimée

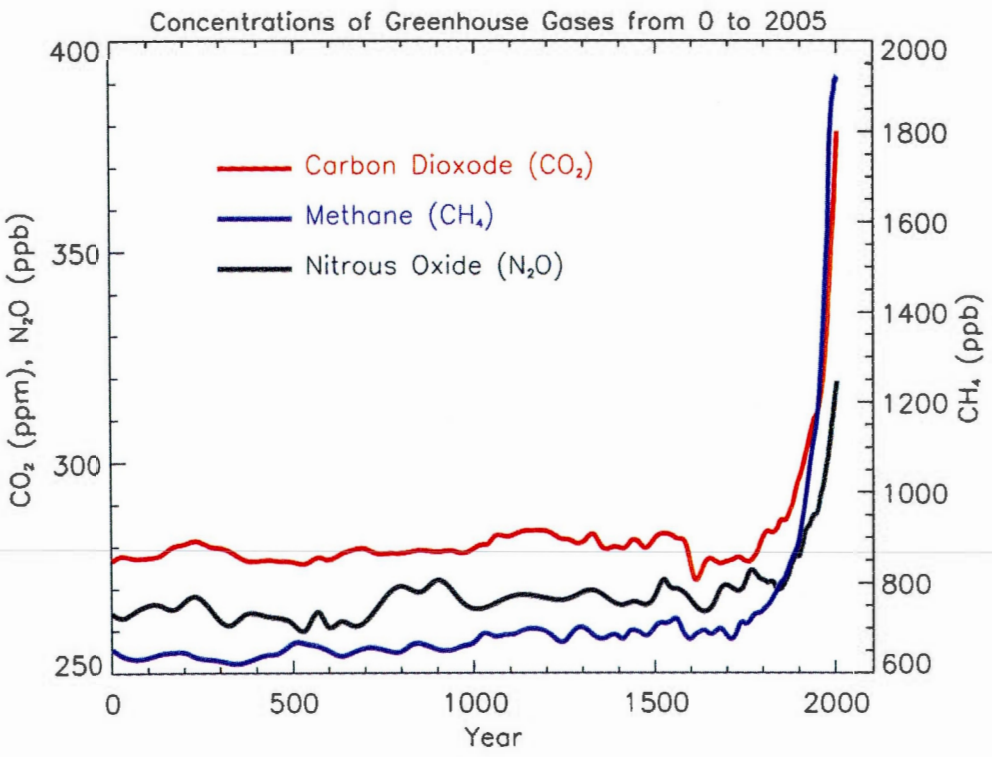

Figure 0.1 Concentration atmosphérique des gaz à effet de serre de longue durée de vie au cours des derniers 2000 ans. Les unités de concentration sont en parties par million (ppm) ou en parties par milliard (ppb), tiré de Solomon *et al.* (2007)

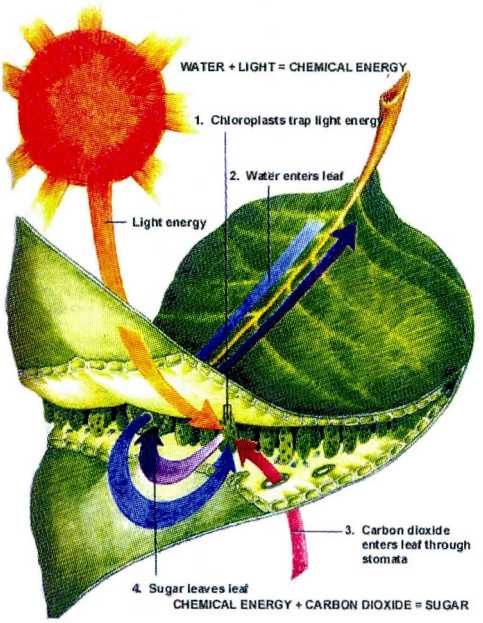

Figure 0.2 La photosynthèse, ©Discover Science, Scott, Foresman & Co. 1993

par les hausses de température, ce qui serait du à une fertilisation au CO_2. Toutefois, Graumlich (1991) et, plus récemment, Jacoby et D'Arrigo (1997) concluent que les indices permettant d'observer un effet de fertilisation au CO en conditions naturelles dans les cernes semblent être très limités. Mais le problème principal reste que le CO et les autres éléments influencés par les changements globaux évoluent lentement d'une année à l'autre. Il y a donc une faible tendance à long terme qui s'est installée. Graumlich (1991) et Jacoby et D'Arrigo (1997) soulignent d'ailleurs qu'avec les méthodes d'analyses utilisées, les tendances comme celle du CO_2 sont difficiles à capter car la croissance des arbres est sujet à d'autres phénomènes climatiques. De nouvelles méthodes d'analyse devraient donc être nécessaires. L'augmentation de la lumière diffuse, l'absorption de la lumière du soleil par des particules aérosol (Hansen *et al.*, 2000; Ramanathan *et al.*, 2001) et les traînées de condensation des avions (Murcray, 1970; Penner *et al.*, 1999; Travis, Carleton et Lauritsen, 2004) pourraient également avoir un effet direct ou indirect sur la croissance des arbres et le bilan de carbone. Le phénomène le plus

visuel est certainement celui des traînées de condensation formées par les avions qui sont constituées de particules de glace. Cette formation de glace est principalement due au réchauffement de l'air et à sa condensation en sortie des réacteurs (Schumann, 2005). Le phénomène est accentué par les impuretés de l'air et la combustion incomplète du kérosène (Schumann, 2005) et peut former des traînées persistantes alors qu'elles disparaissent rapidement en temps normal. Habituellement ces traînées sont présentes en grand nombre (Figure 0.3 b) et leur impact climatique n'était que spéculatif avant la tragédie du 11 septembre 2009. Après cette tragédie, l'espace aérien américain fut interdit (Figure 0.3 a) et, le lendemain, des observations au sol ont montré une augmentation de la différence de température entre le jour et la nuit de 1C (Travis, Carleton et Lauritsen, 2002). Malgré des critiques (Kalkstein et Balling, 2004 ; Solomon *et al.*, 2007), cet impact climatique des traînées d'avions semble réel (Travis, Carleton et Lauritsen, 2004) avec une augmentation de l'ordre de 0.2–0.3°C tous les dix ans (Minnis *et al.*, 2004 ; Stordal *et al.*, 2005 ; Zerefos *et al.*, 2003) même si beaucoup d'incertitudes subsistent (Burkhardt *et al.*, 2008). De plus elles favorisent la formation de cirrus (Mannstein et Schumann, 2005) qui rendent la lumière plus diffuse et contribuent au réchauffement global (Marquart *et al.*, 2005 ; Fichter *et al.*, 2005).

Comme les cirrus, tous les nuages vont diffracter et absorber la lumière. Mais la diffraction et l'absorption de la lumière peuvent également avoir d'autres origines. L'utilisation de combustibles fossiles émet énormément de particules fines et de particles qui forment des aérosols comme les substances organiques volatiles ou le SO_2 (Figure 0.4). C'est également le cas de phénomènes naturels comme les feux de forêts ou les éruptions volcaniques.

Ces particules produisent une baisse des radiations directes et augmentent les radiations diffuses (Dutton et Bodhaine, 2001 ; Robock, 2000, 2005). Ce phénomène agit au niveau de la planète entière (Figure 0.5) et il a été qualifié d'"assombrissement global" (Stanhill et Cohen, 2001 ; Ramanathan *et al.*, 2001). La transparence de l'atmosphère a d'ailleurs diminué graduellement depuis 1850 (Figure 0.6 adaptée de Romanou *et al.*, 2007). Ces particules agissent également comme des nuages, disperçant les rayons de lumière de

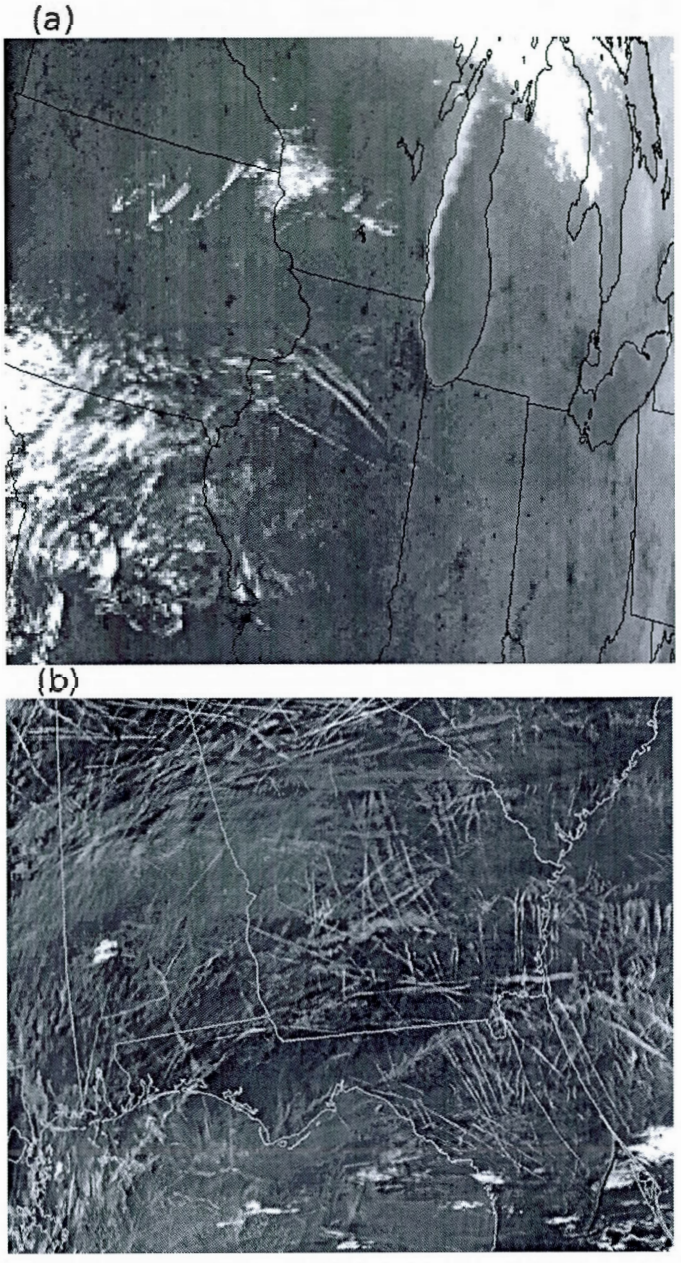

Figure 0.3 Images de Radiomètre Avancé à Très Haute Résolution (AVHRR) infrarouges montrant les traînées de condensation générées par les avions (Photos de la NASA, libre de droits). L'image (a) montre l'avion présidentiel et son escorte le 12 septembre 2001 alors que l'espace aérien était interdit, l'image (b) montre une image normale du ciel américain le 12 septembre 2004.

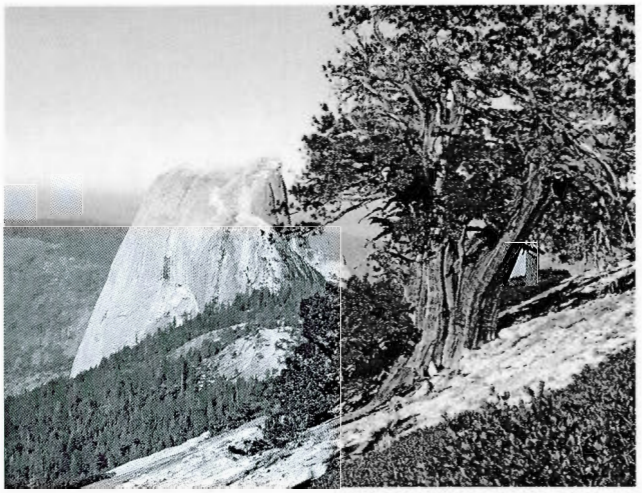

Figure 0.4 Vue du Half-Dome depuis Cloud Rest (2800m) au parc national de Yosemite, Août 2007. La couche grise située au niveau de l'horizon montre la pollution atmosphérique.

façon très complexe (Farquhar et Roderick, 2003), entrainant ainsi un obscurcissement. Cependant, un éclaircissement local a également été observé depuis peu (Wild *et al.*, 2005 ; Wild, Ohmura et Makowski, 2007) dans les régions ou des efforts antipollution ont été fait comme en Europe de l'ouest.

Alors que l'impact de ce phénomène sur la productivité des écosystèmes est potentiellement important, ce n'est que récemment qu'il fut pris en compte (Ramanathan *et al.*, 2001 ; Roderick *et al.*, 2001 ; Roderick et Farquhar, 2002). Cet obscurcissement global, au niveau des radiations solaires a un effet direct sur la température et les précipitations, et au final sur les processus au sein des écosystèmes. La première observation de ce phénomène a été la baisse de l'évaporation au niveau des champs agricoles (Roderick et Farquhar, 2002). De plus, il a été avancé que l'obscurcissement global pouvait augmenter la productivité des plantes et plus particulièrement des arbres (Roderick *et al.*, 2001 ; Gu *et al.*, 2002 ; Roderick, 2006) en diminuant la lumière directe et en augmentant la lumière diffuse. Cet effet non intuitif, a été confirmé par des modèles mathématiques (Cohan *et al.*, 2002), et serait la conséquence de la stimulation de la photosynthèse en

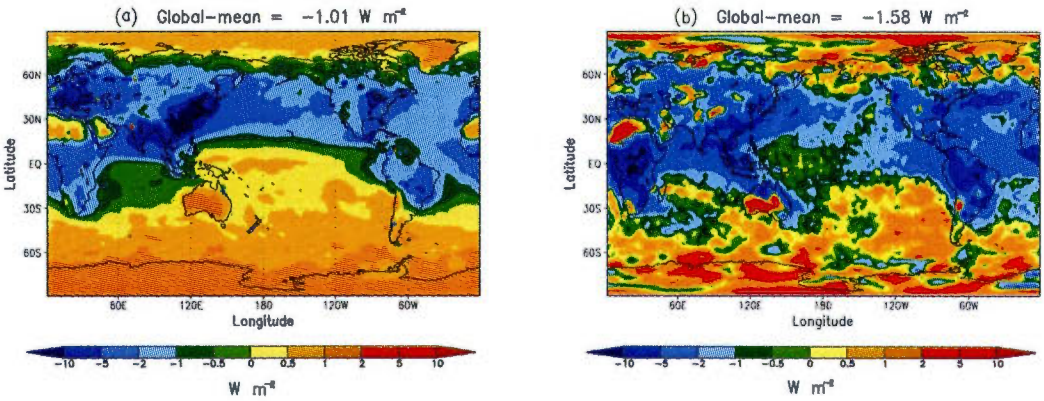

Figure 0.5 Changement dans la répartition spatiale des flux radiatifs nets (énergie solaire et grandes longueurs d'onde) arrivant au sol (W.m) dus aux forçages naturels et anthropiques entre les années 1860 et 2000. (a) correspondant aux résultats en utilisant le model GFDL CM 2.1 (Knutson *et al.*, 2006), (b) utilisant les models MIROC et SPRINTARS (adapted from Nozawa *et al.*, 2005 ; Takemura *et al.*, 2005). Figure tirée de Solomon et al. 2007.

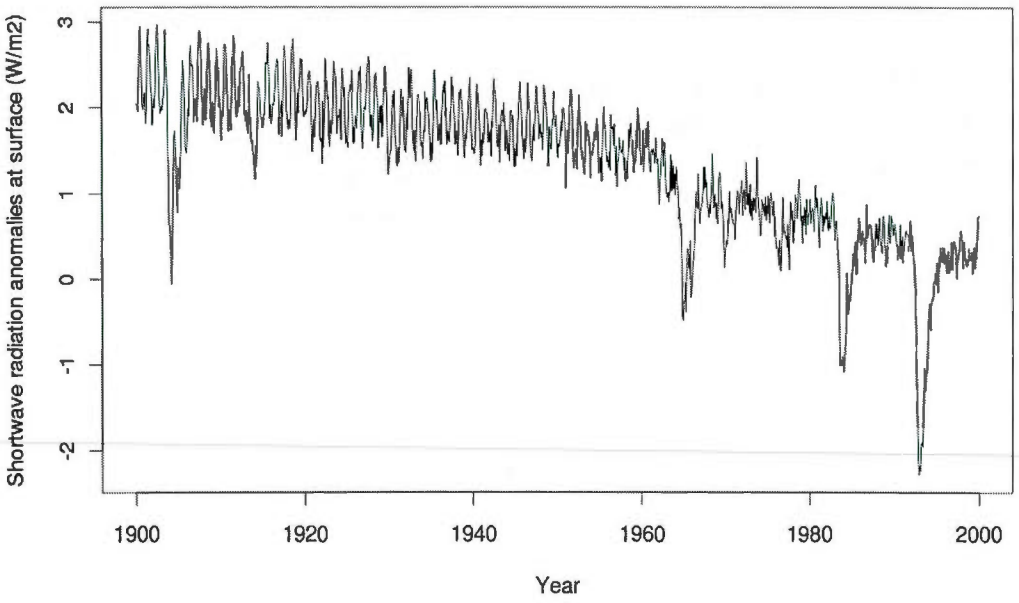

Figure 0.6 Radiations solaires à ondes courtes arrivant au niveau du sol (W/m^2) basées sur la moyenne de 9 modèles (GFDL, CCSM, PCM, GISSAOM, GISSER, GISSEH, HADCM, MIROC, ECHAM) adapté de (Romanou *et al.*, 2007) avec l'aimable autorisation d'Anastasia Romanou.

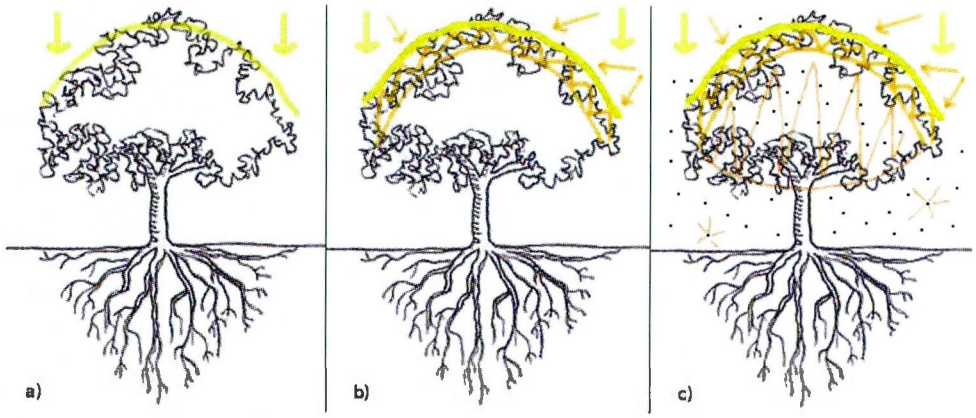

Figure 0.7 Comportement de la lumière diffuse dans la canopée sous trois scénarios : (a) lumière directe uniquement, (b) lumière directe et lumière diffuse telle que produite par les nuages et (c) lumière directe et lumière diffuse telle que produite par de la pollution atmosphérique. Les zones coloriées du feuillage indiquent les zones recevant de la lumière et qui sont donc photosynthétiquement actives.

présence de lumière diffuse dans les canopées complexes. Pour une canopée à plusieurs niveaux, 35% de la photosynthèse est faite par la couche supérieure qui ne représente généralement que 10% de l'indice de surface foliaire (LAI Ellsworth et Reich, 1993). Cela est du aux propriétés physiologiques (teneur en azote) et physiques (surface, angle) de la feuille qui varient à travers le couvert végétal (Sellers *et al.*, 1992) du plein soleil jusqu'à l'ombre pour intercepter la lumière de manière uniforme (Hollinger, 1989). Et même si beaucoup de plantes traquent le soleil avec l'angle de leur feuille (Ehleringer et Forseth, 1980), dans la canopée la fonction de l'angle des feuilles est de réduire la photoinhibition au milieu de la journée, plus que de maximiser les gains en carbone (Falster et Westoby, 2003).

Sous un ciel nuageux, la lumière diffuse créée atteindra la canopée avec une multitude d'angles d'incidence et avec moins d'intensité (Figure 0.7). Les feuilles de lumière s'orientent selon un angle horizontal pour maximiser le gain en carbone et la diversité des angles d'incidence permettra d'atteindre davantage de feuilles d'ombre. Ces radiations

diffuses, supposées uniformes et incidentes, ont été incorporées dans les modèles depuis longtemps (Goudriaan, 1977 ; De Pury et Farquhar, 1997) suivant le modèle de fractions d'ombre, même si le calcul était difficile (Sinclair, 2006). Toutefois, en vertu de l'obscurcissement global, des particules réflechissantes sont également présentes à l'intérieur de la canopée, conduisant à une répartition encore plus complexe de la lumière et permettant d'atteindre davantage de feuilles d'ombre même en l'absence de nuages (Figure 0.7).

Cette augmentation théorique de la photosynthèse à cause de l'augmentation de la lumière diffuse liée aux activités humaines n'a pas encore été mesurée. Mais suite à l'éruption du Mont Pinatubo (Philippines) en 1991, on a observé une augmentation de la productivité forestière (Farquhar et Roderick, 2003). Lors d'une éruption volcanique, des particules sont libérées massivement dans l'atmosphère, particules qui vont également disperser les photons. Gu *et al.* (2003) ont d'ailleurs reporté une augmentation de la photosynthèse localement. De plus une ré-analyse de reconstruction climatique de Mann, Bradley et Hughes (1998) par Robock (2005) montre que les reconstructions basées sur la croissance radiale des arbres sous-estime constamment la baisse de température qui est rapportée par des instruments lors des éruptions volcaniques. Cette sous-estimation pourrait être la conséquence de la stimulation de la photosynthèse par une augmentation de la lumière diffuse et ce, alors que la température globale chute. Mais un doute subsiste quant à l'effet de l'augmentation de la lumière diffuse suite aux éruptions volcaniques sur la croissance des arbres par rapport à l'effet d'une baisse de température (Krakauer et Randerson, 2003).

Plusieurs de ces changements globaux sont également concomitants et stimulés par le soleil. Ainsi le rayonnement cosmique stimulerait l'ionisation et donc la nucléation ce qui créerait plus d'aérosols. Ces particules servent de noyau de condensation pour les nuages et donc augmenteraient la formation de ces derniers (Spracklen *et al.*, 2008 ; Harrison et Ambaum, 2008 ; Marsh et Svensmark, 2000 ; Svensmark et Calder, 2007 ; Usoskin *et al.*, 2004). Des perturbations au niveau de l'atmosphère et surtout celles qui influencent le rayonnement solaire peuvent donc modifier la photosynthèse (Roderick

et al., 2001) et par conséquent la largeur des cernes d'arbres. Le bilan de carbone peut donc être affecté par ceux-ci et peut masquer ou amplifier une possible fertilisation au CO2.

Nous avons discuté de la température et de la lumière mais les précipitations et la disponibilité en eau sont également liées aux changements globaux. Ainsi la baisse observée de l'évaporation (Stanhill et Cohen, 2001 ; Roderick et Farquhar, 2002) peut avoir un impact majeur sur l'écosystème boréal et sur la croissance des arbres par l'augmentation au printemps des périodes d'anoxie dues à la fonte des neiges. En outre, on peut s'attendre à des interactions entre l'activité solaire et le climat (Haigh, 1996, 2001). Toutefois, l'estimation de l'impact de ces interactions sur la hausse des températures au cours des dernières décennies n'est pas réaliste (Laut, 2003), tout comme leurs relations avec El Niño – La Niña et l'Oscillation Nord-Atlantique (Landscheidt, 2000). Nous sommes donc en présence d'un système climatique très complexe (voir figure 3 dans Carslaw *et al.*, 2009) qui évolue lentement sous la contrainte des emissions d'origine humaine.

Comme nous l'avons indiqué précédemment, la principale difficulté consiste à trouver une tendance liée à une variable climatique au sein de multiples tendances liées à d'autres variables climatiques. L'"assombrissement global", dans le cadre de l'analyse de cernes, présente un atout par rapport au CO_2. Ainsi, on peut théoriquement déduire son effet sur les cernes en observant l'évolution de la relation entre les cernes et la lumière. Car la lumière arrivant à la surface du globe suit un cycle déterminé de 11 ans. Ce cycle, le cycle solaire, est bien connu et nous savons qu'il exerce un effet sur les cernes depuis les travaux de Douglass au début du siècle passé. Cette variable est donc connue, ses données remontent à 1761 et elle est facile à étudier. De plus, la lumière, en pénétrant dans l'atmosphère, change quantitativement et qualitativement sous l'influence de l'"assombrissement global", un phénomène variant également localement sous l'effet de la pollution régionale. Par rapport au CO_2, l'"assombrissement global" est donc une variable d'intérêt offrant à la fois des variations régionales importantes ainsi qu'une tendance à long terme suivant l'exploitation des combustibles fossiles. Ces vari-

ations régionales vont pouvoir être exploitées pour vérifier si une relation existe bien entre les cernes et la lumière diffuse.

L'étude de l'effet de l'"assombrissement global" sur les cernes est donc un sujet de choix si l'on veut examiner une variable qui peut induire une changement lent sur le long terme, ou une tendance. Mais il est nécessaire de tester de nouvelles méthodes statistiques et de déterminer si la pollution atmosphérique a un effet sur les cernes avant d'évaluer la tendance à long terme de l'effet de la lumière diffuse sur les cernes de croissance des arbres. Les méthodes traditionnelles d'analyse des cernes de croissance sont mal adaptées à la recherche de telles tendances. En général elles soustraient des courbes théoriques de croissances aux données pour corriger l'effet age et elles se basent sur l'évaluation de modèles dont les erreurs affectent grandement la recherche de tendances. Finalement, grâce à ces nouvelles méthodes, nous pourrons vérifier si la fertilisation au CO_2 a un impact sur les cernes.

Objectifs et Hypothèses

Cette thèse a deux objectifs majeurs avec leurs hypothèses sous-jacentes :

- Offrir un nouveau cadre statistique pour établir des relations entre les cernes et différentes variables climatiques et physiques.
    1. L'utilisation de l'analyse en composante indépendante (ICA) permet-elle de séparer les différents composants d'une série de cernes (l'effet âge, l'effet climatique, les perturbations et le bruit) ?
    2. L'intégration de l'ICA à la démarche d'analyse fournit-elle de meilleurs résultats que les modèles traditionnels ?
    3. Les tendances peuvent-elles être retrouvées par l'approche statistique proposée ?
- Estimer la contribution des phénomènes climatiques et physiques à l'augmentation ou la baisse de la croissance forestière.
    1. L'"assombrissement global" affecte-t-il la croissance de façon directe et/ou indirecte ?

2. Les proportions de croissance expliquée, par le climat, la lumière diffuse, la fertilisation au dioxyde de carbone ... peuvent-elles être estimées ?

Ce travail est divisé en quatre parties, représentant cinq chapitres :

1. Une nouvelle méthode d'analyse des cernes est proposée et testée aux chapitres I et II.
2. La détection et la séparation des différentes tendances possibles sont testées sur des gradients environnementaux contrastés au chapitre III.
3. Le test d'un possible effet de la lumière diffuse sur la croissance est faite dans le chapitre IV.
4. On vérifie si l'effet de l'augmentation de la lumière diffuse engendrée par cette diminution de lumière affecte les cernes ou si c'est l'effet de la baisse de température qui les affecte au chapitre V.

NOTE SUR LES CHAPITRES

Les références des chapitres sont inclusent dans une unique bibliographie à la fin de cette thèse par soucis d'économies.

Le chapitre I après soumission a été jugé trop théorique par la revue Dendrochronologia. Il est actuellement en récriture pour inclure des analyses basées sur des données réelles.

Le chapitre II a subit beaucoup de modification depuis la première version de cette thèse, il devrait être soumis sous peu.

Le chapitre III, "Humbert L. and Berninger F. Tree growth, solar forcing and CO2 fertilization across high altitude and high latitude in Argentina, Nepal and Siberia", est en cours de re-soumission suite à une demande d'analyse supplémentaire pour Global and Planetary Change.

Les chapitres IV et V sont actuellement en préparation avec l'implication de Fernando Valladares et de Daniel Kneeshaw. Fernando Valladares et Daniel Kneeshaw participent à l'interpretation des résultats et à leur rédaction. Fernando Valladares en tant que spécialiste en physiologie végetale et plus précisement au niveau des relations hydriques des plantes méditérranéennes et d'autre milieux arides, m'a aidé dans l'interpretation de l'augmentation de croissance des arbres quand la lumière baisse dans ces milieux. Daniel Kneeshaw nous a apporté ses connaissance des perturbations naturelles en milieu forestier afin de mieux comprendre nos résultats sur cette grande échelle ainsi dans les variations entre les divers types forestiers.

CHAPITRE I

USE OF INDEPENDENT COMPONENT ANALYSIS WITH TREE RING WIDTH SERIES

We test, using simulated data, the utility of Independent Component Analysis (ICA) for the analysis of different superposed signals in tree ring data. According to the standard model of tree ring analysis, tree rings are composed from different signals that express the development of the tree or stand with age, short term disturbances and climatic patterns. Because ICA is effective in the extraction of non-white noise signals from series we tried to apply ICA to the extraction of age related, disturbance related and climate related trends in a single run. We found that ICA is effective in separating an average growth trend and disturbance events from the series. It failed, however, to separate, different simultaneous long term growth trends (like simultaneous growth related declines and CO_2 induced increases). Further pretreatments, like a pre-classification of series owing different growth trends was necessary for complex series where different growth trends were mixed. Differences of ICA and other multivariate methods like principle component analysis are discusses. Overall, the results show that ICA is a promising analysis to separate different non-Gaussian signals from tree ring data.

1.1 INTRODUCTION

Independent Component Analysis (ICA) can be seen as an extension of Principal Component Analysis (PCA) which tries to find a linear representation of non-Gaussian data so that the components are independents (Cardoso, 1989; Comon, 1994). It tries

to capture underlying non-Gaussian processes that explain the variation of the data. Whereas PCA looks for linear combinations of a data matrix that are uncorrelated, ICA seeks linear combinations that are independent (Venable & Ripley, 2002). Independence means here that ICA minimizes the mutual information between components. ICA in it formulation is very closely related to Factor Analysis (FA), a common technique in social sciences, which seek linear combinations of variables, called factors, that represent underlying fundamental quantities of which the observed variables are expressions. Furthermore, PCA analyses the whole variance of a dataset, while ICA and FA analyze only the portion of variance that is correlated across several data series. PCA and FA only estimate the factors up to one rotation, instead, the purpose of ICA is to separate the source signals, that PCA and FA cannot, by seeking for a rotation of spherical data which have independent coordinates (Hyvärinen, Karhunen & Oja, 2001; Stone, 2004).

ICA could be of primary interest in ecological science when we do not require the relative position of the objects but the order of objects. Here, we will test how well ICA might unmix different signals in tree ring series using simulated data.

Tree rings have been described as a mixture of different processes (signals) by Cook (1987); Cook & Kairiukstis (1990) and often referred as the linear aggregated model :

$$S_t = A_t + C_t + \delta D1_t + \delta D2_t + \varepsilon \tag{1.1}$$

where

S is the tree ring indices time series

A is the age effect

C is the climatic component

D1 and D2 are the disturbance events. D1 is the site disturbance effect and D2 is the tree disturbance effect. (see Cook & Kairiukstis (1990) for further details)

ε the noise

1.2 DEFINITION

ICA was proposed by Cardoso (1989), and Comon (1994) defined the basis of the model and made it identifiable. In our case we can describe tree ring width as two linear time series, x_1 and x_2, in this way :

$$\begin{aligned} x_1(t) &= a_{11}s_1(t) + a_{12}s_2(t) \\ x_2(t) &= a_{21}s_1(t) + a_{22}s_2(t) \end{aligned} \tag{1.2}$$

where s_1, s_2 are the original signals and a_{11}, a_{12}, a_{21}, a_{22} are constant coefficients that give the mixing weights. If we assumes that a_{11}, a_{12}, a_{21}, a_{22} are different enough to form an invertible matrix. Using these equations, s_1 and s_2 can be recovered if we know the parameters values, which we, unfortunately, seldom know. The basic definition of ICA is that there is j linear mixture $x_1, x_2, ..., x_j$ of i independent component (s) :

$$x_j = a_{j1}s_1 + a_{j2}s_2 + ... + a_{ji}s_i \quad \text{for all } j \tag{1.3}$$

Now for the next step let be A a matrix with a_{ij} elements, consequently in a vector-matrix notation we can write our mixing problem as :

$$x = As \tag{1.4}$$

Then if A as an inverse matrix W with w_{ij} coefficients, we can separate the s_i as :

$$\begin{aligned} s_1(t) &= w_{11}x_1(t) + a_{12}x_2(t) \\ s_2(t) &= w_{21}x_1(t) + a_{22}x_2(t) \end{aligned} \tag{1.5}$$

or in a matrix form :

$$s = Wx \tag{1.6}$$

Then by considering s_i statistically independent at each time lag t it is possible to estimate W.

In order to identify these components using ICA the values of s must be distributed in a non-normal way. This need of non-normal distribution is not a real problem since ecological data rarely follow the normal distribution. The explanation for this non-Gaussianity of ICA can be found in Hyvärinen & Oja (2000) with an approach to

estimate it. Equation (3) is then call the ICA Model (Hyvärinen, Karhunen & Oja, 2001). ICA Model is a generative model, which means that it tries to describe how the observations are created by the mixing process of components s_i. These components (or signals) are reconstructed (or "generated") by the analysis. In fact, the components s_i are latent variables (a theoretical variables) which are not directly observable. In our specific case, the use of ICA allows the recovery of the variables S, A, C, D1 and D2 of the Cook & Kairiukstis (1990) tree ring model (Equation 1.1).

The ICA is a non parametric method which permit to use it with nearly any kind of data and the initial assumption is simple, *i.e.* all components s_j are statistically independent. There are some underlying problems of the method. The number of components to be extracted is set a priori and their order cannot be determined at the end of the analysis. It is also impossible to determine the proportion of variance explained by independent component. Finally, the analysis is restricted to non-Gaussian data which can describe the ICA as an non-Gaussian factor analysis (Hyvärinen, Karhunen & Oja, 2001).

1.3 SIMULATED DATA AND ANALYSIS

In order to understand how ICA works with tree ring width series we have used simulated growth series data sets base on the tree ring width model proposed by Cook (1987); Cook & Kairiukstis (1990). These series have been construct to test the preservation of trends, the extraction of noise and the influence of disturbances. Tree ring width series have been construct with three components : a trend, a disturbance pattern and 50% of Gaussian noise. Similar test data have been previously used by Rubino & McCarthy (2004) in order to test disturbance detection methods in oak chronologies. Different simulated data sets have been created. Each set contains at least 20 series of 100 years (some examples are shown in figure 1.1) :

1. A data set that mixes a disturbance pattern (*e.g.* Rubino & McCarthy, 2004) with a linear or non-linear trends and some noise. To give a more realistic shape to tree ring width series, the disturbance pattern is not exactly the same for each tree

ring series. It's amplitude in x and y axis varies amongst series, as well as the first and last year of effect. With this set we will test if the different kind of trends are recovered as well as the disturbance pattern.

2. This set mixed a trend with large spikes. Theses spikes try to represent disturbances affecting trees for only one or two years like a severe drought, ice storm ... The value of each spike is set as the mean of the series at the considered year plus x time the standard deviation (σ). We will test the effect of varying amplitudes of spikes, as well as the effect of different number of spikes on the detection of the spike.

3. In order to test spike threshold for the detection, 159 series were created. For this purpose the strategy is different. We have added to one series with one spike an increasing number of non spiky series to understand at what dilution a spike is still detected. The estimation of confidence intervals for the detection and recovery of spikes is not defined in an analytical way. Therefore, a bootstrap with 1000 permutations, when possible, was made. This re-sampling replaces the non spiky series then, ICA was restarted.

4. A set of complex data was generated in order to simulate real tree ring series by mixing a trend, disturbances, noise and a cyclicity pattern. The cyclicity was simulated using two sine waves simultaneously : a 12 years and a 60 years. This set was made of four different trends (two linear and two non-linear) containing 20 series each.

Our initial analyses revealed that under some conditions the ICA algorithm was unable to separate trends and cyclic patterns in the data. The principal problem is that there are more potential component to be extracted than there are series in the analysis. Unfortunately, ICA is not able to extract more component than the number of input series. To solve this problem, we propose to analyze trends by ICA separately (Figure 1.2). A classification method can used to separate series with different trends. Then a second ICA is performed on the four independent components representing the mixture of recovered trends and cycles. Two extractions have to be done separately because

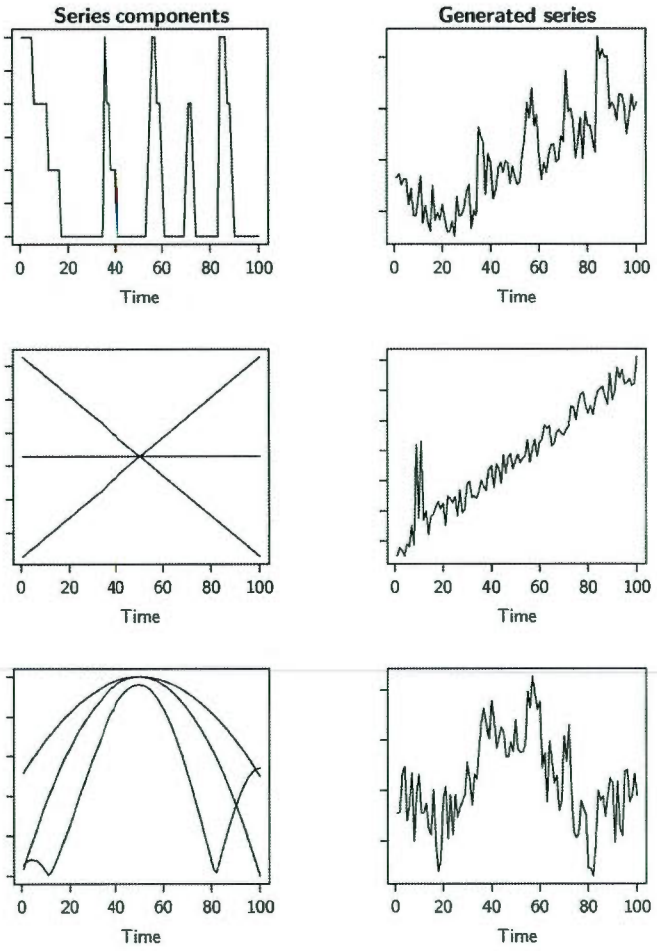

Figure 1.1 Example of constructed series with the components used to build it. The component column shows from top to bottom a disturbance pattern, then linear trends and non-linear trends. The right column shows some example of generated series with from top to bottom positive trended disturbances, then a spike with a trend and a non-linear trended disturbance.

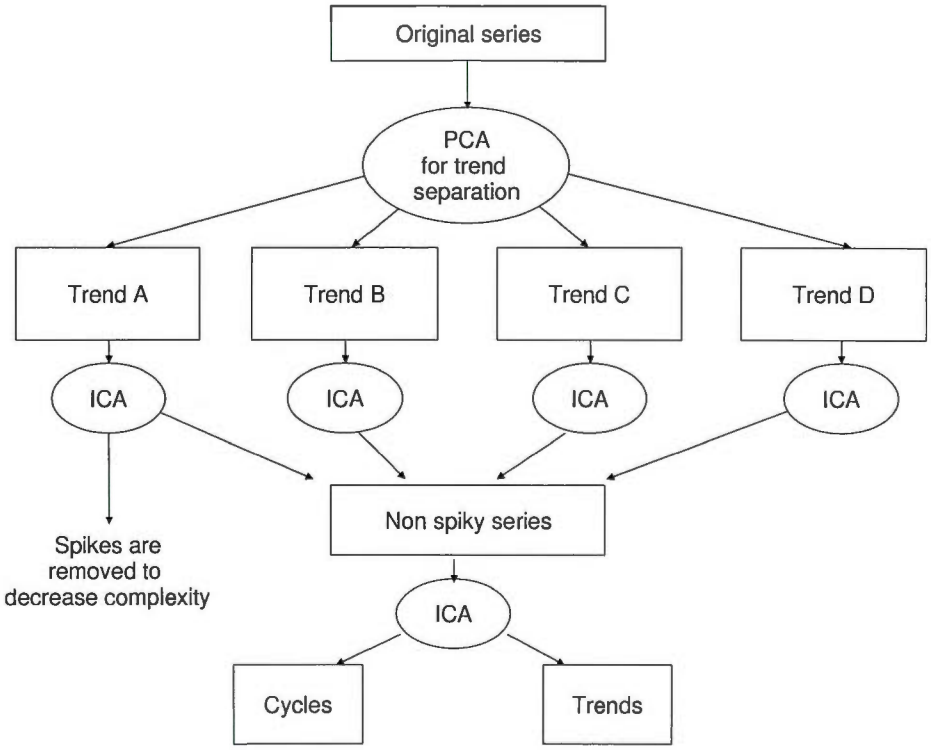

Figure 1.2 Analysis of complex series schematic representation

ICA provide statistically independent results. This independence mean that a second analysis cannot be done on some component extracted from the same first analysis due to the lack of interaction (different coordinates) between input data.

We used the FastICA algorithm (Hyvärinen & Oja, 2000) to do the ICA. This algorithm, after data are centered, projects the data onto a n dimensional space where n is the number of components to extract (specified by the user). This algorithm used the fixed-point iteration scheme for maximizing the neg-entropy with the constraints that the estimated un-mixing matrix is an orthonormal matrix. In practice Principal Component Analysis can be used as preprocessing tool for ICA in order to set the number of component to extract (Stone, 2004). However, in the case of constructed data this pre-process is not necessary because we know a priori the number of components to extract. We, however, tested the usability of the PCA to set the number of components.

A comparison of ICA is made with the mean series which is a year to year mean of the series.

As a measure of the goodness of the ICA we used the surface recovered by series. We calculated the common surface the original data (without noise) and the surface of the ICA components. This was compared to the mean series (with noise).

1.4 RESULTS AND DISCUSSION

1.4.1 Trend Recovering within Data Set 1

ICA recovers the trends and disturbances of our data. However, these two pattern appears mixed together in the same component (Figure 1.3). Moreover, further analysis shown that this performance is better than that of a mean series for non-linear trends as shown in figure 1.3, whereas mean series do better with linear trend. This comparison is given by the per cent of common area between the recovered series (by ICA or mean) and the original series without noise (Table 1.1). With linear trend the ICA explained is 17% less than a simple mean, while for non-linear trends the ICA was of 11% better than a simple mean.

If series with the three different trends of the same kind (linear or non linear) are used as input data, ICA recovered them but seems to be unable to separate positive and negative trends and the performance (measured again as common surface under the mean curve) is less good than results of a single trend (Table 1.1), but far better than the mean which erases the positive and negative trends.

Results of ICA done in the same way with non-linear trends are much better than the mean of the series (Table 1.1), but it is just able to distinguish three trends of the four trends present in the series and the perturbation pattern disappears like with the mean series. When applied on all these data simultaneously, ICA recovered the same three non-linear trends and the perturbation pattern with a slightly positive trends. The series obtained by the mean is non-linear with the perturbation.

We tested principal components analysis (PCA) to set the number of component to

extract (Himberg & Hyvärinen, 2001; Stone, 2004) in a subsequent ICA. The main three axis of the PCA explained 83% of the variance (result not shown) of all data. Other axis did not explained a significant par of the variance (under 2%). Consequently, an ICA with three components to extract was done (Table 1.1). This was one component less than there are signals in the simulated data. The analysis recovered two linear trends and the non linear which was not recovered when four components were extracted. Generally we observed that if we decreased the number of components to extract, the non linear trends extracted look like more and more the average non linear trend. It is probably good to try both methods for real data. An extraction with the number of components set by a PCA and an extraction with the maximum number of components that can be obtained from the ICA. In order to set a number of components to extract equals to the number of source signal various methods exist and are discussed in Penny, Roberts & Everson (2001) but in tree ring width the number of "anomalies" and other sources can be larger than the number of input series. Setting the number of component to extract equal to the number of input series can be a good idea.

1.4.2 Detection of Spikes and Recovery of Their Values within Data Set 2 and 3

As described before, our aim is to determine the minimum size of a spike that is detected and the minimum proportion of series that contain a spike required for spike detection. Also, we wanted to understand the consequences of having several spikes in a tree series on the detection of a spike.

The detection threshold (Table 1.2) is as low as the definition of a spike used by us. ICA always detected spikes as low as 4σ that occur in 5 series. The larger is a spike, the more easily it is detected, even if it occurs less frequently. Spikes of 4σ were detected if they occur in 1/15 series, spikes of 5σ in 1/16 and spikes of 10σ in 1/128 (Table 1.2). This representation of spikes within series, in order to be able to detect it, is effectively non-linear (Figure 1.4). In order to test more robustly this detection threshold, the detection of a single 10σ spike was tested with an increasing number (up to 160) of

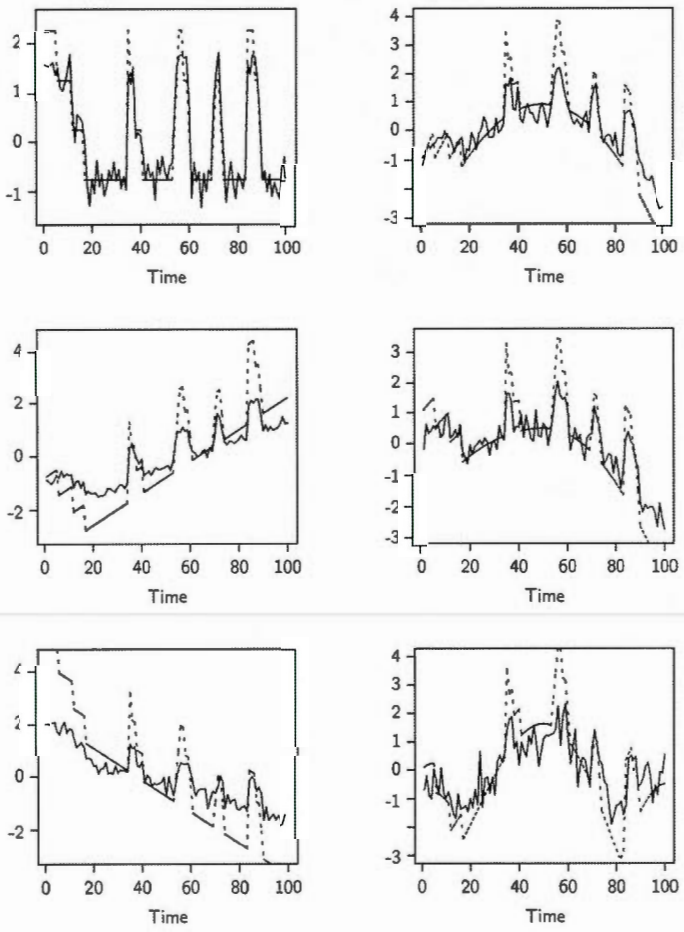

Figure 1.3 Results of the recovered trends and disturbance pattern. Dotted lines represent original components centered on the mean and plain lines represent the recovered components by the independent component analysis.

Tableau 1.1 Performance of the independent component analysis compared to a mean series in trends and disturbance pattern recovering express by the proportion of surface recovered. Values shows how the analysis performed by comparing the share proportion of area under recovered curves with the original non noisy curve. Symbol " — " is use for series without trends, " / " for positive trends, " \ " for negative trends, " $\sim\frown$ " for linear trend becoming non linear, " $\frown\sim$ " for non linear trend becoming linear, " $\frown$ " for non linear hyperbolic trend and " Ω " for non linear " omega like " trend. " One " refers to a test applied on just one trend, " Mix s.t. " refers to a test applied to all linear or all non linear trends and " Mix all " to a test applied to all trend at the same time. " - " shows non obtained results. PCA ICA shows results of ICA done with the number of components to extract set by PCA.

			Linear	trend		Non Linear	trend	
Input		—	/	\	$\sim\frown$	$\frown\sim$	$\frown$	Ω
One	ICA	0.621	0.775	0.723	0.872	0.880	0.760	0.781
One	Mean	0.691	0.909	0.936	0.777	0.807	0.663	0.612
Mix s.t.	ICA	0.726	0.737	-	0.782	0.467	-	0.733
Mix s.t.	Mean	0.734	-	-	-	-	0.774	-
Mix all	ICA	-	0.630	-	0.801	0.425	-	0.729
Mix all	Mean	-	-	-	0.828	-	-	-
Mix all	PCA ICA	0.686	0.726	-	-	-	0.814	-

non spiky series. Moreover, a bootstrap with 1000 permutations was used to calculate a confidence interval of the recovered spike's size. Bootstrap gave two results as shown in figure 1.4 : the value recovered vary by 2 units or more within the confidence interval and the detection is affected by the noise. A value to be recovered of 10σ has a maximum dilution of 1/8 series with a threshold of detection set at 125% the noise maximum value and sometime, it can be detected in 1/128 series. Our capacity to detect multiple spikes is not directly related to the magnitude of the spikes. In table 1.2 we compared results of a 5σ spike versus the addition of one 4σ and one 1σ spike where detection works better with the 5σ. The ICA was always more able to detect a single large spike (*e.g.* a single spike of 5σ) than the detection of several simultaneous spikes of the same cumulative magnitude (*e.g.* two spikes of 2.5σ). The sign of the spike (positive or negative) did not affect the detection due to rotation if only one spike is present in the series. For two spikes of opposite sign, the difference of sign between them is preserved. Moreover, ICA attempt untie, if possible, spikes in order to recover each spike in a single component. In figure 1.5 we have recovered five spikes. These spikes appeared at year 9, 11, 15, 25 and 41, and are mixed differently. In order to untie each spike, the number of components to extract has to be set correctly. However, it is impossible to extract more components than the number of series in the analysis. The proximity of spikes (*e.g.* one year between two spikes) did not affect their recovery as shown in figure 1.5 (top row).

1.4.3 Complex Series Analysis of the Data Set 4

The analysis of simulated complex data gave similar results to the trend and disturbances recovering tests. Spikes were recovered separately, but the other parts (trend, cyclicity and disturbance) were mixed together. The principal problem is that there is more potential component to be extracted than the number of data in the analysis. Consequently, data were separated according to their trend and two ICA were made as explain in the methods. Results of this second analysis (Figure 1.6) show that it was able to recover the two cyclicity patterns. However, the trends are in two components as a mix of a linear trend and a non-linear trend whereas we were expecting to have six

Tableau 1.2 Results of the detection of spikes in a set of series without spikes by the independent component analysis. Nb. Spike give the number of spike involved at the same year, σ Add. referred as the number of time the standard deviation is added with Val. the value in the input matrix. Nb. S. referred to the number of series used in the analysis. Val. Rec. is the absolute value of the spike recovered. Mean, Sd., Max and Min referred to the mean, the standard deviation, the maximum value and the minimum value without the spike of the recovered series. * give the detection threshold, which is in reality 1/(Nb. S.). The first line of data gives the characteristics of other values at the same year than the spike, and the second line reproduce the same values but centered on the mean.

Nb. Spikes	σ Add.	Val.	Nb. S.	Val. Rec.	Mean	Sd.	Max	Min
One	4σ	2.51	5	3.17	-0.03	0.96	2.12	-2.11
One	5σ	2.79	5	3.76	-0.04	0.93	2.07	-2.12
One	6σ	3.07	5	4.56	-0.05	0.89	1.83	-1.80
One	7σ	3.35	5	5.12	-0.05	0.86	1.73	-1.73
One	8σ	3.63	5	5.62	-0.06	0.83	1.63	-1.67
One	9σ	3.91	5	6.06	-0.06	0.80	1.55	-1.60
One	10σ	4.19	5	6.45	-0.06	0.77	1.47	-1.55
One	11σ	4.47	5	6.80	-0.07	0.74	1.37	-1.46
One	4σ	2.51	5	3.24	-0.03	0.95	1.95	-2.08
One	4σ	2.51	10	2.97	-0.03	0.96	2.10	-2.25
One	4σ	2.51	15*	2.90	-0.03	0.97	2.38	-2.22
One	5σ	2.79	5	4.11	-0.04	0.92	2.00	-1.84
One	5σ	2.79	10	3.38	0.03	0.95	2.28	-1.97
One	5σ	2.79	16*	3.22	0.03	0.96	2.30	-2.17
One	10σ	4.19	10	6.53	0.00	1.01	1.85	-1.76
One	10σ	4.19	20	6.71	0.01	1.00	1.85	-1.85
One	10σ	4.19	100	4.76	-0.05	0.96	2.67	-2.14
One	10σ	4.19	128*	3.40	-0.03	0.95	2.85	-2.23
Two	4σ & 1σ	2.51 & 1.67	5	3.12	-0.03	0.97	2.07	-2.14
Two	4σ & 2σ	2.51 & 1.95	5	3.17	-0.03	0.96	1.95	-2.04
Two	4σ & 3σ	2.51 & 2.23	5	3.35	-0.03	0.95	1.92	-1.97
Two	4σ & 4σ	2.51 & 2.51	5	3.68	-0.04	0.94	2.07	-1.85
Two	4σ & 5σ	2.51 & 2.79	5	4.36	-0.04	0.91	2.07	-1.71
Two	4σ & 6σ	2.51 & 3.07	5	4.98	-0.05	0.87	2.07	-1.76
Two	5σ & 6σ	2.79 & 3.07	5	5.23	-0.05	0.86	2.04	-1.68

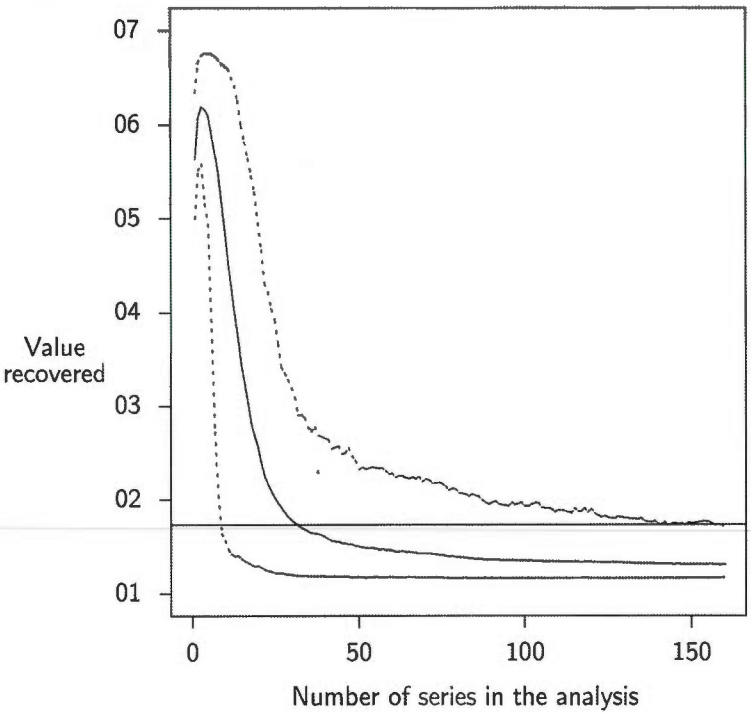

Figure 1.4 Recovering of one spike with increasing number of series without spike. The plain line represents the mean and dotted lines the 90% confidence obtained by bootstrap with 1000 permutations when possible. The vertical line gives the threshold of detection (125% of noise maximum value).

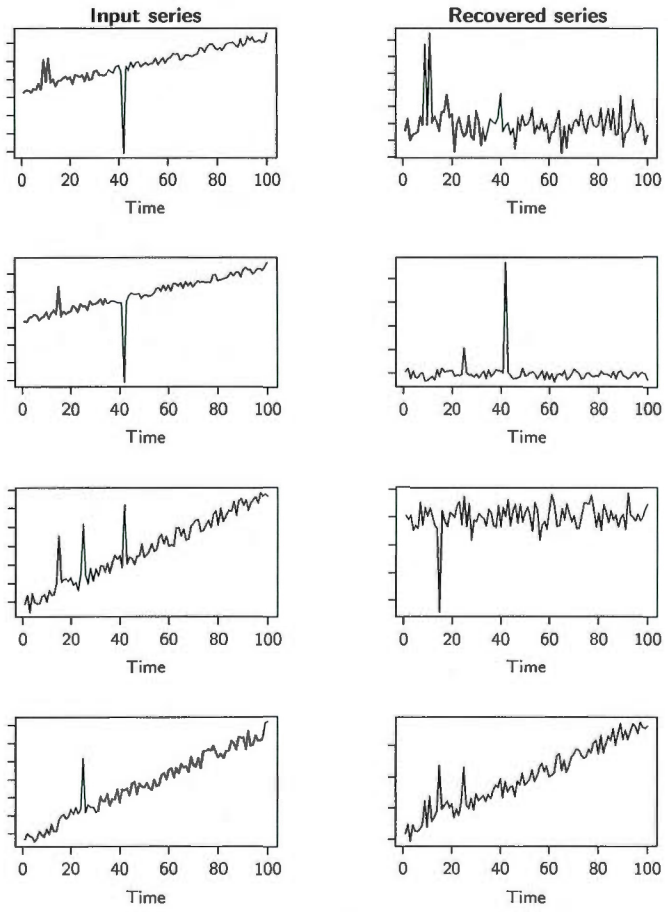

Figure 1.5 Spikes recovering from independent component analysis

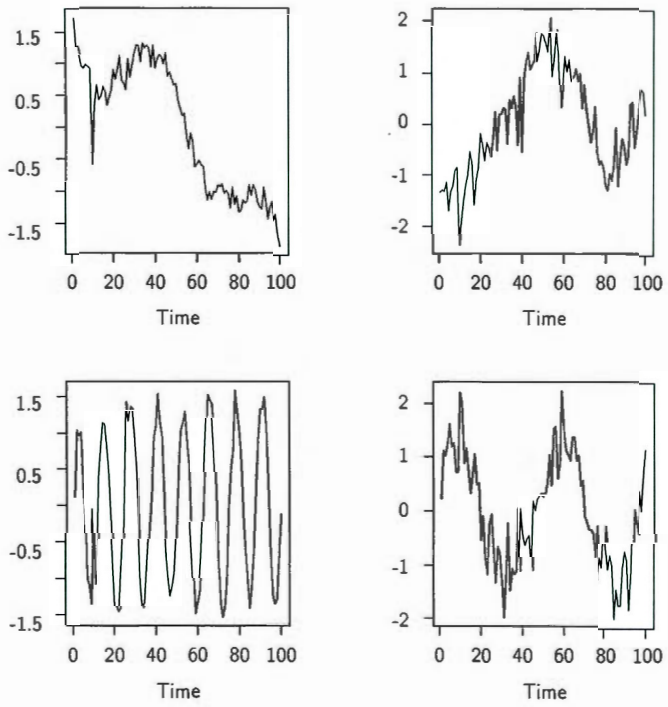

Figure 1.6 Resulting trend and cycle of independent components extracted during the analysis of complex simulated data

different trends recovered.

1.5 CONCLUSION

Independent component analysis is a relatively new statistical methodology. It success in medical science for the electroencephalographic brain dynamics had show the power of the methods applied to time series (Vigário *et al.*, 1998; Hyvärinen, Karhunen & Oja, 2001). However, their is major differences in the kind of analysis made with electroencephalographic and the dendrochronological approach. In climate dendrochronology we are interested in all extracted components, like in financial analysis, whereas medical science seek for anomalies and more generally spikes detection. Recently, ICA has been applied to try to uncover hidden patterns in the observed financial data (Back & Weigend, 1997; Moody & Wu, 1998; Moody & Howard, 1999) or in seismic records

(Ham & Faour, 1999) which is closely related to our goal in tree ring width analysis.

In this paper multiple tests have been done to test the applicability in dendrochronology. Like in medical science spike recovering is done without problems. Moreover, ICA seems to improve trends and large disturbance detection in comparison with the classical mean series made in dendrochronology approach. Where ICA improve tree ring width analysis is in the recovering of cyclicity and it seems to be an efficient method to recover disturbance. Whereas classical analysis try to identify such patterns with the estimation of parameters in hypothetical relationship, ICA extract it directly. This direct extraction will permit to work on other independent components or on this cyclicity without the offset introduced by their estimation. Moreover, the recovered patterns are statistically independent, which can be of great interest especially for detecting co-occurring disturbances. Also a mean tree ring width series can be obtained without disturbance effect which can be precious for studies dealing with long term trends.

In the applicability of ICA for particular contexts lies the power of this technique for tree ring research. In particular, spike recovering can improve the resolution of insect outbreak detection and other disturbances.

DE LA THÉORIE À LA PRATIQUE

Le premier chapitre nous a permis de tester une nouvelle méthode pour l'étude des cernes de croissance des arbres. Différents tests furent appliqués sur des données simulées, avec succès. Mais, un test sur de vraies données doit être fait avant d'aller plus loin. Pour cela nous avons utilisé des données provenant de trois articles scientifiques qui utilisent les cernes pour détecter les épidémies d'insectes passées. Nous espérons ainsi obtenir les mêmes résultats et voir si notre méthode ne pourrait pas aboutir à une recherche plus affinée dans ce domaine.

CHAPITRE II

IDENTIFYING INSECT OUTBREAKS : A COMPARISON OF A BLIND-SOURCE SEPARATION METHOD WITH HOST VS NON-HOST ANALYSES

The identification of past insect outbreaks is often determined using a comparison of host and non-host tree-ring growth chronologies. Yet this may be a problem when non-hosts are either affected by the outbreaking insect or when the growth of host and non-host trees does not respond similarly to the same climatic factors. In this paper, we investigate the use of a blind source separation method to identify past outbreaks. This method, used in neurology and called independent components analysis (ICA), directly identifies disturbance patterns in time series data. We re-analyzed the tree-ring data from three papers dealing with insect outbreaks for which data were available. These papers focus on western spruce budworm, pandora moth and Douglas-fir tussock moth outbreaks. We compared the results of the original analyses in these papers conducted using a comparison of tree growth in host and non-host trees with results from ICA. We detected the five outbreaks identified in the original papers using the ICA for host series. However, the start and end dates for the outbreaks were different in 75% of the ICA analyses compared to the dates reported in the original paper. On the other hand, we were able to detect growth reduction in non-host ponderosa pine chronologies during western spruce budworm outbreaks with generally 50% of the trees affected by a growth reduction for the considered site. Other non-host chronologies tended to show increased growth during outbreak periods by at least 60% of the average growth occurring in

non-outbreak periods. Since conventional methods may be less robust when the growth of non-host trees is affected, the ICA may provide a powerful new method to identify outbreaks when there are overlaps in effects in host and non-host trees. However, for ICA to work most optimally the number of tree ring width series needed is high. There are multiple advantages of this new approach ; there is no need to assume that outbreaks do not decrease the growth of non-host species and there is the potential ability to identify other disturbance events.

2.1 INTRODUCTION

Forests are subject to many disturbances varying in scale and severity : fire, windthrow, insects, etc. The understanding of these events is fundamental for a better comprehension of forest dynamics, the conservation of biological diversity (Lindenmayer & Franklin, 2002) and the development of sustainable forest management (Bergeron *et al.*, 2002; Burton *et al.*, 2003; Franklin *et al.*, 2002). Knowledge about the frequency of disturbances provides an understanding of the historical factors affecting forests in a region. However, reconstructing the history of these events is not easy and different non-destructive methods have been used, such as associating disturbances with recruitment peaks in tree age structures or associating ages to crown area distribution. However, tree ring growth patterns provide the most direct identification of past disturbances (Lorimer, 1985; Frelich, 2002). Recent statistical advances in fields such as neurology (Vigário *et al.*, 1998; Jung *et al.*, 2001) have been used to detect disturbance events in brain records; such methods may be of interest to ecologists attempting to identify disturbances that decrease growth in tree ring chronologies. Here we focus on the possibility of using a blind source separation method called Independent Component Analysis (ICA, Cardoso, 1989; Comon, 1994) for identifying insect outbreak history from tree ring width series.

As a disturbance, insect outbreaks are a primary driver of forest productivity and nutrient cycling (Romme, Knight & Yavitt, 1986). Defoliating insects reduce growth and can cause high mortality (McCullough, Werner & Neumann, 1998; Kulman, 1971a), whereas

growth increases can occur in unaffected neighboring non-host trees when released from competition. The analysis of tree ring series is often used to reconstruct insect outbreaks (Morrow & Lamarche, 1978; Swetnam, Thompson & Sutherland, 1985). Although direct analysis of a host tree ring series has been used in some papers (Bouchard, Kneeshaw & Bergeron, 2006) a favored dendrochronological approach involves using a non-host growth chronology to detect decreases in the growth of host species (Nash, Fritts & Stokes, 1975; Swetnam, Thompson & Sutherland, 1985). A key assumption in this approach is that the growth of the non-host species is not affected by the disturbances (or at least is less affected). The non-host species should also react to the same climatic variations as the host species in order to limit misinterpreting climatically induced growth fluctuations as being due to insect outbreaks *e.g.* a moisture sensitive outbreaking insect host species matched with a drought tolerant non-host species could lead to interpreting reduced growth in the host because of a dry period being interpreted as an insect outbreak. Although limitations of the host–non-host correction procedure are well recognized in the literature (Ryerson, Swetnam & Lynch, 2003), this method has been one of the only ways of detecting past outbreaks when direct observations were not available. The ICA can help prevent these problems by viewing data differently and complying with tree growth components (age effect, disturbance events, ...) as described in the traditional linear aggregated model (Cook, 1987). Actually ICA views data as a mixture of information based on the physically realistic assumption that if these information are from physical processes, then those information are statistically independent and thus can be recovered. The objective of this paper is therefore to test whether ICA can be used to identify outbreaks and to what extent it can be used to help or replace the host–non-host correction procedure.

2.2 MATERIALS AND METHODS

2.2.1 Data and Insect Information

We analyzed ponderosa pine (*Pinus ponderosa*) ring width data from three papers : Swetnam *et al.* (1995), Speer *et al.* (2001) and Ryerson, Swetnam & Lynch (2003), the only species in these papers with data available in the International Tree-Ring Data Bank (http ://www.ncdc.noaa.gov/paleo/treering.html, last accessed 09/09/2009). The outbreak reconstruction of these papers targets some of the most important generalist defoliators in western North America : the western spruce budworm (*Choristoneura occidentalis*), the pandora moth (*Coloradia pandora*) and the Douglas-fir tussock moth (*Orgyia pseudotsugata*).

We obtained 10, 14 and four sites from these papers with an average of 24 trees per site (Table 2.1). In the case of data obtained from Swetnam *et al.* (1995) and Ryerson, Swetnam & Lynch (2003), Ponderosa pine was used as a non-host species for western spruce budworm in their original paper (see below), as well as tussock moths in Swetnam *et al.* (1995), and as a host species for pandora moth in the paper by Speer *et al.* (2001). We will use the same distinctions in our analyses.

The primary hosts of the western spruce budworm are Douglas-fir (*Pseudotsuga menziesi*), grand fir (*Abies grandis*), white fir (*Abies concolor*), subalpine fir (*Abies lasiocarpa*), western larch (*Larix occidentalis*), blue spruce (*Picea pungens*), Engelmann spruce (*Picea engelmannii*) and white spruce (*Picea glauca*) (Furniss & Carolin, 1977; Fellin & Dewey, 1982; Hagle, Gibson & Tunnock, 2003). Secondary hosts include non-native Norway spruce (*Picea abies*), scotch pine (*Pinus sylvestris*), native western hemlock (*Tsuga heterophylla*), and ponderosa pine (Fellin & Dewey, 1982; Hagle, Gibson & Tunnock, 2003), which has often been used as a non-host species in outbreak reconstructions (Weber & Schweingruber, 1995).

The Douglas-fir tussock moth's primary hosts are Douglas fir, all true firs and spruces (Wickman, Mason & Trostle, 1981; Fellin & Dewey, 1982; Hagle, Gibson & Tunnock,

2003) while secondary hosts include ponderosa pine and bitterbrush species (*Purshia tridentata* and *Purshia glandulosa*), which are in the Rosaceae family.

The pandora moth's primary hosts are ponderosa pine, Jeffrey pine (*Pinus jeffreyi*) and lodgepole pine (*Pinus contorta*), while secondary hosts include Coulter pine (*Pinus coulteri*) and sugar pine (*Pinus lambertiana*) (Carolin & Knopf, 1968; Fellin & Dewey, 1982; Hagle, Gibson & Tunnock, 2003).

Ponderosa pine can therefore be attacked by these three insects as well as other less damaging insects (Fellin & Dewey, 1982; Hagle, Gibson & Tunnock, 2003), such as the sugar pine tortrix (*Choristoneura lambertiana*), the defoliating weevil (*Magdalis gentilis*), the pine looper (*Nacophora mexicanaria*) or the elegant weevil (*Scythropus elegans*).

Tableau 2.1: Summary of data used in analyses. "ITRDB" refers to the International Tree-Ring Data Bank data with the "site name" as it appeared in the original database and the site name abbreviation used in the paper in brakets, "# trees" refers to the number of trees for the site under consideration, "Start" gives the beginning of tree ring records and "End" their end. "ICA" refers to the data used in the Independent Component Analysis. For example, in the first line, three fewer trees were used for the ICA than found in the ITRDB and the time period analyses started 135 years after the first year with data in the ITRDB.

ITRDB				ICA		
Sites name	# trees	Start	End	# trees	Start	End
Ryerson, Swetnam & Lynch (2003) *Pinus ponderosa* non-host chronologies for *Choristoneura occidentalis*						
co557 (PTP)	23	1654	1997	20	1889	1997

Continued

Tableau 2.1: Summary of data used in analyses (continued)

ITRDB				ICA		
Sites name	# trees	Start	End	# trees	Start	End
co558 (RDS)	29	1605	1997	27	1892	1996
co559 (TLP)	23	1600	1997	21	1800	1997
co560 (WIR)	23	1675	1997	23	1880	1996
Speer *et al.* (2001) *Pinus ponderosa* host chronologies for *Coloradia pandora*						
or046 (LML)	19	1529	1995	19	1835	1993
or047 (PPF)	30	1354	1991	18	1747	1991
or048 (PF)	29	1476	1993	29	1785	1990
or049 (EF)	24	1334	1993	22	1723	1993
or050 (SVF)	10	1747	1995	10	1863	1995
or051 (DES)	21	1574	1995	19	1714	1993
or052 (JCT)	27	1419	1995	24	1849	1995
or053 (SKB)	19	1639	1995	19	1887	1994
or054 (DLK)	20	1513	1995	20	1776	1990
or055 (BJS)	28	1423	1995	26	1803	1995
or056 (TLD)	20	1570	1995	19	1797	1990
or057 (TDS)	15	1442	1995	14	1811	1987
or058 (CLK)	24	1572	1990	20	1838	1990
or059 (CAB)	20	1653	1995	20	1879	1994
Swetnam *et al.* (1995) *Pinus ponderosa* non-host chronologies for *Choristoneura occidentalis*						

Continued

Tableau 2.1: Summary of data used in analyses (continued)

ITRDB				ICA		
Sites name	# trees	Start	End	# trees	Start	End
or029 (CCT)	33	1485	1991	25	1773	1991
or030 (GBP)	34	1502	1991	33	1867	1991
or031 (DHR)	10	1672	1990	10	1824	1990
or032 (IDC)	27	1550	1990	26	1852	1990
or033 (BLM)	21	1469	1990	15	1886	1990
or034 (ESP)	19	1761	1990	18	1892	1990
or035 (LO)	19	1665	1990	16	1770	1990
or037 (SSP)	24	1760	1990	23	1862	1989
or038 (BSK)	42	1665	1990	40	1815	1990
or039 (FLP)	44	1585	1991	42	1874	1990
or040 (LSP)	21	1675	1991	19	1817	1991
or041 (WH)	8	1714	1991	8	1877	1991

2.2.2 Analyses

The traditional linear aggregated model (Cook, 1987) is as follows :

$$R_t = A_t + C_t + \delta D_{1t} + \delta D_{2t} + \epsilon \tag{2.1}$$

where R is the tree ring width, A is the age effect, C is a climatic component, D are disturbance events and ϵ is noise. If we consider trees : R_1, R_2 and R_3, this linear model can be written :

$$R_1(t) = \alpha_{1A}A(t) + \alpha_{1C}C(t) + \alpha_{1D1}\delta D_1(t) + \alpha_{1D2}\delta D_2(t) + \alpha_{1\epsilon}\epsilon_1 \tag{2.2}$$

$$R_2(t) = \alpha_{2A}A(t) + \alpha_{2C}C(t) + \alpha_{2D1}\delta D_1(t) + \alpha_{2D2}\delta D_2(t) + \alpha_{2\epsilon}\epsilon_2 \tag{2.3}$$

$$R_3(t) = \alpha_{3A}A(t) + \alpha_{3C}C(t) + \alpha_{3D1}\delta D_1(t) + \alpha_{3D2}\delta D_2(t) + \alpha_{3\epsilon}\epsilon_3 \tag{2.4}$$

where α is a coefficient linked to each tree for each growth component (A, C and D). Here, we assume that ϵ, the random noise, is time-independent. We can then write this in a matrix form :

$$R = \alpha S \tag{2.5}$$

with R as the original data matrix, α the coefficients matrix and S the components matrix (grouping A, C, Ds and ϵ). If we assume that the αs are different enough to make the matrix non-singular, which we will call ω, then :

$$S = \omega R \tag{2.6}$$

In this form, we simply have to find ω to obtain S, which is the objective of ICA. ICA can be seen as an extension of Principal Components Analysis (PCA) which tries to find a linear representation of non-Gaussian data so that the components are independent (Cardoso, 1989; Comon, 1994). ICA attempts to capture underlying non-Gaussian processes that explain the variation in the data. Whereas PCA looks for linear combinations of a data matrix that are uncorrelated, ICA seeks linear combinations that are independent (Venable & Ripley, 2002). ICA in its formulation is very closely related to Factor Analysis (FA), a common method in social sciences, which seeks linear combinations of variables, called factors, that represent underlying fundamental quantities of which the observed variables are expressions. Furthermore, PCA analyses the entire variance of a dataset, while ICA and FA analyse only the portion of variance that is correlated across several data series. PCA and FA only estimate the factors up to one rotation, instead, the purpose of ICA is to separate the source signals, that PCA and FA cannot, by seeking a rotation of spherical data which have independent coordinates by evaluating ω (Hyvärinen, Karhunen & Oja, 2001; Stone, 2004). This independence means that ICA minimizes the mutual information between components.

Spikes, or disturbance events in our case, have been successfully detected by ICA in numerous fields of science, such as neurology (Vigário *et al.*, 1998; Jung *et al.*, 2001), and seismology (Ham & Faour, 1999). Moreover, this analysis is very sensitive and is thus capable of detecting small disturbances (see Appendix A).

ICA uses raw data (no de-trending) that are normalized (mean of zero and standard deviation of one). Since ICA does not handle missing values, they must be removed. We therefore deleted trees or years with missing values (see Table 2.1), trying to maximize the information by giving preference to the number of trees rather than the length of the series. The trade off is whether a researcher wants to maximize the length of the reconstruction or its robustness (see Appendix A). We used the FastICA algorithm (Himberg & Hyvärinen, 2001) developed in R (Comprehensive R Archive Network, 2009). We then identified disturbance events within extracted components as the ones containing values lower than -1.6 or higher than 1.6, which excludes 90% of the values within a normal distribution of (0,1) parameters. These extreme values have to occur consecutively for at least two years since outbreaks generally affect trees for several years (Kulman, 1971b; Furniss & Carolin, 1977), thus setting a minimum number of consecutive years of extreme values excludes short term disturbances like wind breakage or ice storms. Here each identified growth reduction or increase can be due to a single tree or to all trees. Thus, growth reductions were then compared with the site average growth series (mean of the normalized tree ring width series). When this average contains the same reduction or period, we considered the extracted independent components to involve not only a single tree but rather all trees at the site.

The peak year of growth reduction or increase is then determined from the average series. The maximum percentage of growth reduction or increase is based on the peak year growth value and the 20 years of growth before and after the peak year (it therefore includes some years of the disturbance). We also counted the number of trees showing this change in growth.

2.3 RESULTS

The ICA was able to detect disturbances for all sites, and the periods of growth reduction or growth increase evaluations noted in historical data, and in the results from the original papers were also successfully identified.

2.3.1 Analysis of Ponderosa Pine as a Host Species of Pandora Moth

When analyzing data for Ponderosa pine as a host species for pandora moth, we found five main growth reduction periods (Figure 2.1) : 1967–1988 for six sites, 1914–1941 for seven sites, 1863–1910 for ten sites, 1827–1846 for six sites and 1795–1813 for four sites. They correspond to outbreaks detected by Speer *et al.* (2001) in 1967–1989 (six sites), 1919-1925 (seven sites), 1870–1875 and 1889–1895 (seven sites), 1836–1847 (12 sites), and 1794–1803 (nine sites) respectively. The number of affected sites identified by the ICA is most similar to those identified by Speer for outbreaks after 1870. Differences for earlier outbreaks are due to the length of tree ring width series used (Table 2.1).

Moreover, we detected a greater number of growth reduction periods per site than reported in the original papers. For example, site SVF shows three growth reduction periods : one starting in 1870 and also detected in the original paper, and two minor ones in 1960 (22% growth reduction) and 1971 (17% growth reduction) respectively, which were not detected by Speer *et al.* (2001).

The amplitude of growth reduction cannot be directly compared due to the de-trending carried out in Speer *et al.* (2001), and problems with site names and correspondence between figures and tables in the paper (*e.g.* site EF in their Figure 4 was affected by an outbreak in 1989–1992, but no growth reduction value is reported in their Table 3). Nevertheless, values appear to be consistent. For example, we detected a maximum growth reduction of 33% in 1992 at the JCT site, and the 1990–1995 period reduction is 17%. During the same period, Speer *et al.* (2001) reported a growth reduction between 21% and 32%.

2.3.2 Analysis of Ponderosa Pine as a Non-host Species for Western Spruce Budworm and Tussock Moths

Although the ICA detected changes in the growth of Ponderosa pine when treated as a non-host species these changes were not always decreases but also included growth in-

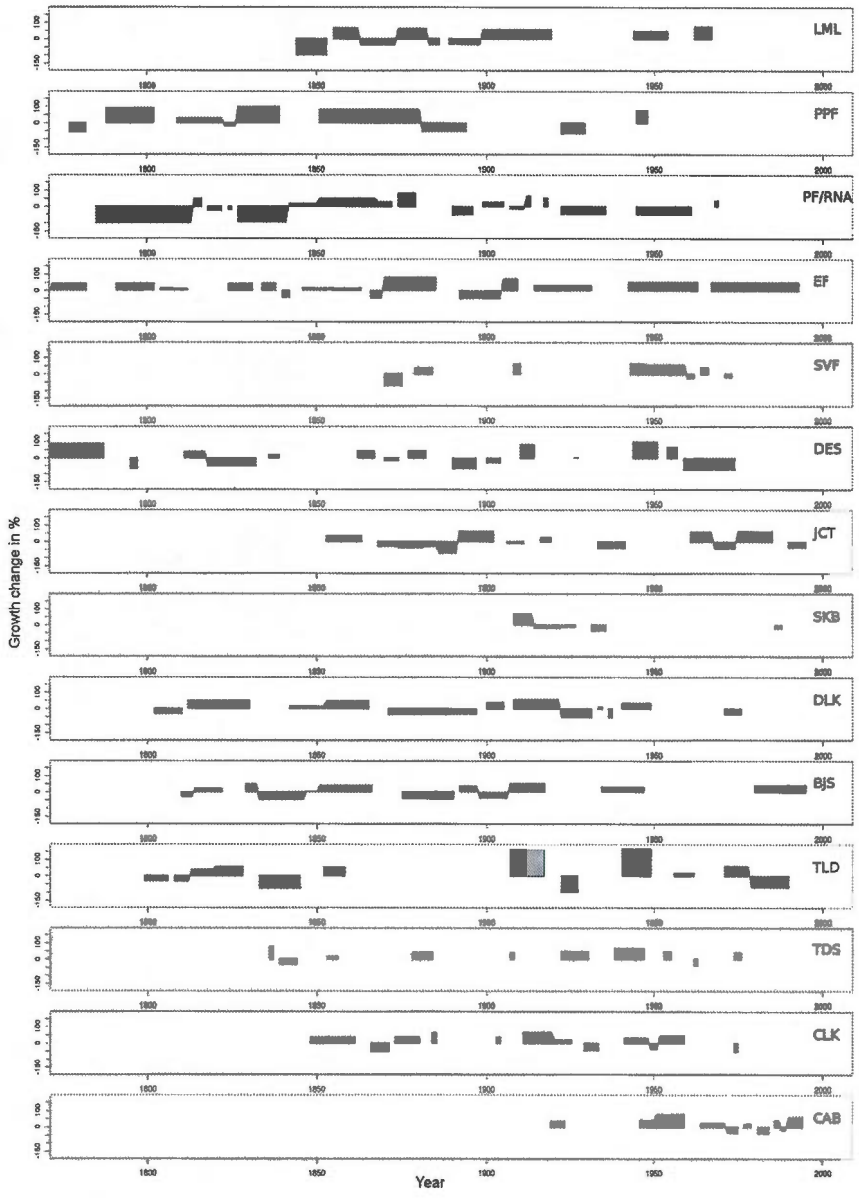

Figure 2.1 Results from the re-analysis of the host species data of Speer *et al.* (2001). Site name abbreviations (BJS, CAB, ...), as they appeared in the original paper, are indicated to the right of each result. The black boxes show decreases in growth and the grey boxes increases in growth. Box lengths show the duration of the change in growth and their height shows the maximum growth change.

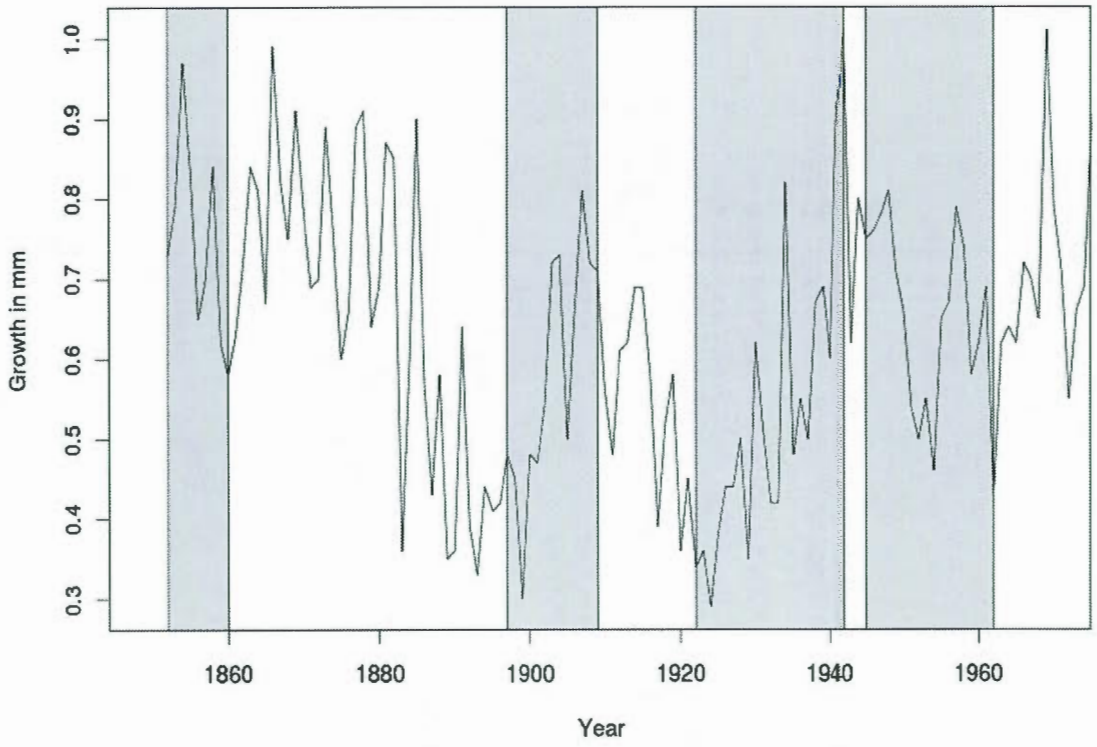

Figure 2.2 Growth of a single non-host tree from Swetnam *et al.* (1995), site number or032 in the ITRDB (abbreviated IDC in the original paper) , with outbreak periods they detected in grey.

creases. We found major increases or decreases in growth during the originally reported outbreak periods (Tables 2.2 and 2.3). Increases in growth could be up to 600 % compared with the average growth 20 years before and after the period of change, whereas decreases were only as low as -113 %. These increases in growth are not marginal, for example, the maximum reached in Table 2.2 of a 600% growth increase, was an event that affected 90% of the analyzed Ponderosa pines. Moreover, during the 1925–1939 outbreak period (Table 2.3), the average growth reduction observed in four sites out of ten was -48.5%, whereas the average growth increase in the remaining sites was 33.7%.

Tableau 2.2 Results from the re-analysis of non-host species data of Ryerson, Swetnam & Lynch (2003). "Outbreak" refers to outbreak periods and "peaks" are the peak years appearing in the original paper. "Sites" gives the names of the re-analyzed sites as they appear in the International Tree-Ring Data Bank and in brakets their abbreviated name as the appear in the original paper, "start" is the beginning of the outbreak, "peak" is the year of maximum change in growth with a half-year indicating that the maximum lasted two years, "end" is the end of the outbreak, "#" the number of trees showing a change in growth with the percentage in brackets, and "%" the maximum change in growth in percent.

	Outbreaks	1984–1997	1960–1977	1936–1952	1903–1932
Sites	peak year	1990	1971	1942	1913
co557	start	1985	1960	1939	1907
(PTP)	peak	1992.5	1968	1945	1921.5
	end	1994	1974	1955	1935
	#	12	9	11	16
	%	145	61	0	73
co558	start	1985	1965	1935	1902
(RDS)	peak	1990.5	1971	1942	1916.5
	end	1996	1974	1945	1933
	#	4	18	16	21
	%	35	242	70	140
co559	start	1984	1966	1940	1905
(TLP)	peak	1987	1972.5	1946.5	1916.5
	end	1990	1978	1953	1931
	#	16	10	14	19
	%	125	130	-48	600
co560	start	NA	1968	1946	1900
(WIR)	peak	NA	1968	1947	1915
	end	NA	1973	1948	1932
	#	NA	7	5	22
	%	NA	115	61	130

Tableau 2.3: Results from the re-analysis of non-host species data of Swetnam *et al.* (1995). "Outbreak" refers to outbreak periods and "peaks" are the peak years appearing in the original paper. "Sites" gives the names of the re-analyzed sites as they appear in the International Tree-Ring Data Bank and in brakets their abbreviated name as the appear in the original paper, "start" is the beginning of the outbreak, "peak" is the year of maximum change in growth with a half-year indicating that the maximum lasted two years, "end" is the end of the outbreak, "#" the number of trees showing a change in growth with the percentage in brackets, and "%" the maximum change in growth in percent.

	Outbreaks	1946–1958	1925–1939	1898–1910	1851–1867
Sites	peak year	1950	1934	1904	1858
or029	start	1937	NA	1900	1860
(CCT)	peak	1956	NA	1904	1861
	end	1961	NA	1904	1872
	#	11	NA	14	18
	%	167	NA	83	53
or030	start	1946	1920	1895	NA
(GBP)	peak	1952	1934	1904	NA
	end	1965	1940	1904	NA
	#	13	14	15	NA
	%	40	-31	25	NA
or031	start	NA	NA	1900	1853
(DHR)	peak	NA	NA	1907	1861
	end	NA	NA	1908	1866
	#	NA	NA	8	4
	%	NA	NA	59	57

Continued

Tableau 2.3: Results from the re-analysis of Swetnam *et al.* (1995) non-host species data (continued)

	Outbreaks	1946–1958	1925–1939	1898–1910	1851–1867
Sites	peak year	1950	1934	1904	1858
or032	start	1945	1922	1897	1852
(IDC)	peak	1949	1929	1905	1861
	end	1962	1942	1909	1860
	#	1	12	14	13
	%	-113	49	-110	53
or033	start	1950	1925	1896	NA
(BLM)	peak	1950	1934	1907	NA
	end	1956	1928	1911	NA
	#	2	9	10	NA
	%	-52	13	72	NA
or034	start	NA	1924	1901	NA
(ESP)	peak	NA	1928	1903	NA
	end	NA	1928	1910	NA
	#	NA	9	10	NA
	%	NA	19	35	NA
or035	start	1950	1925	1904	1853
(LO)	peak	1960	1930	1908	1857
	end	1963	1931	1922	1866
	#	9	5	7	5
	%	95	53	74	28

Continued

Tableau 2.3: Results from the re-analysis of Swetnam *et al.* (1995) non-host species data (continued)

	Outbreaks	1946–1958	1925–1939	1898–1910	1851–1867
Sites	peak year	1950	1934	1904	1858
or037	start	NA	1925	1890	NA
(SSP)	peak	NA	1928	1904	NA
	end	NA	1931	1913	NA
	#	NA	15	14	NA
	%	NA	37	89	NA
or038	start	1941	1921	1903	1849
(BSK)	peak	1952	1925	1907	1858
	end	1963	1928	1914	1862
	#	9	17	20	36
	%	101	-25	-32	42
or039	start	1948	1921	1899	NA
(FLP)	peak	1951	1931	1907	NA
	end	1955	1937	1911	NA
	#	20	13	23	NA
	%	-36	31	113	NA
or040	start	1944	1923	1896	NA
(LSP)	peak	1947	1933	1907	NA
	end	1955	1937	1908	NA
	#	10	15	11	NA
	%	73	-55	76	NA

Continued

Tableau 2.3: Results from the re-analysis of Swetnam *et al.* (1995) non-host species data (continued)

	Outbreaks	1946–1958	1925–1939	1898–1910	1851–1867
Sites	peak year	1950	1934	1904	1858
or041	start	NA	1935	NA	NA
(WH)	peak	NA	1936	NA	NA
	end	NA	1938	NA	NA
	#	NA	6	NA	NA
	%	NA	-83	NA	NA

2.4 DISCUSSION

ICA vs Traditional Analyses

Our results show that the Independent Component Analysis (ICA) is able to detect all changes in growth reported in the original papers as having been caused by insect outbreaks. Ponderosa pine was considered to be a non-host species for western spruce budworm and tussock moth, and as a pandora moth host species. However, in situations where it was considered to be a non-host species (Tables 2.2 and 2.3) both growth increases and decreases were observed.

The traditional host–non-host method is theoretically based on there being no decrease in non-host species growth during periods of host species growth reduction (although there are a number of examples of authors using secondary hosts as non-hosts, *e.g.* Weber & Schweingruber (1995), in which reductions are expected to be minor compared to primary hosts), and the non-host species should respond to climatic variations like the host species. These requirements are often difficult to achieve (Swetnam *et al.*, 1995) due to the absence of such perfect "non-host species" at the location of interest. In

such cases, using the ICA approach with dendroecological data could help in avoiding problems associated with not being able to respect these premisses.

The ICA approach should also strengthen host-only approaches that have been used when non-host comparisons are difficult. A number of papers have used such methods when appropriate non-host chronologies are not available (*e.g.* Bouchard, Kneeshaw & Bergeron, 2006). The ICA approach thus offers an alternative that may permit researchers to more objectively determine the occurrence of outbreaks or at least act as an objective validation. The main power of the ICA lies in the simple assumption that source signals are statistically independent and can thus be recovered through the analysis. In other words, it means that we observed a mixture of independent signals. However, this requires that the number of mixtures is at least equal to the number of independent signals. Therefore, the number of tree ring series has to be equal to or greater than the number of possible events. For example, we recommend using a 100-year-long window and 30–40 tree ring series, this recommendation would permit the analysis of series containing 30-40% disturbances. This number of series should be adjusted based on ecological knowledge of the site location. For example, for mountainous sites that could suffer from spring frosts, as well as summer droughts and insect outbreaks, a larger number of tree growth series would be needed. The statistical independence of ICA results implies that the probability of one event occurring is not affected by a change in the probability of a second event. For the tree ring width series, it means that disturbances detected in growth are not affected by other factors, such as an age effect (A in Equation 2.1) or due to long-term climate changes. Traditionally, eliminating misinterpretations about the causes of growth reductions has been the strength of using non-host growth comparisons. However, when using a secondary host the independence of ICA results allows us to make a strong statement that the disturbance observed is not just due to the difference between host species growth and non-host species growth. Where doubts arise about the choice of the non-host species, ICA should be employed. In other situations, using ICA or the host non-host approach will lead to equivalent results.

2.4.1 Growth Changes

The decreases in growth that we observed may be due to insect defoliation of the non-host species during the outbreak (Figure 2.2), since the peak year in these cases generally occurred the same year or after the peak year of the host species as identified in the original papers. Given that Ponderosa pine is considered to be a secondary host to western spruce budworm and tussock moth, growth reductions are not unreasonable during peak outbreak years. Many papers have reported growth reductions in secondary host species (*e.g.* Muzika & Liebhold, 1999) and discussed the "spill-over" effect of outbreaking insects from primary hosts to secondary hosts species (Sturtevant *et al.*, 2004). Thus in the case where Ponderosa pine is a secondary host of an insect species, its growth decreases could occur in high severity outbreaks. This growth reduction could be more important for secondary hosts since the species may lack the defenses and physiological adaptations that prevent or minimize damage of the attacking herbivore (Oleksyn *et al.*, 1998). Another interpretation, as reported in other papers, is that sudden modification of environmental conditions following canopy disruption (Bouchard, Kneeshaw & Bergeron, 2005) could lead to stresses that cause high mortality for non-host species such as paper birch (*Betula papyrifera*) after outbreaks. Thus, similar effects would not be unreasonable in other species like Ponderosa pine.

On the other hand, periods of increased growth are expected in non-affected species or individuals due to the increase in resources, such as light and water. Growth releases have been used to detect past disturbances (Caron *et al.*, 2009; Nowacki & Abrams, 1997) especially when the disturbance event leads to tree mortality precluding the testing of residual trees for growth depressions. However, some research on the growth of competing plants released by herbivory has not shown a response of non-defoliated plants (Lee & Bazzaz, 1980), but these kind of studies are sparse and conflicting results have been observed (Hamback & Beckerman, 2003). Some studies have suggested that a physiological response to defoliation is the compensation or the enhancement of growth of host species (Edenius & Danell, 1993) that can be important when herbivory is low

(Lee & Bazzaz, 1980). This could, for example, be important in secondary host species or during light infestations, especially in early years.

2.5 CONCLUSION

In this paper, we present the Independent Component Analysis as a new approach for researchers interested in outbreak reconstruction and dealing with the problem of non-host species availability. This method could also be applied to analyze other disturbances affecting ecosystems or to remove disturbance effects from master chronology.

TEST DU SEUIL DE DÉTECTIONS DES TENDANCES CLIMATIQUES DANS LES CERNES DE CROISSANCE

Au cours des chapitres précédents nous avons montré l'utilité de l'analyse, en composants indépendants, appliquée sur les cernes de croissance. Maintenant nous devons montrer que l'application de cette analyse permet de supprimer les écarts de croissance liés aux perturbations et ainsi récupérer la partie liée aux constantes climatiques. Dans le chapitre suivant, on évalue l'importance du climat sur la croissance d'arbres dans un contexte de faible productivité en utilisant de forts gradients de température et précipitations. Nous estimerons également l'impact du cycle solaire ainsi que le niveau de pollution sur cette croissance.

CHAPITRE III

TREE GROWTH, SOLAR FORCING AND CO_2 FERTILIZATION ACROSS HIGH ALTITUDE AND HIGH LATITUDE FORESTS IN ARGENTINA, NEPAL AND RUSSIA

The effects of atmospheric changes on the biosphere are difficult to detect since changes are gradual and occur concurrently with natural climatic variation. In this paper, we investigate tree growth along three contrasting climatic gradients : two altitudinal and one latitudinal. The gradients were located in Nepal, Argentina and Russia. We asked whether the relationship between temperature, precipitation and the solar cycle (as a surrogate for light quantity and quality) and tree growth are stable or not since the onset of the industrial revolution in the early XIXth century. The results show a running correlation of growth with temperature and precipitation that are linked in Nepal and Argentina. During periods when trees are more sensitive to precipitation, they become less sensitive to temperature, and vice versa. No trend was found between the solar cycle and growth, the except for a positive one in Nepal. This positive trend means that changes in solar irradiance have a greater impact on tree growth in this area. The quantities of diffuse light seems to be an explanation for this trend, which is confirmed by the results obtained during the eruption of the Tambora volcano in 1815. In Nepal, due to the proximity of the most densely populated areas in the world in adjacent India, the level of anthropogenic emissions (CO_2, SO_2 and NO_x) in the atmosphere is high, which leads to more diffuse light than in the other areas studied. We discuss the effects of increases of the proportion of diffuse light on tree growth that is caused by

these aerosols. We conclude that it will be difficult to detect a CO_2 effect, since as with diffuse light, aerosols can lead to an increase in the carbon gain by plants. This could explain why there is little consensus in the literature about the effect of the increase in atmospheric CO_2 concentration on tree growth.

3.1 INTRODUCTION

The response of forest growth to climate change and the existence and size of a CO_2 fertilization effect on tree growth is still uncertain. Studies using CO_2 enrichment and tree rings disagree with each other on which ecosystems are sensitive to changes in CO_2(Huang *et al.*, 2007). Studies using in situ CO_2 enrichment seem to predict large initial increases in growth that are not maintained over time (Körner, 2003b; Körner *et al.*, 2005). However, results vary greatly among species (woody and non-woody), and trees seem to be the most influenced by fertilization in the free-air CO_2 enrichment (FACE) project (Ainsworth & Long, 2005). Generalizations to ecosystem level processes are also difficult to make since not many replications of FACE experiments with different stand ages have been made (Karnosky, 2003). FACE studies indicate that CO_2 does not necessarily limit tree growth on the long term since the observed growth increase was usually lower than expected and often transitional (Ainsworth & Long, 2005; Millard, Sommerkorn & Grelet, 2007). Eddy covariance-based research has been used to detect carbon sinks in forests, but analysis of long-term changes in the carbon balance are difficult, due to the large effect of stand age on the forest carbon balance (Magnani *et al.*, 2007, and references therein). Also, eddy covariance is a relatively new technique and cannot explain the fate of the large amount of carbon that has disappeared in the residual terrestrial carbon sink (often call "missing sink" Solomon *et al.*, 2007) since the beginning of the industrial revolution. These meteorological methods provided an extremely insightful but short-term snapshot of forest responses to the environment. Also, many ecological processes are asymptotic and tend to saturate at a high level of limiting variable. Therefore the absence of a CO_2 fertilization effect at 700 ppm does not provide any idea about its possible influences during the increase from the pre-

industrial to present concentrations. Moreover, the growth response is probably also constrained by nitrogen availability (Reich *et al.*, 2006) due to the low mineralization rates, particularly in high elevation and high latitudinal forests (Vitousek & Howarth, 1991; Tamm, 1991).

In this paper, we used an approach based on tree ring width chronologies along three strong and contrasted climatic gradients : two elevation gradients (one in Nepal and one in Argentina) and one latitudinal gradient (from Mongolia to Northern Russia). This gradient design is used to reduce the site effect related with elevation and latitude since no on site data were available for temperature, precipitation and air pollution, or for local non stand replacing disturbances (*e.g.* insect outbreaks ...). As a result, changes observed over the gradient should not be due to local variations at one site but rather to a global change in the region. Moreover, if contrasts within the gradients changes over time, these changed will be more easly interpreted than with a random selection of sites (Ellis & Schneider, 1997).

One well-documented main effect of air pollution is the reduction of the quantity of light reaching the ground due to the reflection of solar radiations by aerosols. However, as the proportion of diffuse light increases, the penetration and availability of light beneath a plant canopy might actually increase (Ramanathan *et al.*, 2001; Roderick *et al.*, 2001). Diffuse irradiance penetrates more evenly than direct solar irradiance into canopies (Sinclair, Shiraiwa & Hammer, 1992). As a result the photosynthetic production of shaded leaves increases and may enhance the photosynthetic production of the plant canopy(Stanhill & Cohen, 2001; Gu *et al.*, 2003). Moreover, growth models seem to corroborate these expectations (Cohan *et al.*, 2002; Mercado *et al.*, 2009). The ratio of the diffuse irradiance to direct irradiance is closely correlated with global irradiation. According to (Roderick, 2006) the highest rates of photosynthesis are reached at intermediate levels of diffuse to direct radiation since high ratios are usually associated with low irradiance. Another variable that interacts with the availability of irradiance is the solar cycle. It is recognized that the solar cycle can affect tree growth (Douglass, 1927), and recent studies using more advanced statistical analysis have confirmed this (Rigozo

et al., 2003, 2007; Dengel, Aeby & Grace, 2009). If the correlation between solar cycle and growth change exists, it could be modified due to increases in diffuse radiation and other mechanisms linked to the presence of aerosols.

Here, the solar cycle is defined as the total solar irradiance (TSI) arriving at the surface of the atmosphere, or the sun spots, but with an unvarying amplitude since TSI does not vary in amplitude from cycle to cycle (Foukal *et al.*, 2006). Even though the amount of these TSI changes are small (1–2%), they apply to the TSI, not to the UV part that undergoes 32% change between the maxima and minima of the solar cycle (Lean, 1989). These UV having large implications for stratospheric ozone (Haigh, 1996; Hood, 1997), infrared radiative forcing (Haigh, 1994), production of aerosols (Dickinson, 1975; Yu, 2002) and tropospheric climate (Shindell *et al.*, 1999; Reid, 2000) that could lead to a stronger response of trees to the solar cycle by combined effects. Moreover, the quantity of aerosols can also amplify the importance of the solar cycle for tree growth. This indirect solar contribution could either decrease or increase cloudiness (Ramanathan *et al.*, 2001; Ackerman *et al.*, 2000) leading to more or less diffuse light. This paper bases its tree ring analysis on a blind source separation technique derived from signal processing and applied for the first time on tree ring width series in Chapters I and II.

The objective of the paper is determine if (1) an effect of solar irradiance on tree growth is detectable and (2) to detect if the responses of trees to climatic factors are modulated by the sunspot cycle and long term environmental changes.

3.2 DATA

Data were selected either along elevation gradients (with sites being located as close to each other as possible) or along a latitudinal gradient (with sites being located approximately at the same longitude). We wanted two altitudinal gradients with differences in precipitation, one being relatively dryer than the second one. Potential differences in air pollution being a plus. For the latitudinal gradient, we wanted a large homogeneous region with sufficient data. We selected Argentina and Nepal for the altitudinal gradi-

ents and Siberia (Russia and Mongolia) for the latitudinal gradient. Argentina being relatively dry compared to Nepal since they are on two different mountainside considering wind and clouds origin, and the higher pollution levels due to air pollution context also being potentially different since Nepal could suffer from its proximity with high population density areas of India.

The raw tree ring width series was obtained from the International Tree-Ring Data Bank (http ://www.ncdc.noaa.gov/paleo/treering.html, last accessed on 09/07/2009). We selected all tree ring chronologies that were present in the ITRDB matching these requirements : raw data (Measurements only), ending time at least between 1980-1990, no archaeological data or dead trees and if possible data collected for climatic reconstruction. Amongst these sites, we selected those sites forming an uniform site distribution along the gradient.

We obtained 31 sites in Argentina, 18 sites in Nepal and 20 sites in Russia and Mongolia (Table 3.1 and mapped in Appendix B). The average number of individual tree ring series per site is 29. Tree species are different on each gradient and vary sometimes from one site to another (Table 3.1).

The elevation gradients range from 1,320 to 3,600 meters in Nepal, and from 15 to 2,800 meters in Argentina. The latitudinal gradient ranges from 47^o to 73^o N with high-altitude (2000 m) sites dominating in the south (Mongolia) and low altitude sites in the north, which leads to homogeneous temperatures across this gradient. See Appendix B for sites maps.

Temperature and precipitation series have been derived from a grid of climate data made available by the International Research Institute for Climate and Society (IRI at http ://iridl.ldeo.columbia.edu/docfind/databrief/cat-atmos.html, last accessed on 09/07/2009). The temperature grid (NOAA NCDC GCPS Monthly Gridded; Eischeid *et al.*, 1995) is a cell of 5^o latitude by 5^o longitude from January 1851 to December 1993, and the precipitation grid (UEA CRU Global; Hulme, 1992, 1994) is 2.5 per 3.75^o cells from January 1900 to December 1996. These data were selected for their large temporal

Tableau 3.1 Tree ring width data summary. For each studied region, # site gives the number of sites used, # tree the average number of trees per site, Length the average tree ring width series length in years, % growth the average remaining proportion of growth after ICA and Species list all species with data in the considered region.

Region	# sites	# trees	Length	% growth	Species
Argentina	31	30	255	95	araucaria, cedar, cypress, nothofagus, walnut
Nepal	18	28	243	94	fir, hemlock, poplar, pine, juniper, spruce
Russia and Mongolia	20	29	254	96	larch, spruce, pine

coverage. Sunspot data are from the National Oceanic and Atmospheric Administration (NOAA). Atmospheric pollution was assessed by the aerosol optical depth given by the AErosol RObotic NETwork Project (NASA; Holben *et al.*, 2001).

3.3 METHODS

Our statistical analysis proceeded in three stages : (1) We extracted climate related growth components from the tree ring width series; (2) we used running correlations to establish environment climate relationships; and (3) we analyzed systematic changes in these environment climate relationships. The first step was done using Independent Component Analysis (ICA) on raw tree ring width series for each site separately. ICA is a signal processing blind source separation method (Cardoso, 1989; Comon, 1994) that has been used various fields, such as neural activity signals (Vigário *et al.*, 1998) and seismology (Ham & Faour, 1999). It seems to be suitable to separate climate and different disturbance signals in tree ring series (Chapter I and II). The purpose of

ICA is to separate the source signals by seeking a rotation of spherical data, which have independent coordinates (Hyvärinen, Karhunen & Oja, 2001; Stone, 2004). This independence means that ICA minimizes the mutual information between components. As shown in Chapter I and II, this decomposition of the original data can be interpreted within the linear aggregated conceptual tree ring model proposed by Cook (1987); Cook & Kairiukstis (1990) : This model decomposes each tree ring series into a climatic, a disturbance, an age and an error component. The ICA was carried out using the FastICA algorithm (Himberg & Hyvärinen, 2001) under R (R Development Core Team, 2009). Previous work (Chapter I) has shown that the main utility of ICA result is the separation of all disturbance effects from the basal growth, which will be called an environmental related independent component (abbreviated here as ICE). These disturbance patterns, such as insect outbreaks, diseases, etc., would have otherwise masked an important portion of the climate effects on tree growth. Next, in order to identify and ensure that one of the extracted independent components is an ICE, a distribution of series values, autocorrelation function and spectral analysis were performed. All subsequent analysis (correlation with climate and solar activity) were done only on this ICE. The main characteristic of an ICE is that it has a low kurtosis shape (from 2 to 4) compared with disturbance-related independent components, which are spiky or high pitched with a kurtosis higher than 4. The autocorrelation function (ACF) provides information about trends, and spectrum analysis identifies periodicity in the series. Moreover, we checked whether ICE contained white noise, which is described as a Gaussian distribution (mean of zero and standard deviation of four) or a uniformly distributed, following the method proposed by Lobato & Velasco (2004). The ICA is not able to determine the variance explained by the ICE. We have tried to approach this statistic through the percentage of the mean tree growth series (MTGS) contained within the ICE. Since the ICA centers and normalizes series, we have also centered and normalized MTGS. Next, the % of growth explained by the ICE was determined by random selection of 50 years of growth and their comparison to the measured values as in Chapter I. In the second step, we have calculated a running correlation with a running window length of 11 years between the ICE and the solar cycle, temperature and precipitation. This method is widely used

in dendrochronological climate research (D'Arrigo *et al.*, 2008; Pauling, Luterbacher & Casty, 2006) to investigate the stability of these types of relationships. We simply compute the linear correlation inside a window, which is moved along the time series. The 11-year size of the window permitted to capture a full solar cycle. Moreover, data for the temperature also shows an 11-year cycle, and the precipitation data shows a five-year cycle (*e.g.* Appendix C). Correlations made this way are not affected by any long-term growth (Lorimer & Frelich, 1989; Payette, Filion & Delwaide, 1990) or climatic trends present in the input data. They can, however, detect changes in the relations between environmental factors and growth (Nowacki & Abrams, 1997). As a preliminary analysis, we checked the differences in the influence between monthly and yearly values of the three environmental variables that will be used (solar cycle, temperature and precipitation). It appeared that monthly values were not well-suited for this study since different months affect growth in varying ways at different locations along the same gradient. Therefore, an analysis based on yearly values was considered to be more robust.

A major problem with running correlation is that, locally trends can be present for each variable in the defined window. This often leads to spurious regression. The problem is even larger when the data is cyclic. With trends in both dependent and independent variables t and F statistics are altered, and the correlation coefficient is overestimated. In the field of econometrics, Granger (1969) introduced the concept of co-integration to deal with this problem. The aim of co-integration is to detect a stable long-run relationship among non-stationary variables. If two series are co-integrated, then a stationary vector exists between these variables. In this paper, we test whether the series are co-integrated, because if such a co-integration exists, at least one of the series must "Granger cause". The Engle-Granger (Engle & Granger, 1987) two-step estimation of co-integration is performed between ICE and the solar cycle, temperature and precipitation. The first step tests the unit root and the second step estimates an error correction model. De-trending has to be performed before the second step of the analysis can be done. In this case, we took the differential of the series. When spurious correlation is not encountered, we averaged site results to obtain a single result for each region.

3.4 RESULTS

3.4.1 Independent Component Analysis

We analyzed data from each site using the components, extracted by the ICA, which appear to record variations in the environment (ICE). As explained in the methods section, to ensure that these components are possibly related to the environment, an autocorrelation analysis and a spectral analysis were performed. All extracted ICEs were cyclical with a cycle length ranging from 7 to 13 years. The most common cycle length was 11 years (*e.g.* Appendix C). Other superimposed cycles were detected, but the 11-year cycle was usually the most common one. Moreover, the ICEs represented an average 95% of the original growth of the MTGS (Table 3.1).

3.4.2 Running correlations

A running correlation was made with an 11-year lag between the selected ICE and environmental variables. This correlation involved the ICE and each environmental variable (sunspots, temperature and precipitation). As explained in the Methods section, running correlations are prone to spurious correlation. We used the Engle-Granger co-integration test to evaluate the significance of the correlation. Table 3.2 provides the results of this test. They differed greatly among region, but, for ICE and solar cycle correlations, $\approx$70% (50/69) of them are significant and are generally bi-directional. This means that each series changed direction simultaneously, leading to, a priori, both Granger causing the other. This issue will be fully discussed in the next section. Noise was also tested using two different kinds of distributions. No ICEs had a uniform distribution of their values, whereas white noise appeared only in four (4) Nepalese sites out of 18, half of Russian sites were "noisy" (11 out of 20), and in Argentina 14 out of 31 sites were "noisy". However, results for the average running correlation in these regions are slightly affected (Figure 3.2). For example, the resulting time series without noisy ICEs for sun spots does not differ from the averaging of all series. Overall, the presence of noise partially concealed the cyclical pattern, but the overall trend was not affected (Table 3.3).

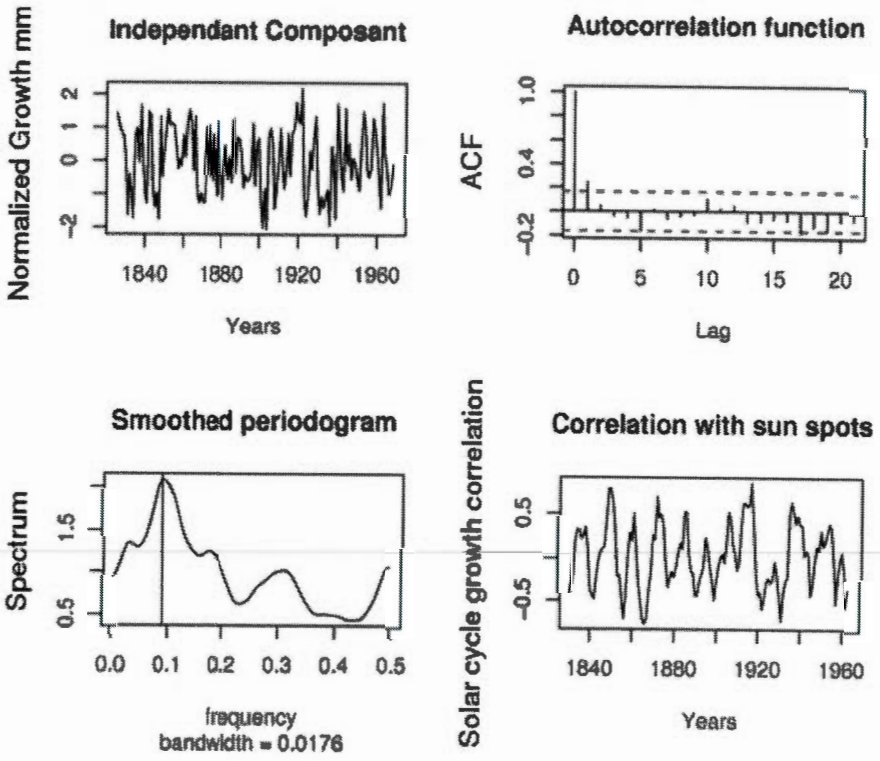

Figure 3.1 Autocorrelation function, spectrum analysis and solar cycle correlation with growth of an extracted environmental component from a Russian site

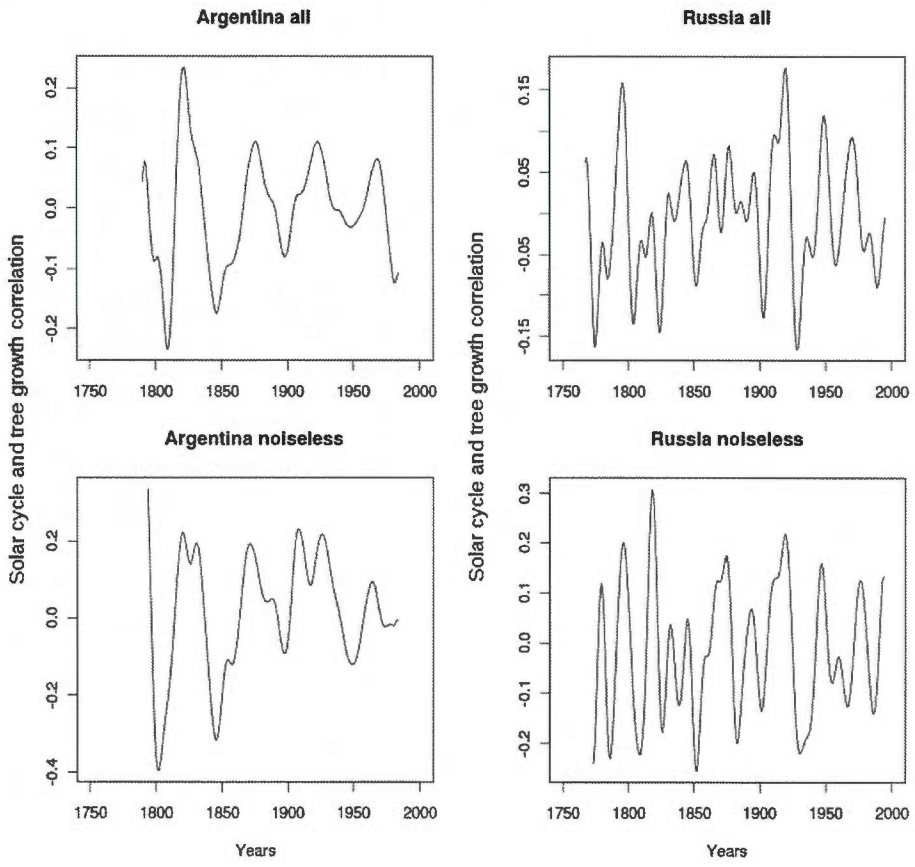

Figure 3.2 Solar cycle correlation with noisy and noiseless tree growth data from 1780 to 1990 in Argentina and Siberia

Tableau 3.2 Cointegration test and Granger causation results between tree growth (G) and the solar cycle (S), temperature (T) and precipitation (P). This table display the number of series with significant cointegration result ($p < 0.05$) per region, NA stands for the absence of results. Arrows show the Granger causality direction between the express variables. For example in G and S, -> means that tree growth Granger cause solar cycle, <- means that solar cycle Granger cause tree growth and <-> implies a bi-directional Granger causality.

	G and S			G and T			G and P		
	->	<-	<->	->	<-	<->	->	<-	<->
Argentina	NA	NA	31	NA	NA	25	NA	3	6
Nepal	NA	NA	18	2	NA	4	NA	NA	2
Russia	NA	NA	1	NA	NA	NA	NA	NA	NA

It should be noted that a regional averaging of the resulting correlation coefficients of all series, maintained the periodicity patterns detected by the spectrum analysis (*e.g.* Russian results or the correlation between ring width and sun spots in figure 3.2).

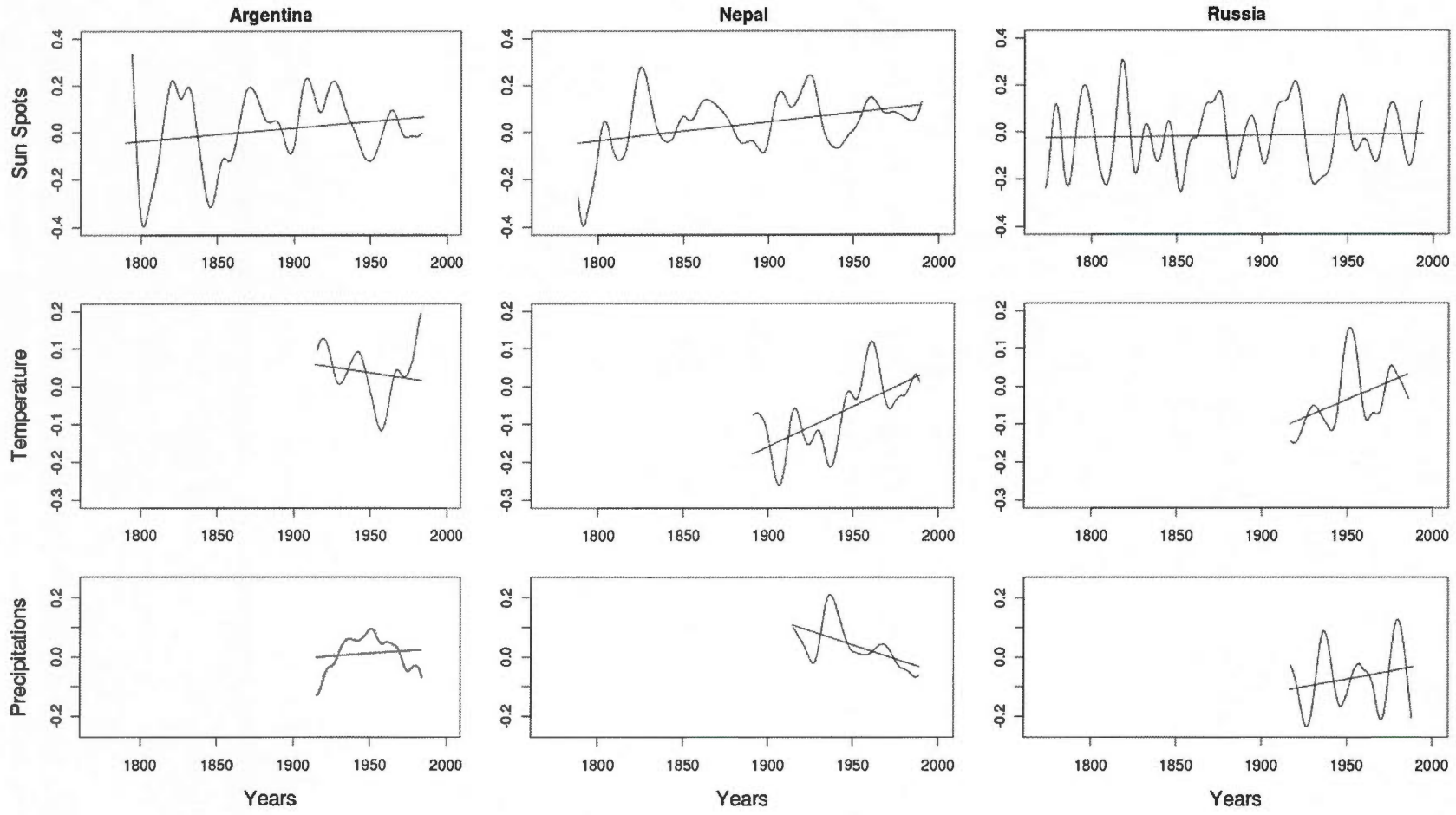

Figure 3.3 Correlation of temperature, precipitation and solar cycle with tree growth from 1750 to 2000 along two altitudinal and one latitudinal gradients in Nepal, Argentina and Siberia. The strait line represent the calculated trend of the plotted data.

For the elevation gradient in Nepal, correlations of tree ring width with temperature and precipitation were of opposite signs and changed systematically with time and their slopes were significantly different from 0 (Table 3.3). They tended to cancel each other : while the correlation of the ICE with temperature increased by 2.1 10^{-3} per year, the correlation with precipitation decreased by 1.9 10^{-3} per year (Table 3.3). Temperature was always negatively correlated with tree growth, while the relationship with precipitation was positive until the 80s. As well, the cross-correlation functions between these variables (results not shown) did not indicate any interaction. Plus a positive and significant trend (Table 3.3) exists for the ICE relationship with the sunspot index in Nepal. This slope was very steep from 1800 to 1850, and then slowed down. Moreover, we found that some bumps in correlations corresponded to major volcanic eruptions. The biggest bump observed for the 1815–1825 period corresponds with the Tambora (Lesser Sunda Islands, Indonesia) eruption of 1815 (Figure 3.4), the major event of the last millennium (Smithsonian Global Volcanism Program Web site, last accessed 15 July 2010).

Temperature was positively correlated to the ICE in Argentina, but the strength of the correlation decreases over time. For precipitation, the correlation with the ICE was positive from 1930 onward and increases. These two bell-shaped trends compensate each other (Figure 3.3). The relationship between sunspot indices and change in growth as indicated by a small long-term positive and significant temporal trend in the correlation (Table 3.3), which follows the trend observed in Nepal.

In Russia, the correlation of growth with temperature and precipitation are both increasing over time. This correlation with temperature has been generally positive since 1900, but, for precipitation, the correlation shifted recently from a negative to a positive one. No long-term correlations change with sunspot indices was found. However, short-term periodic changes are observed with 11-year cyclicity.

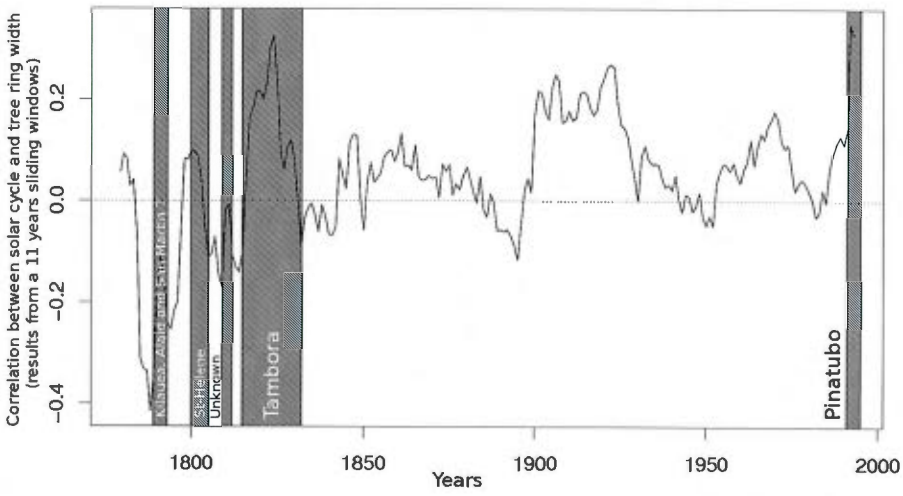

Figure 3.4 Volcanic events affecting the correlation between solar cycle and growth in Nepal. Grey boxes refers to volcanic eruption which are named by volcano based on the Smithsonian Global Volcanism Program data, and their width refers to the length of the disturbance recorded in the tree ring and "?" indicates an uncertainty.

Tableau 3.3 Student's t-test results concerning the slope of the linear regression made on regional estimated correlation between the independent component of interest and the considered variable. * indicates significant results.

Location	Variable	Slope	Std. Error	t value	Pr(>| t |)
Nepal	Sun	0.0007973	0.0001378	5.787	2.72e-08 *
	Temperature	0.0021117	0.0002456	8.598	1.42e-13 *
	Precipitation	-0.0019020	0.0003103	-6.130	4.08e-08 *
Argentina	Sun	0.0005636	0.0001975	2.853	0.00481 *
	Temperature	-0.0005802	0.0004273	-1.358	0.179
	Precipitation	0.0003807	0.0003403	1.119	0.267
Siberia	Sun	7.544e-05	1.353e-04	0.558	0.578
	Temperature	0.0019153	0.0004229	4.529	2.45e-05 *
	Precipitation	0.0010446	0.0005458	1.914	0.0597

3.5 DISCUSSION

3.5.1 Independent Component Analysis

This is the first time that independent component analysis methods were applied to tree ring in a geophysical context. The main interest in this paper was to separate the effects of non-climatic variables and disturbances from tree growth. The common use of ICA is spike detection (Hyvärinen, Karhunen & Oja, 2001), we however just kept a non-peaky component in order to evaluate tree growth without disturbance effects. Selection of the ICE among the independent components was usually not very difficult (see chapter Chapter I and II). As reported in Table 3.1, 95% of the mean growth remain in the ICE. The 5% that was removed is due to spikes and attributed to disturbances. However, we were not able to confirm this, since site disturbance histories are not available. Another important aspect of the recovered components is that they are statistically independent. This means that the extracted components do not affect other components. Practically it means that we can analyse each component individually and ignore the others.

3.5.2 Granger Causality and Running Correlation Robustness

The Granger causality has been previously used with climatic data (Kaufmann & Stern, 1997). However, this method has been highly criticized (Triacca, 2001, 2005), because it was applied to data as a final analysis instead of with the goal of ensuring that spurious correlations were not found as we did in this paper. Seventy percent (70%) of the co-integration tests between solar activity and the independent components related to the environment (ICE) are significant. The same test is less convincing for temperature and precipitation. This may be due to the presence of a trend in the series, because trend removing can be difficult, and we do not know up to which point we have to de-trend (Wu *et al.*, 2007). In this study, we have just made a differential in order to remove the trend. Carbohydrate reserves that buffer growth responses to climatic variations and allow the growth to respond over prolonged time periods can also explain why temperature and precipitation relationships are less convincing.

Moreover, causality is nearly always bi-directional. Statistically, a bi-directional causality means that there is "feedback" between the two variables or that the two variables change nearly at the same time. However, the speed of adjustment is not the same, and it is always faster for the direction : sunspot indices Granger cause growth (*c.f.* Appendix D). In other words, when the solar cycle changes, growth adjusts faster than in the other direction. The explanation of bi-directionality is simply the fact that we are in the presence of two annual variables that are highly related without lags, and there is no direct way of inferring causal relationships. As well, noise does not sidestep this issue.

We also have some indirect evidence that the correlation is not spurious based on the anomalies found (for exemple in figure 3.4) related to volcanic eruptions (Mount Tambora), which follow the re-analysis of tree ring data from Mann, Bradley & Hughes (1998) by Robock (2005). Tree ring based temperature reconstruction is heavily biased (underestimated) during volcanic events due to diffuse light Robock (2005).

3.5.3 Regional Estimate and Pollution Effect

We observed that the strength of the correlation between tree ring width and the solar cycle changes in the altitudinal gradients of Nepal and Argentina, but not in the latitudinal gradient from Mongolia to Russia (Table 3.3). These trends are not likely to be to the result of an indirect effect of temperature and precipitation since the correlation of these two variables with growth have an exact opposite slope. Moreover, as shown by Foukal *et al.* (2006), total solar irradiance (TSI) did not change in amplitude from solar cycle to cycle, which permitted us to perform the same analysis with TSI reconstruction using sunspot indices. The results were exactly identical.

Thus the solar activity cannot cause the observed trend directly. Even though the energy gain is just 2 W/m^2 between the maximum and minimum of one cycle (Foukal *et al.*, 2006), amplification factors are likely to enhance this role. We argue that only a change in the atmosphere during the considered period can cause this trend. If this would be an effect of the increase in atmospheric CO_2 concentration, responses of trees everywhere around the globe would be similar, since the increase in CO_2 atmospheric concentration is global. However, no trend was observed in Russia, whereas the slope of the correlation in Nepal (7.9 10^-4) was nearly twice the slope observed in Argentina (5.6 10^-4). Moreover, values after 1950 in Nepal were far higher than those observed in Argentina. We argue that only local atmospheric changes such as high levels of atmospheric pollution could create the trend we observe in Nepal and Argentina. Particularly in Nepal due to the proximity of India and its most populated province (*c.f.* Kanpur data in Table 3.4). We argue that light scattering by atmospheric particles can explain this constant increase of the correlation with solar radiation, especially in a region subject to high pollution levels. Tree growth will increase by a higher proportion of diffuse light (Stanhill & Cohen, 2001; Gu *et al.*, 2003) and the general trend will follow increases in anthropogenic releases. Nitrogen can also be seen as a possible explanation. However, nitrogen inputs into the terrestrial biosphere increased only after ~1950 due to automobile traffic and fertilizer inputs, whereas we found a change starting at the

beginning of the XIXth century. Here again, volcanic eruptions also offer arguments in favor of a diffuse light effect : in 1815 (Figure 3.3), the correlation with solar cycle increased abruptly, and arrived at a summit in 1820, which corresponded to the eruption of the Tambora volcano. This eruption is known to cause some anomalies in temperature reconstruction based on tree rings (Robock, 2005, based on Mann, Bradley & Hughes (1998) reconstruction). Tree rings give a temperature anomaly of -0.1°C compared with -0.65°C with other proxy methods. This difference is attributed to an increase in growth due to diffuse light (Robock, 2005). The results show that light scattering effect were substantial for tree growth in more polluted areas. In Nepal and Argentina, solar cycle results (Figure 3.3) show some oscillations varying in amplitude : from the beginning of the XIXth century until 1960, oscillations were very wide. Then they slowed down and oscillated between 0 and 0.2, following the global change of atmospheric transparency (Romanou *et al.*, 2007). The amount of diffuse light has driven tree growth to become less and less sensitive to change in irradiance with a general gradual increase in carbon assimilation. Whereas in Siberia, with low pollution levels, the oscillations seem to remain more constant. Consequently, it can be very difficult in these polluted regions to separate the effects of light scattering from those of CO_2 enrichment, both leading to an increase in the carbon sink. This results can explain why there is little consensus and uncertainty on the effect of CO_2 on tree growth (Schimel *et al.*, 2001; Joos, Prentice & House, 2002). Numerous models indicating a significant reduction in the forest carbon sink during the last years of the XXth century (Falkowski *et al.*, 2000; Hurtt *et al.*, 2002) and enrichment-based studies show little or no long term effects of increased atmospheric CO_2 effect on tree growth (Körner, 2003b; Körner *et al.*, 2005). Recent "brightening" observed locally (Wild *et al.*, 2005; Wild, Ohmura & Makowski, 2007) has surely confused the issue even more.

3.5.4 Light and Temperature Limitation in Northern Forest

In Figure 3.3, the results of Russia show a clean periodic pattern. In our view, this result indicates that light or at least the energy induced by light seems to be a limiting factor

Tableau 3.4 Aerosol optical depth (AOD) daily average. AOD is given for 7 different wavelength and is a measure of how much airborne particles prevent light from passing through a column of atmosphere. A low AOD (less than 0.1) indicates a crystal clear sky with maximum visibility, whereas values greater than 1.0 indicate dust or smoke with very low visibility. Data are at Level 2.0 (cloud screened and quality-assured) and values give the daily AOD average for the whole period of measurement ranging from 1998 to 2007 depending on location. The 4 first locations provide reference values. One very clear site, the Amsterdam Island (situated in the Indian ocean at 77.573^o east and -37.810^o south) and three important cities : Beijing, Los Angeles at UCLA and Mexico City. Other columns give values of the nearest location available in the database for the gradient used in this study. Kanpur is the nearest big city in India for the Nepalese gradient (400km to the nearest site). Tomsk, Krasnoyarsk indicate values for Siberia and Ulaangom for Mongolia. Cordoba gives values for the Argentinian gradient and Santiago give an idea of Andes other slope.

Wavelength	Amsterdam Island (Indian Ocean)	Beijin	UCLA	Mexico city	Kanpur
1020	0.074	0.377	0.077	0.123	0.336
870	0.074	0.442	0.089	0.159	0.378
675	0.075	0.578	0.115	0.230	0.464
500	0.078	0.824	0.162	0.367	0.596
440	0.084	0.869	0.186	0.434	0.653
380	0.092	0.978	0.217	0.522	0.736
340	0.098	1.048	0.289	0.592	0.800
Wavelength	Tomsk	Krasnoyarsk	Ulaangom	Cordoba	Santiago
1020	0.070	0.078	0.085	0.049	0.057
870	0.080	0.087	0.077	0.059	0.075
675	0.107	0.124	0.109	0.073	0.102
500	0.167	0.172	0.157	0.108	0.160
440	0.200	0.198	0.196	0.125	0.192
380	0.236	0.233	0.256	0.152	0.239
340	0.265	0.271	0.280	0.175	0.273

in the region. The justification of this conclusion lies in the fact that, in order to obtain a perfect signal, the noise has to be very low. If light is the limiting factor, then other environmental conditions play only a minor role in growth and will generate only a little noise in the correlation with the solar signal. This can be strange conclusion, since, in the boreal forest, nitrogen has historically been regarded as the limiting factor (Vitousek & Howarth, 1991). However, nitrogen deposition due to anthropogenic activities has dramatically increased since the 60's (Galloway & Cowling, 2002). The link between low temperatures and the low energy provided by light rays at these latitudes can be the answer. Photosynthetic capacity has been identified depending on low temperatures (Linder & Flower-Ellis, 1992; McMurtrie *et al.*, 1994; Makela *et al.*, 2004) for boreal trees, which can explain our results. Altitudinal and boreal ecosystem productivity is mainly limited by temperature (Körner, 1999). Temperature limitation is due to (1) a 6 to 7°C limit for cell formation (Grace, 1989; Körner, 2003a) and (2) the strong relationship between temperature and decomposition (Burke *et al.*, 2003; Jenkinson & Coleman, 2008). This increase in solar radiation, even if the energy gain is just 2 W/m^2 between the maximum and minimum of one cycle (Foukal *et al.*, 2006), can affect the photo-synthetically active period (Gea-Izquierdo *et al.*, 2010), the threshold of cell formation and increase decomposition, which makes trees in these ecosystems sensitive to solar cycle.

ACKNOWLEDGMENTS

We would like to thanks all the contributors of the International tree ring databank : N. Baatarbileg , A. Bhattacharyya, J. Boninsegna, B. Buckley, O. Byambasuren, E. Cook, R. D'Arrigo, N. Davi, D. Frank, R. Holmes, G.C. Jacoby, J. Keegan, P.J. Krusic, G. Lazzarini, N. Lovelius, N. Pederson, N. Raj Khanal, F. Roig Junent, F. Schweingruber, O. Shumilov, R. Villalba, R. Zuber and many others. We also thank B. Holben, J. Sciare, P. Goloub, C. Hong-Bin, L. Kuo-Nan, A. Leyva Contreras, M. Panchenko and their staff for establishing and maintaining the 10 sites of the AERONET project used in this investigation.

POSSIBILITÉ D'UN EFFET DE L'ASSOMBRISSEMENT GLOBAL SUR LA CROISSANCE DES ARBRES

Les résultats du chapitre précédent pour les données du Népal nous ont laissé croire que la pollution atmosphérique pouvait affecter la croissance. Par pollution atmosphérique on entend la diminution de la lumière directe à cause des particules émises lors de l'utilisation des combustibles fossiles. En effet, depuis le début de l'ère industrielle on estime que nous avons perdu plus de 20% de lumière directe, mais gagné de la lumière diffuse. Cette lumière diffuse pourrait augmenter la croissance des arbres en stimulant la photosynthèse du feuillage situé dans la canopée. Ce chapitre évalue cette possibilité en utilisant des données mondiales de croissance d'arbres et en s'appuyant sur le réseau de stations de pollution atmosphérique, mis en place par la N.A.S.A.

CHAPITRE IV

THE INFLUENCE OF ATMOSPHERIC TRANSPARENCY ON TREE GROWTH VARIES ACROSS ECOSYSTEMS

Short-term variations in atmospheric transparency, such as those due to volcanic eruptions, are known to affect ecosystem function and productivity. However, only scant information is available on long-term ecological effects due to changes in atmospheric transparency, particularly for the recent decrease in transparency due to anthropogenic aerosol emissions (the so-called "global dimming"). Our goal is to evaluate these effects on tree growth across forest ecosystems worldwide. We present results for 841 tree ring sites selected across the globe and representing four major ecosystems : Mediterranean and sub-arid, temperate, boreal, and high elevation and mountainous areas. These sites were within either 50 or 150 km of aerosol optical depth (AOD) stations (67 and 183 stations respectively). These stations give a snapshot of the global dimming and the regional air pollution at the location. Results show that atmospheric transparency had a significant influence on the relationship between solar irradiance and tree growth : their decrease increased the negative impact of solar irradiance on growth during most of the XXth century. This influence was present for Mediterranean and sub-arid, temperate and high elevation ecosystems for sites within 50 km of AOD stations. For sites within 150 km, the relationship remains for the Mediterranean and sub-arid ecosystems, and was still present but weaker for high elevation ecosystems. Atmospheric transparency influence on the relationship between growth and solar irradiance increased constantly and became positive in the 60s-70s. Decreases in atmospheric transparency involved less

radiation for photosynthesis, but also involved a higher fraction of diffuse over direct irradiance. Overall, plant photosynthesis in complex, multilayer canopies can benefit from the increased diffuse irradiance associated with global dimming. Our results reveal that this positive effect of global dimming is significant only for those ecosystems that have irregular precipitations and a pronounced dry season (*i.e.*, Mediterranean and sub-arid ecosystems). We propose that this growth enhancement is due to a decrease in leaf overheating, photo-inhibition and water stress in the sun parts of the foliage, and to an increase in productivity under increased diffuse light in shaded leaves. These findings have major implications for modeling forest responses to anthropogenic changes in the atmosphere, the impacts of which vary across ecosystems depending on other factors beyond irradiance such as water availability and temperature.

4.1 INTRODUCTION

Solar radiation is scattered in the atmosphere during clear sky days by anthropogenic and naturally emitted particles resulting in a decrease in direct irradiance and an increase in diffuse irradiance (Dutton & Bodhaine, 2001; Robock, 2000, 2005). During the last fifty years the quantity of anthropogenic aerosols has been increasing, resulting in a decrease in the global and direct irradiance and an increase in the amount and proportion of diffuse radiation. This phenomena has been well documented in different parts of the globe ("global dimming" ; Stanhill & Cohen, 2001; Ramanathan *et al.*, 2001). Although, a recent reverse trend has been also documented for some regions ("brightening" ; Pinker, Zhang & Dutton, 2005; Wild *et al.*, 2005; Wild, Ohmura & Makowski, 2007), model simulations indicate that the atmospheric transparency has decreased gradually since 1850 (Romanou *et al.*, 2007). According to Romanou *et al.* (2007) aerosols were the main causes for the long-term decline, while variations in cloudiness cause much of the short-term variations. Despite its potentially large impact on ecosystem productivity, this change in light quality and quantity has received the attention of ecologists only recently (Ramanathan *et al.*, 2001; Roderick *et al.*, 2001; Roderick & Farquhar, 2002). Changes in irradiance might affect ecosystem functioning directly

through changes in photosynthetic production and indirectly through changes in temperature and precipitation. For example, a global decrease pan evaporation as described by (Peterson, Golubev & Groisman, 1995), have been associated to the global dimming (Chattopadhyay & Hulme, 1997; Roderick & Farquhar, 2002; Hobbins, Ramírez & Brown, 2004; Wild *et al.*, 2004). Moreover, it has been argued that global dimming may enhance plant productivity, in general, and tree growth in particular (Roderick *et al.*, 2001; Gu *et al.*, 2002; Roderick, 2006). This counter-intuitive effect, confirmed by plant growth models (Cohan *et al.*, 2002; Mercado *et al.*, 2009), would be a consequence of an increase in the photosynthetic production due to an increase in the amount of diffuse light in complex canopies. Changes in photosynthesis and for the carbon cycle reported following the Pinatubo eruption have also shown this productivity enhancement (Farquhar & Roderick, 2003). After the massive increases in light scattering aerosols, Gu *et al.* (2003) found an increase in photosynthesis at local scales. Moreover, a re-analysis of the work of Mann, Bradley & Hughes (1998), Robock (2005) shows that tree rings always underestimate temperature when used as a proxy for temperature reconstruction during volcanic events. Thus we can attribute this difference in reconstruction to an increase in diffuse irradiance.

A way of improving our understanding of globally changing ecosystem processes is by analyzing tree growth, which can be viewed as the result of all the environmental variables influence. In this regard, tree rings offer a unique opportunity (Carrer & Urbinati, 2006; Jump, Hunt & Penuelas, 2006). For instance, tree rings can be useful in irradiance studies since they have been reported to respond to changes in the solar cycle (Rigozo *et al.*, 2003, 2007), and Dengel, Aeby & Grace (2009) reported a direct relationship between galactic cosmic radiation and tree rings. A decrease in atmospheric transparency leads to a decrease in direct irradiance and an increase in the proportion (and usually also the amount) of diffuse irradiance (Robock, 2000; Dutton & Bodhaine, 2001). Diffuse irradiance penetrates more evenly inside plant canopies. As proposed by the model of Roderick (2006), this effect potentially increases the sensitivity of tree photosynthesis and growth to solar irradiance changes. We hypothesized that the cor-

relation between irradiance and tree growth will be increased by diffuse irradiance. We further hypothesized that it should vary across ecosystems, due to differences of growth limiting factors for their nature and intensity, such as water and temperature. In this paper, we investigated the stability of relationships between irradiance and tree ring width series from 841 sites around the globe with different atmospheric optical depth (AOD). These sites were located near stations recording AOD from the aerosol robotic network project (Holben *et al.*, 2001).

4.2 MATERIAL AND METHODS

4.2.1 Data

Atmospheric pollution has been assessed by the optical depth given by the aerosol robotic network project (Holben *et al.*, 2001) stations. Aerosol optical depth (AOD) is given for seven (7) different wavelengths (1020, 870, 675, 500, 440, 380 and 340 nm) and is a measurement of how much light airborne particles prevent from passing through a column of atmosphere. A low AOD (less than 0.1) indicates a very clear sky with maximum visibility, whereas values greater than 1.0 often indicate dust or smoke with very low visibility. Data are cloud screened and values give the daily AOD average for the whole period of measurement ranging from 1998 to 2007, depending on the location. AOD data are lacking before 1998. However models (Romanou *et al.*, 2007; Solomon *et al.*, 2007) indicate a gradual linear and global change in irradiance at the surface level, except some local increases found since 1990 (Wild *et al.*, 2005; Wild, Ohmura & Makowski, 2007). Thus, AOD values recorded during the 1998–2007 period can be used in a global analysis context. For the analysis, only wavelengths in the photosynthetic active radiations (PAR) have been used : 675 and 440 nm (500 nm was not used due to missing values and 380 nm is outside the PAR). Raw tree ring width (TRW) series have been obtained from the international tree-ring data bank (NOAA). We selected all available TRW site within a distance of 50 and 150 km from the AOD stations. The number of records per year in a TRW site varies (different age, or dead tree), years and

trees with missing values were removed to maximize the length (years) of the each site data. All data have been extracted from their original data base during the winter of 2007–2008. These data were mostly collected for climatic reconstruction. After selection, 197 AOD stations remain with at least one TRW site within 150 km, and 81 with at least one within 50 km. We found 1,074 TRW sites with an average of four (4) TRW sites within 50 km of an AOD station, and an average of 13 sites within 150 km. Each TRW site consisted of tree ring series for 10 to 50 trees with a segment length of at least 40 years of growth. The last tree ring was usually between 1970 and 2006. From the 1,074 TRW sites available, 842 were suitable for ICA analysis (sites were removed due to too many missing values and/or too few trees), which permitted to have enough data for 66 AOD stations at 50 km and 179 AOD stations at 150 km for a time period ranging from 1700 to 2006 (Figure 4.1). However, 95% of the data were available for the 1933–1954 period (Appendix E), a percentage that decreases quickly after 1960.

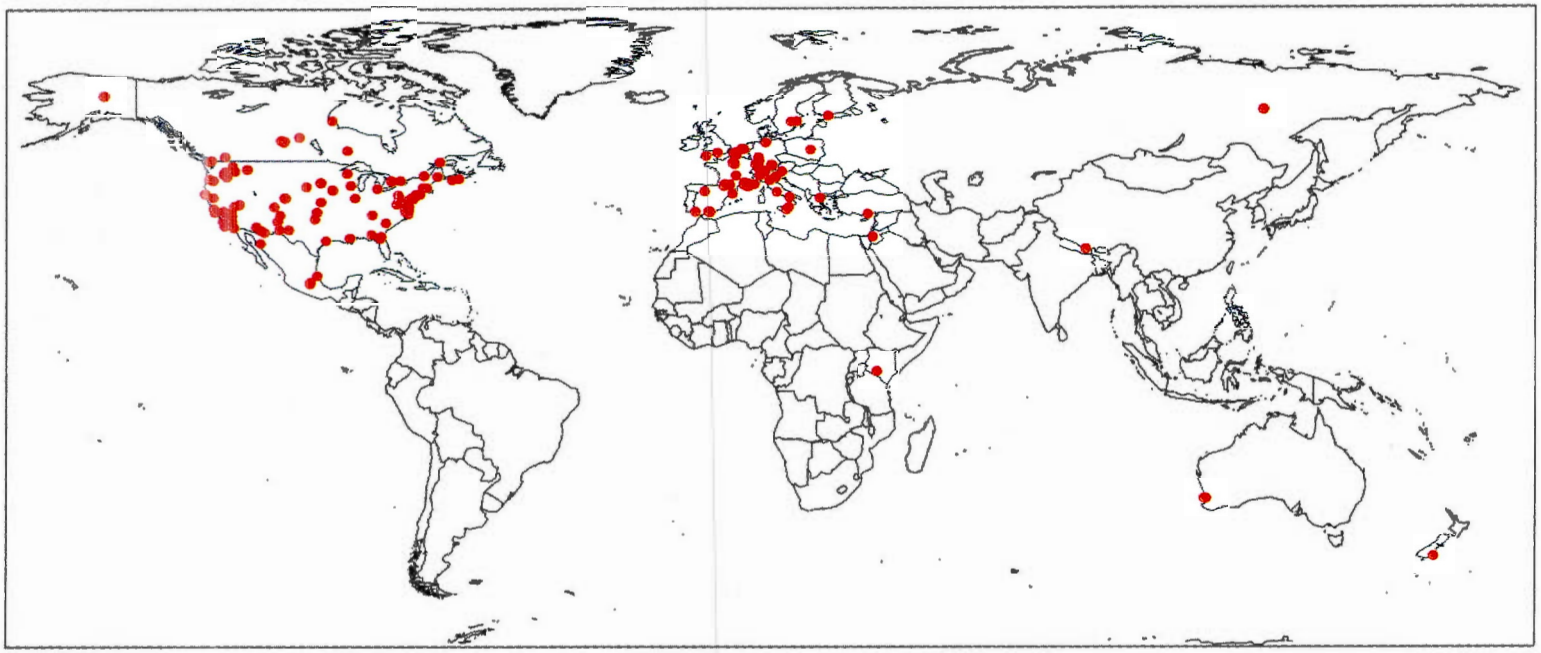

Figure 4.1 Map with the aerosol optical depth site locations highlighted in red

According to the level and regularity of yearly precipitations, the mean annual temperature, and the elevation, each AOD stations environment was labeled as Mediterranean and sub-arid, temperate, boreal or high elevation and mountainous area (> 1000 m) following Rakonczay (2002). Precipitation, temperature and cloud cover were extracted from UEA CRU TS 2.1 monthly data (Mitchell & Jones, 2005) for the 1971–2000 period at a 0.5-degree scale. The annual mean, monthly mean and seasonal mean were calculated for each variable at each AOD location. A summary of data is provided in the Appendix C. We have made the assumption that tree growth within 50 km and 150 km was representative of the AOD stations environmental conditions. Moreover, the high elevation environment can overlap with the others. We used yearly mean sunspot numbers as a representation of the solar activity. These data were obtained from the National Oceanic and Atmospheric Administration (NOAA).

4.2.2 Data Analysis

Our statistical analysis proceeded in three stages. (1) We separated climate-related growth signals from tree ring width series. (2) We used running correlation analysis to establish a relationship between tree growth and solar cycle. (3) We analyzed changes in these correlation in respect to the variation of AOD. TRW series were first analyzed with a blind source separation technique : the independent component analysis (ICA). This method separates the input data into components that are statistically independent (see Hyvärinen, Karhunen & Oja, 2001, for further detail) and is used to detect spikes (abnormal data) in numerous field of science, such as neurology (Vigário *et al.*, 1998) or seismology (Ham & Faour, 1999), and also work with tree ring width series (Chapter I and II). The goal here was to clean TRW from disturbance patterns, such as volcanic eruptions, insect outbreaks, or windthrows (breakage by wind). The results of ICA consist generally of a large number of spiky series and some non-spiky ones (Chapter I and II). We have selected only the non-spiky series, with a kurtosis below four and containing a cyclic pattern of near 11 years, corresponding to 90–95% of the initial growth. Moreover, TRW sites displaying one single non-spiky series correspond

to homogeneous sites, and only those were kept for further analyses. More than one non-spiky series means that the TRW sites are a mix of trees showing different growth pattern. Secondly, a running correlation of these non-spiky series within an 11-year window was performed with the solar cycle as in Chapter III. Such running correlations are widely used in dendrochronological analysis (D'Arrigo *et al.*, 2008; Pauling, Luterbacher & Casty, 2006) to investigate the stability of these relationships. Moreover, these correlations are not affected by any long-term growth (the age effect, *e.g.* Lorimer & Frelich, 1989; Payette, Filion & Delwaide, 1990) or climatic trends present in the input data. They can, however, detect changes in the relations between environmental factor and growth (Nowacki & Abrams, 1997). The use of sunspot numbers against TSI can be seen as a problem (Foukal *et al.*, 2006) : The TSI cycle amplitude is stable from cycle to cycle, whereas sunspots amplitude varies greatly from cycle to cycle. However, by restricting the correlation to within an 11-year window, we avoid the effect of these changes in amplitudes. As well, preliminary analysis shows no spurious correlation using Engle-Granger (Engle & Granger, 1987) causality test like in Chapter III. Thirdly, for each AOD station and for each scale (50 km and 150 km), a general tree growth result was obtained using the median value of each year and by smoothing with a modified Daniell (3,3) kernel. Linear regressions were made on the resulting series for their entire duration and for consecutive periods of 10 years. The effect of the sun on tree growth was measured by the slope of the regressions. Finally, we investigated for potential relationships between these slopes and the AOD, precipitation, temperature and clouds cover by linear correlation. We hypothesized that the correlation occurring between the solar cycle (the amplitude of which is stable from cycle to cycle) and tree growth should be affected by a change in the atmospheric composition as measured by the AOD.

4.3 RESULTS

The values of AOD at the wavelengths (440 nm and 675 nm) were linearly correlated with an adjusted r^2 of 0.93 and a slope of 0.58. Consequently, we present only results at 440 nm. We used only mean annual values for precipitation, cloud cover and temperature

since none of our results was significantly better using monthly or seasonal values. The distribution of the AOD values is similar across the different ecosystems (Figure 4.2). Temperate conditions showed higher level of AOD and a more Gaussian distribution center at 0.2, which is consistent with the location of human activities.

The analysis of the relationship between atmospheric transparency and the trend of the correlation between solar cycle and growth has been made for the two scales (50 and 150 km) for which AOD stations could be found. However, data at the 50 km scale were sparse and did not provide less robust results (Figure 4.3a). When we plotted the correlation of growth with the sunspot index as a function of the mean site AOD we found that the correlation coefficient was decreasing with AOD for Mediterranean and sub-arid ecosystems, and for the mountainous area during the 1934–1954 period (Figure 4.3), where most data were available. This trend means that, when AOD is low, an increase in solar irradiance enhances growth, whereas for high AOD, it decreases in growth. This trend was positive for the temperate environment leading to opposite effects.

These results cannot be explained by the distribution of the values used (Figure 4.4), since no differences among environments exist for the correlation between solar cycle and growth. Furthermore, no linear relationships were found between atmospheric transparency and environmental variables (precipitation, temperature). We followed the temporal variation of the correlation between sunspots and the tree growth over time for different 20 year periods : 1874–1894, 1894–1914, 1914–1934, 1934–1954, 1954–1974 and 1974–1994 (Table 4.1). For convenience we used the center of these periods (1885, 1905, 1925, 1945, 1965 and 1985) in the text and figures. For all these periods, significant relationships between the sunspots/tree growth correlation and the AOD were decreasing (negative slope coefficient) at the one exception in 1945 for the temperate environment.

Until 1960–1970 (Figure 4.5) for the high elevation and the Mediterranean and sub-arid ecosystems, the sunspots/tree growth correlations were decreasing when AOD increased

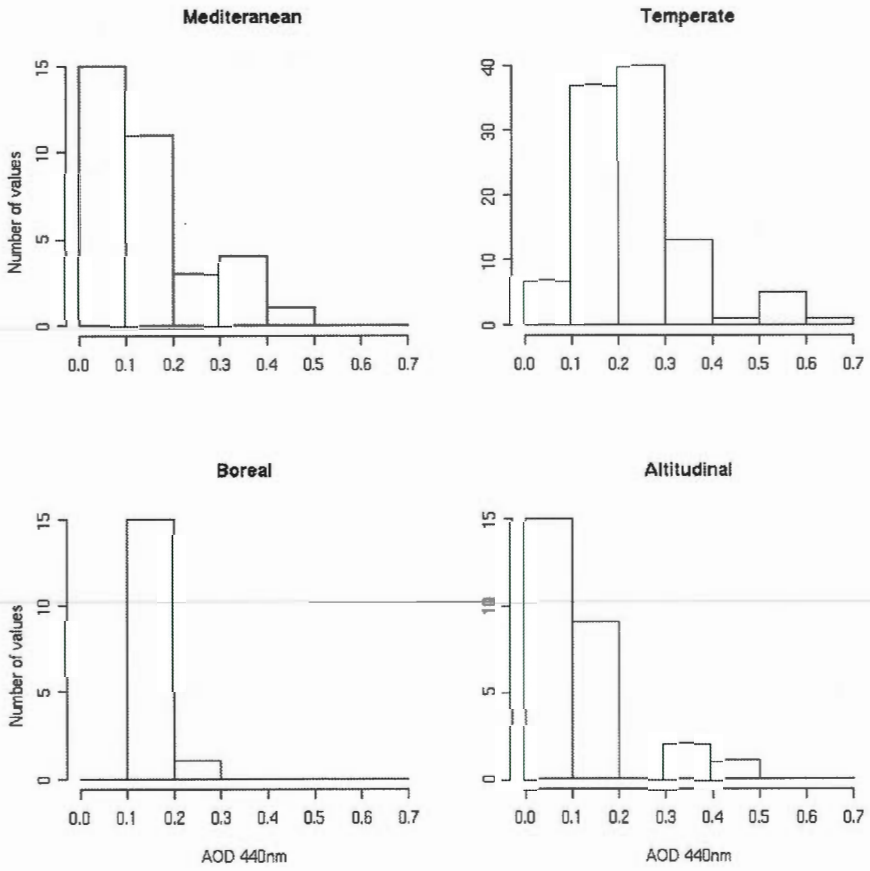

Figure 4.2 Distribution of the values for aerosol optical depth (AOD), with values of 0.1 indicating a clear sky and values of 1 a smog, for all ecosystems covered in this study.

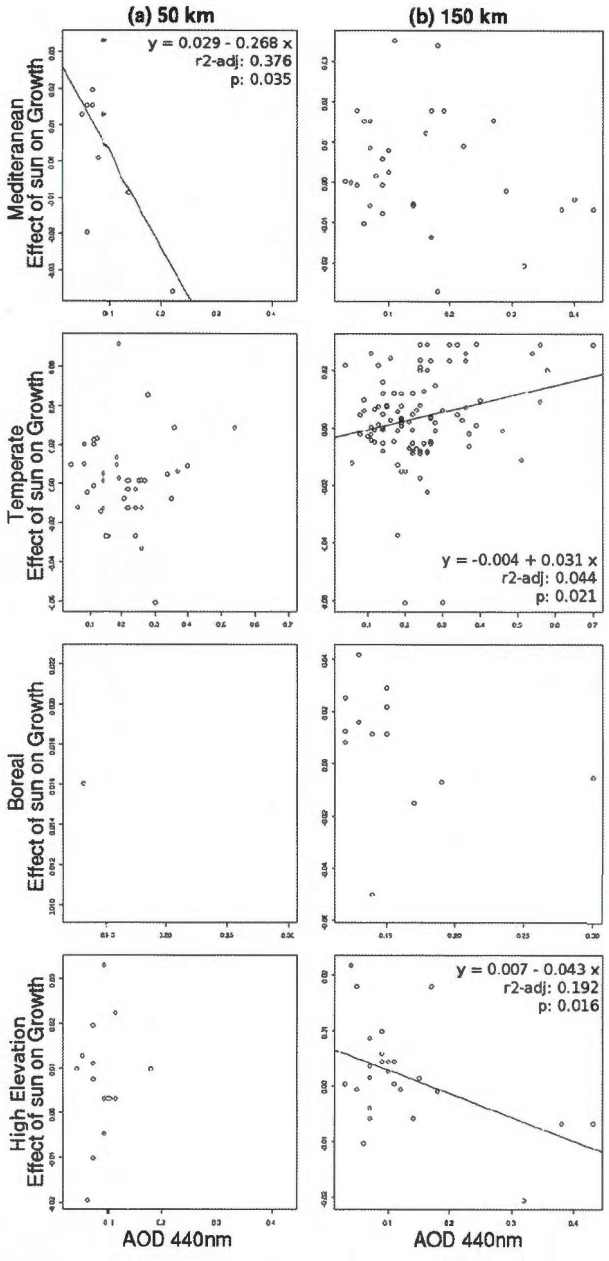

Figure 4.3 Relationship between the atmospheric transparency (AOD 440 nm) and the correlation between solar cycle and growth during the 1933–1954 period. Only significant simple linear relationships are shown by their regression with their coeficients, adjusted r^2 and p-value.

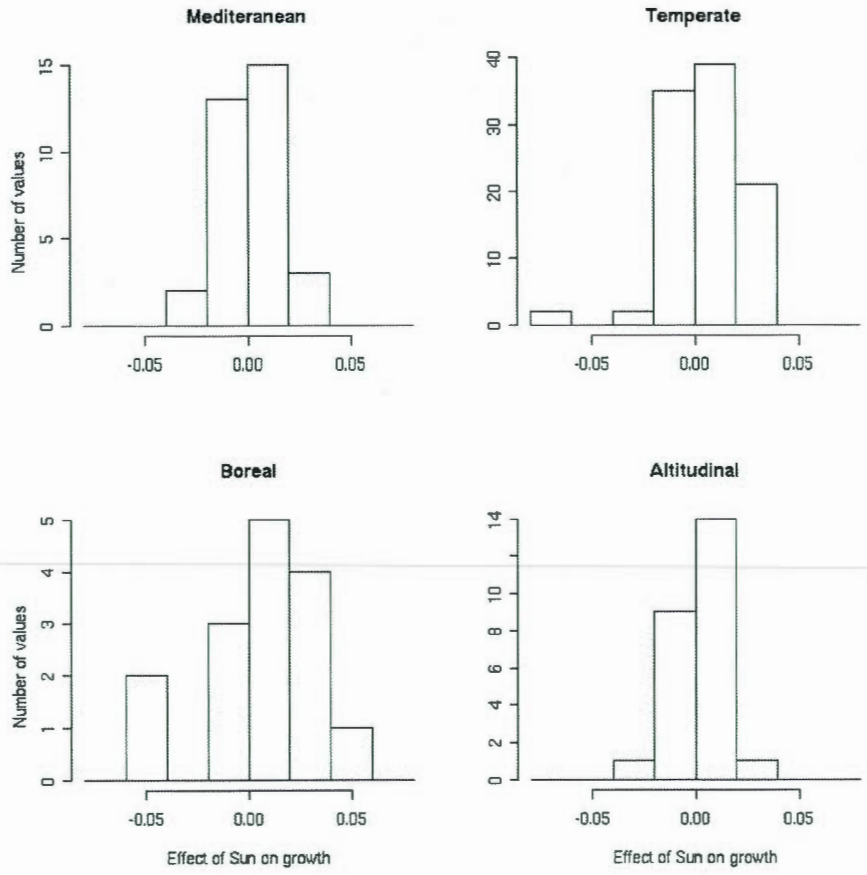

Figure 4.4 Frequency distribution of the correlation values between solar cycle and growth for the different ecosystems covered in this study

Tableau 4.1 Evolution of the relationship between Aerosol Optical Depth and the correlation between Solar Irradiance and Growth. Years refers to the center of the 20-year window and values represent the slope of the relationship and * significant values at 0.05.

Years	1885	1905	1925	1945	1965	1985
Mediterranean	-0.09*	-0.06*	0.01	-0.03	0	0.05
Temperate	0	0.03*	-0.04*	0.03*	-0.03*	0.04
Boreal	0.61	-0.43	-0.19	-0.18	0.14	NA
Altitudinal	-0.11*	-0.08*	-0.01	-0.05*	0.06	0.04

, and, after 1960–1970 it reverses, showing increase sunspots/tree growth correlations when AOD increased. No changes in the correlation between growth and sunspots was linked to AOD for the temperate and boreal ecosystems. However, some cyclicity was found in the responses of temperate ecosystems (Table 4.1) where the trend was positive in 1905, then negative in 1925, positive in 1945, and again negative in 1965. Years around 1985, even if the result was not significant, followed the same pattern by changing this trend to a positive one.

4.4 DISCUSSION

Our results confirmed that changes in the relative importance of diffuse irradiance influence tree growth at global scale as assumed in Chapter III. In fact, changes in atmospheric optical depth (AOD) act on the sensitivity of tree growth to small changes in irradiance during the solar cycle. In our records, the influence started with a negative effect from 1885 to 1965, and then a global positive effect. In the literature, models present a large and rapid change in atmospheric transparency for the period from 1940–1960 (Appendix G adapted from Romanou *et al.*, 2007), which is caused by the abrupt increase in fossil fuel use after the Second World War (Siegenthaler & Sarmiento, 1993). Loss in irradiance was in an order of 2% per decade before 1960, and then increased at 6% per decade (Stanhill & Cohen, 2001).

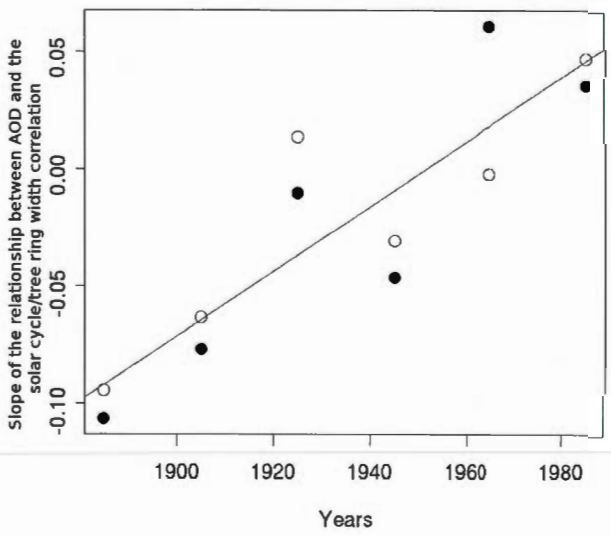

Figure 4.5 Long-term change of the relationship between atmospheric transparency and the solar cycle/tree growth correlation. Filled circles refer to high elevation (> 1000 m) and open circles to Mediterranean and sub-arid ecosystems.

The process by which growth might increase under diffuse irradiance involves a more even penetration of scattered light into multilayer crowns (Gu *et al.*, 2002). Whole plant carbon gain thus increases because deeper foliage layers are better reached and shade leaves receive more irradiance and contribute more to carbon fixation (Valladares & Pearcy, 1998; Roderick *et al.*, 2001; Gu *et al.*, 2002). Besides, the decrease in direct irradiance associated with an increased AOD reduces light exposure of sun leaves and the risk of photo-inhibition and overheating (Long, Humphries & Falkowski, 1994; Niyogi, 1999; Horton, Ruban & Walters, 1996; Roderick *et al.*, 2001; Gu *et al.*, 2002). It is well-known that, despite a lower photosynthetic capacity compared with sun leaves, carbon gain of shade shoots can be similar to that of sun shoots under a number of environmental conditions (Valladares & Pearcy, 1998); or at least they can contribute to a significant part of whole plant carbon gain (*e.g.* Beyschlag & Ryel, 2007). We can thus expect a significant increase in carbon gain in trees growing with an increased fraction of diffuse irradiance. However, only a few studies are available to corroborate this expectation (Farquhar & Roderick, 2003; Niyogi *et al.*, 2004). These result applied only to Mediterranean and sub-arid, and high elevation (> 1000 m) ecosystems. These ecosystems are highly subject to drought, which confirms some counterintuitive results observed for shrubs (Valladares & Pearcy, 2002; Niinemets & Valladares, 2004) where shade plants exhibit more photo-inhibition, showing that their photosynthesis is stimulated by diffuse light. However, at the same time, these shrubs suffer more from drought. We argue that diffuse light can reduce the negative impact of water stress in these ecosystems, leading to an increase in net carbon gain for canopy trees, since their root systems are deeper than those of shrub species reducing water restrictions. Moreover, as proposed by Kulmala *et al.* (2009) it is possible that if cosmic ray flux induces ionization in the atmosphere (Harrison & Carslaw, 2003; Usoskin *et al.*, 2004; Svensmark & Calder, 2007; Svensmark, Bondo & Svensmark, 2009) it could affects the electrical properties of the trees by modifying their water uptake. This indirect effect of solar cycle could be one of the require amplification factors that would be necessary to enhance it role for tree growth. Calculations made with a model of diffuse light effects on photosynthesis (Roderick *et al.*, 2001; Roderick, 2006) suggest that photosynthesis

should be maximum at $\sim$ 50% of atmospheric transparency, when the loss of energy due to the decrease in direct irradiance is over-compensated by the gain made by an increase in diffuse light. In this study, AOD is generally low, with an average of 0.21 (standard deviation of 0.11) at 440 nm and 0.12 (s.d. of 0.07) at 675 nm, reflecting a low level of pollution and a relatively low increase in diffuse irradiance. Our AOD values are therefore far from the 50% suggested as being the optimal amount for maximum photosynthesis, and even farther from an excess of fractional diffuse irradiance. Future work should focus on places with an intense reduction in the atmospheric transparency in order to determine the compensation point between a net gain in growth due to diffuse irradiance and a loss due to reduced irradiance.

ACKNOWLEDGMENTS

We would like to acknowledge contributors to the international tree-ring databank (IGBP PAGES/World Data Center for Paleoclimatology, NOAA/NCDC Paleoclimatology Program, Boulder, Colorado, USA), as well as contributors and site managers of the AERONET program, especially B, Holben. We also wish to thank Anastasia Romanou for making her data available, Stephane Daigle for the statistical support, and Elise Filotas for her comments. This project was supported by the Fond Quebecois de Recherche en Nature et Technologies. Fernando Valladares was funded by the Spanish Consolider Grant Montes (CSD2008_00040).

TEMPÉRATURE OU LUMIÈRE DIFFUSE

La pollution atmosphérique en générant de la lumière diffuse stimule la croissance dans les écosystèmes ayant des périodes de déficit hydrique. Or, la diminution de la lumière directe a également comme conséquence de diminuer la température. Il y a donc un doute sur les résultats précédents. Il faut donc évaluer si la lumière diffuse est véritablement à l'origine des variations de croissance que l'on observe. Pour cela nous allons analyser la croissance durant les deux dernières éruptions volcaniques d'importance. En effet lors des éruptions stratosphériques du SO_2 est libéré dans l'atmosphère et va générer énormément de lumière diffuse. Lors de l'éruption de El Chichón, au Mexique en 1982, un épisode de El Niño a également eu lieu qui annula la baisse de température liée à la présence de SO_2 dans l'atmosphère. Alors qu'aucun phénomène n'a masqué la baisse de température durant l'éruption du Mont Pinatubo (Philippines) en 1991. Nous avons donc une comparaison de choix.

CHAPITRE V

TREE GROWTH FOLLOWING PINATUBO AND EL CHICHÓN ERUPTION : A GLOBAL ANALYSIS

Tree growth response to volcanic events is still an open debate in the literature. Whereas some observed increases in tree growth have been attributed to the induced cooling, others were linked to diffuse light, which, by entering more evenly inside the canopy, reaches more leaves and enhances plant photosynthesis. In this paper, we look closely at the growth response of trees around the world, as measured by tree ring width, in terms of intensity of the response, its duration and the year of maximum intensity following the last two major volcanic events : the El Chichón and Mount Pinatubo eruptions. These two events differ greatly due to a cooling compensation induced by El Niño starting one year after the El Chichón eruption, whereas during the Pinatubo eruption, even if present, the El Niño event was not able of such compensation. The goal of this study is to identify potential differences in tree growth during these two events in order to evaluate the effect of temperature on growth response. Our results indicate that tree growth is independent of the intensity, duration and year of maximum intensity following the two volcanic eruptions despite 30 to 40% of the tree ring sites showing an increase in growth. In fact, the maximum intensity was reached the year after the eruptions, or the same year than the El Niño event following El Chichón, which excludes temperature as the main driver of tree response. These results were confirmed by two different multivariate analyses. By showing that diffuse light enhances photosynthesis and overpowers differences in temperature, at least for volcanic events, our investigation

has fundamental implications for climate models. These results can be projected for the global dimming and global temperature phenomenon, the first one having probably more importance for tree growth than the second.

5.1 INTRODUCTION

Volcanic eruptions can be major driver of climate (Robock, 2002). Two major events from the past century – El Chichón (Mexico) eruptions of March 28^{th} and April 3^{rd}, 1982 and Mount Pinatubo (Philippines) eruption of June 15^{th}, 1991 – have acted greatly on global temperature and on the amount and quality of light reaching the ground (Dutton & Bodhaine, 2001). They are rated using the volcanic explosivity index (VEI Simkin *et al.*, 1981; Newhall & Self, 1982), 4 and 5 respectively for El Chichón, and 6 for Mount Pinatubo (Robock & Mao, 1995). The VEI giving an estimation of the quantity of material send in the atmosphere (See comparison and discussion between VEI and dust veil index, DVI, in Robock, 1991) on a scale ranging from 1 to 7, 1 refers to minor eruption, whereas 7 (*e.g.* : Tambora eruption of 1815) refers to major events having released more than 100 km^3 of particles. Shortly after both events, aerosols were uniformly distributed from the tropics to the poles (Strong, 1984; Robock & Mao, 1995). After El Chichón eruptions temperature decreased (Bandeen & Fraser, 1982; Gerber & Deepak, 1984) and transmission of solar radiation to the earth surface dropped by 10% during two years (Dutton & Bodhaine, 2001), with a maximum loss of 45% in May 1982 recorded at Mauna Loa (Garcia & Yasukawa, 1983). However, the earth cooling was limited in 1983 by the beginning of the largest El Niño event of the last century (Rasmusson & Wallace, 1983). The Pinatubo eruption on the other side has decreased global temperature by about 0.5 K with a peak 18 months after (Soden *et al.*, 2002), and solar transmission by 10% (Hansen *et al.*, 1992) with a significant decrease during three years (Dutton & Bodhaine, 2001). Unlike during El Chichón, even if present, the El Niño event was moderate and did not mask its cooling effect. Some early work on tree growth following the eruption of the Pinatubo (Gu *et al.*, 2003; Farquhar & Roderick, 2003) showed a local increase and attributed it to an increase in diffuse light. It has been

proposed that an increase in diffuse light as observed globally (Roderick *et al.*, 2001; Roderick & Farquhar, 2002; Stanhill & Cohen, 2001) can enhance photosynthesis by permitting light to penetrate more evenly inside the canopy. Moreover, simulation model of plant growth seems to corroborate this expectation (Cohan *et al.*, 2002; Mercado *et al.*, 2009), as well as chapters III and IV of this thesis. In a study of the effects of volcanic eruptions on tree growth (Krakauer & Randerson, 2003) found a global decrease in net primary productivity (NPP) following major eruptions since 1026 A.D. for about eight years. However, although discussing the problem of light availability, they attributed this decline to cooling and not in light drop, raising once more the delicate divergence problem (D'Arrigo *et al.*, 2008).

However, the problem is whether the scattering of light increased or, if it is too great, decreased growth that has not been considered by Krakauer & Randerson (2003). This trade-off between diffuse and direct light is fully discussed by (Roderick, 2006), and an increase in growth will occur only for an intermediate ratio between these two kinds of light. More recently, Robock (2005) proposed that some anomalies found in temperature reconstruction using tree rings (results of Mann, Bradley & Hughes, 1998), and following volcanic eruptions were due to an increase in diffuse light, since tree rings base reconstruction always underestimated cooling compared with other proxy methods. However, the shape of tree ring response is always identical to other proxy except following the Tambora 1815 eruption (VEI 7), which become, if the reference for temperature anomalies is set to the 19^{th} century mean temperature, a warming period. This increase in temperature as seen by the tree ring proxy can only be attributed to diffuse light considering the large impact of the Tambora eruption on temperature, which seems to have had a peak of 0.6^{o}C and the cooling had last at least ten years (Robock, 2005).

The purpose of this study is to determine whether cooling has an effect on tree ring width or not by comparing the eruptions of Mount Pinatubo and El Chichón, the cooling caused by the latter having been offset by a strong El Niño event. We look at whether an increase in scattered light had a significant impact on growth by comparing the results at different latitudes and altitudes. Our hypothesis is that, if the scattered light plays

a role, there is a latitudinal gradient ranging from no gain in growth, to an increase and then a decrease caused by too much scattering, following the model proposed by Roderick (2006). Here, we assumed that if the angle of incidence of light rays decrease (following latitude), the ratio between diffuse light and direct light should increase due to the longer trajectory of light rays in the atmosphere. Moreover, the transportation of stratospheric aerosol emitted by these volcanoes was composed of three layers (Reiter *et al.*, 1983; Jäger, 1992). The first layer of low altitude reach the mid-northern latitudes in two weeks, the second layer higher in the atmosphere reach these latitudes in one month and the third layer was discernible four months after the eruptions. Thus, in the first year, a relationship between the intensity of trees response and the distance to volcanoes could exist for the same latitude especially for short growing season ecosystems like the boreal forest.

5.2 METHODS

5.2.1 Data

Raw tree ring width series have been obtained from The International Tree-Ring Data Bank (http ://www.ncdc.noaa.gov/paleo/treering.html). Sites were randomly selected – 210 in total – in order to have an even distribution of distances from site to volcano (Figure 5.1). These distances were calculated as the shortest distance on the surface of the WGS84 Ellipsoid world model. These sites were located in 14 countries and six states of the United States of America. This indication of geographic localization is call "state" in this paper. They were composed of 37 species from 13 genus collected mainly for climatic reconstruction. Latitude and elevation were also retained for analysis.

5.2.2 Tree Ring Width Analysis

TRW series were analyzed using a blind source separation technique. This method, the independent component analysis (ICA), separates the input data into components that are statistically independent (see Hyvärinen, Karhunen & Oja, 2001, for further details)

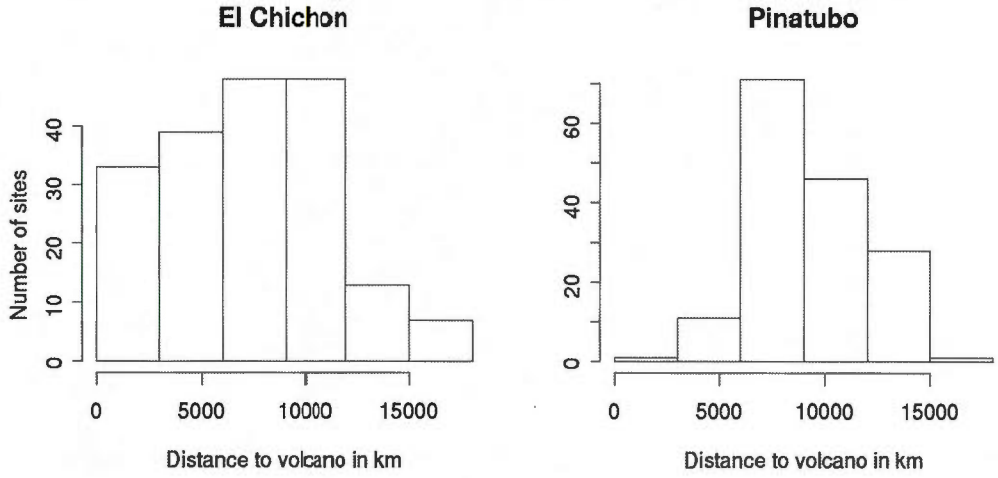

Figure 5.1 Distribution of data with regard to their distance to the volcano

through an unmixing process and is used to detect spikes in fields such as neurology (Vigário *et al.*, 1998), seismology (Ham & Faour, 1999), etc., where, components or sources signals are the underlying mechanisms producing the mixture. Following the conceptual model proposed for tree rings (Cook, 1987; Cook & Kairiukstis, 1990), these sources are a climatic component, disturbances, an age effect and an error component. In this paper, we have applied ICA in order to recover spikes, or disturbances, caused by the decrease in solar radiations or temperature following volcanic eruptions. The ICA was conducted using the FastICA algorithm (Himberg & Hyvärinen, 2001) for R (CRAN 2008). Note the algorithm standardizes the data before processing by setting the mean of each series to 0 and its standard deviation to 1. This will be helpful for later comparisons by canceling tree species differences in term of growth rate and its variations while not affecting the interactions between climate, tree growth and disturbance events. From the output of the ICA volcanic eruption induced spiky series (Figure 5.2) were then identified as any series containing a spike occurring during the year of eruption or the following year. A spike was defined as any values lower than -1.5, or 1.5 times the standard deviation . Then spikes were characterized by :

- the intensity of the disturbance, defining as the lowest value observed during the period
- the timing (year) of the largest growth effect
- the duration of the disturbance, defines as the number of years of values lower than -1.5

5.2.3 Statistics

The output of the spike detection described above was used for further analysis. We combined the data on spike duration, intensity and occurring year with information on the location of the series. The data was then used in a regression tree (Rpart, Breiman *et al.*, 1984; Ripley, 1996; De'ath & Fabricius, 2000; De'ath, 2002) to identify, which variables environmental characteristics influence most the tree growth reaction to the volcanic eruptions. All combinations of the three response variables were tested as a function of distance to volcanoes, latitude, elevation, species and state. As a parallel analysis we applied redundancy analysis (RDA, Van Den Wollenberg, 1977; Ter Braak, 1986) with Helinger transformation to the data (Legendre & Legendre, 1998). We used a matrix including all sites (with or without volcanic induced disturbances) as data. The data included presence and absence of disturbance events (based on the spike detection described above) for each species by site, whereas the second matrix contains characteristics of tree growth response to disturbance, and location data (state, elevation, etc.). Volcanic eruptions can have a positive or negative effects on growth. Therefore we analyzed the amplitude of the spike was analyzed as absolute (only positive) and non-transformed values. This double analysis was used to understand if species or sites react in a similar way (positive or negative) to the volcanic eruptions.

Finally, we provide some descriptive statistics per category or groups (made according to Rpart and RDA results) that cannot be tested for the reasons given above. All analyses were made with R (CRAN, 2009) using rpart (Therneau and Atkinson, 2002) and vegan (Oksanen et al., 2009) packages.

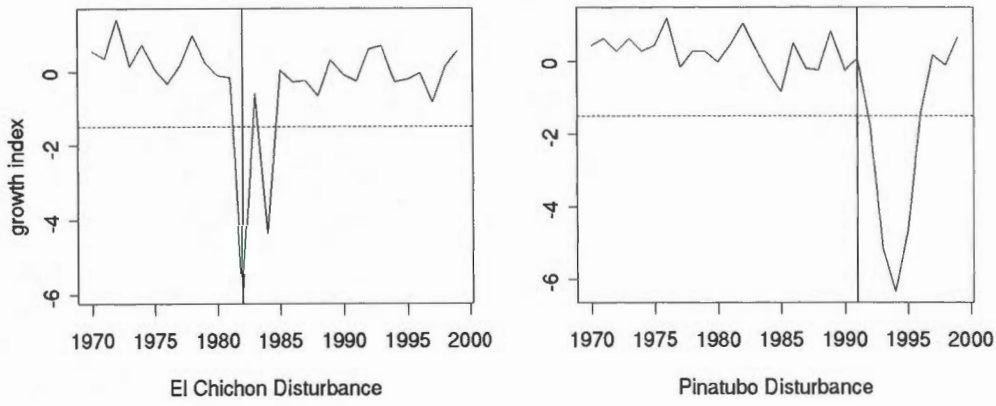

Figure 5.2 Example of volcanic disturbance affecting tree growth extracted by ICA in Arizona site number 558. Vertical lines indicate volcanic event, and horizontal dashed line the -1.5 threshold.

5.3 RESULTS

5.3.1 Detection

From the original 210 sites, 157 were affected by volcanic events and a total of 346 disturbance components were extracted by ICA. In most cases, no abrupt change in tree growth was observed in the years following a disturbance event. For El Chichón 188 disturbances were found, and 158 for the eruption of Mount Pinatubo.

5.3.2 Volcanoes

The median and mean responses of tree growth for each volcanic eruption appeared equivalent based on the intensity, duration and year of the maximum intensity (Table 5.1). The only difference seems to be that the effect of El Chichón lasted longer (higher values for the upper quartile) and its maximum was also higher. However, distinct results were found when comparing the two events using the average tree species response

Tableau 5.1 Descriptive values for tree growth response following the volcanic eruption of El Chichón and the Pinatubo. Int. refers to intensity, Dur. to duration and Year to the year of the intensity. Pos and Neg give the number of trees with positive and negative intensity (increase or decrease in growth).

	El Chichón			Pinatubo		
	Int.	Dur.	Year	Int.	Dur.	Year
Minimum	-8.76	1	0	-8.96	1	0
Lower quartile	-4.97	1	0	-5.12	1	0
Median	-3.07	2	1	-2.92	2	1
Upper quartile	3.83	4	2	3.50	3	2
Maximum	9.48	8	5	8.48	6	4
Mean	-1.10	2.65	1.09	-1.03	2.14	0.98
Pos	75			66		
Neg	113			92		

(Values available in Table 5.2). The average intensity during El Chichon is identical with both methods of calculation (global average and averaging species average); however, the one for Mount Pinatubo is 0.21 using species average (0.30 without rounding up values) against -1.03 for global average (Table 5.1). This difference is explained by the influence of extreme values for the mean. It turns out that, whereas they are globally equivalent, some species show more extreme responses during the Mount Pinatubo eruption. The complete data for species response are presented in Appendix H. Furthermore, no differences were found in the ratios between a growth increase and decrease : 0.71 (92/113) for El Chichón and 0.66 (66/92) for Mount Pinatubo.

5.3.3 Multivariate Analysis

The Rpart (Figure 5.3) and RDA (Figure 5.4) suggest that species response is globally affected by latitude and elevation. Results were identical with both absolute and real values for intensity; just a 180^o rotation in the axis for the RDA. Each analysis separates species into three distinct groups. The response of RDA groups following the two

eruptions seems inconsistent compared with Rpart groups (Table 5.3). For example, the +RDA2 exhibits the highest decrease in growth during El Chichón, whereas it exhibits the lowest decrease in growth during the Mount Pinatubo event. This shows that intensity, duration and the year of the maximum intensity have no impact on the structure of the data during the RDA. The Rpart groups are formed at the first node leading to two groups (1 and 2). The first group is further subdivided into two groups (1a and 1b). The three groups are distinguished as follow : Group 1a groups species with an increase in growth for a short duration, Group 1b with a response varying according to latitude, and Group 2 with a response varying according to elevation (Figure 5.3). Groups are composed of :

- Group 1a : Austrian pine, Calabrian pine, Dahurian larch, Lenga, Pink pine, *Pterocarpus angolensis*, Sitka spruce, Teak and White oak.
- Group 1b : Black pine, Black spruce, Californian sycamore, Cedar of Lebanon, Chir pine, Cyprian cedar, Douglas fir, Himalayan cedar, Himalayan spruce, Montezuma cypress, Norway spruce, Pinyon pine, Ponderosa pine, Whitebark pine and White spruce.
- Group 2 : Armand's pine, Blue oak, Grecian juniper, Himalayan fir, Jeffrey pine, Limber pine, Lodgepole pine, New Zealand cedar, Qilianshan juniper, Scots pine, Umbrella pine, Valley oak, Western juniper.

For the RDA, groups follow axes. The first axis is negatively correlated to latitude with a score of -0.99 and the second axis is positively correlated to elevation with a score of 0.95 (Figure 5.4). Elevation contributes also to the first axis (score of 0.32) as well as states (score of 0.38). Species groups can be separated by their correlation with the axes :

- Negatively to the first axes (-RDA1) : Black spruce, Dahurian larch, Norway spruce, Scots pine, Sitka spruce, White oak, White spruce.
- Positively to the first axes (+RDA1) : Blue oak, Calabrian pine, Californian sycamore, Lenga, Montezuma cypress, New Zealand cedar, Pink pine, *Pterocarpus angolensis*, Teak, Umbrella pine, Valley oak.
- Positively to the second axes (+RDA2) : Armand's pine, Austrian pine, Black pine,

Cedar of Lebanon, Chir pine, Cyprian cedar, Douglas fir, Grecian juniper, Himalayan cedar, Himalayan fir, Himalayan spruce, Jeffrey pine, Limber pine, Lodgepole pine, Pinyon pine, Ponderosa pine, Qilianshan juniper, Western juniper, Whitebark pine

RDA inertia (variance explained) has a total value of 0.104, in which constrained axes represent 0.11 and unconstrained 0.93. These low inertia values are easily explained by the low number of replications per tree species. Moreover, +RDA2 seems to group trees from water-stressed habitat, whereas, +RDA1 groups species with higher water availability from warm latitudes and -RDA1 from cold latitudes.

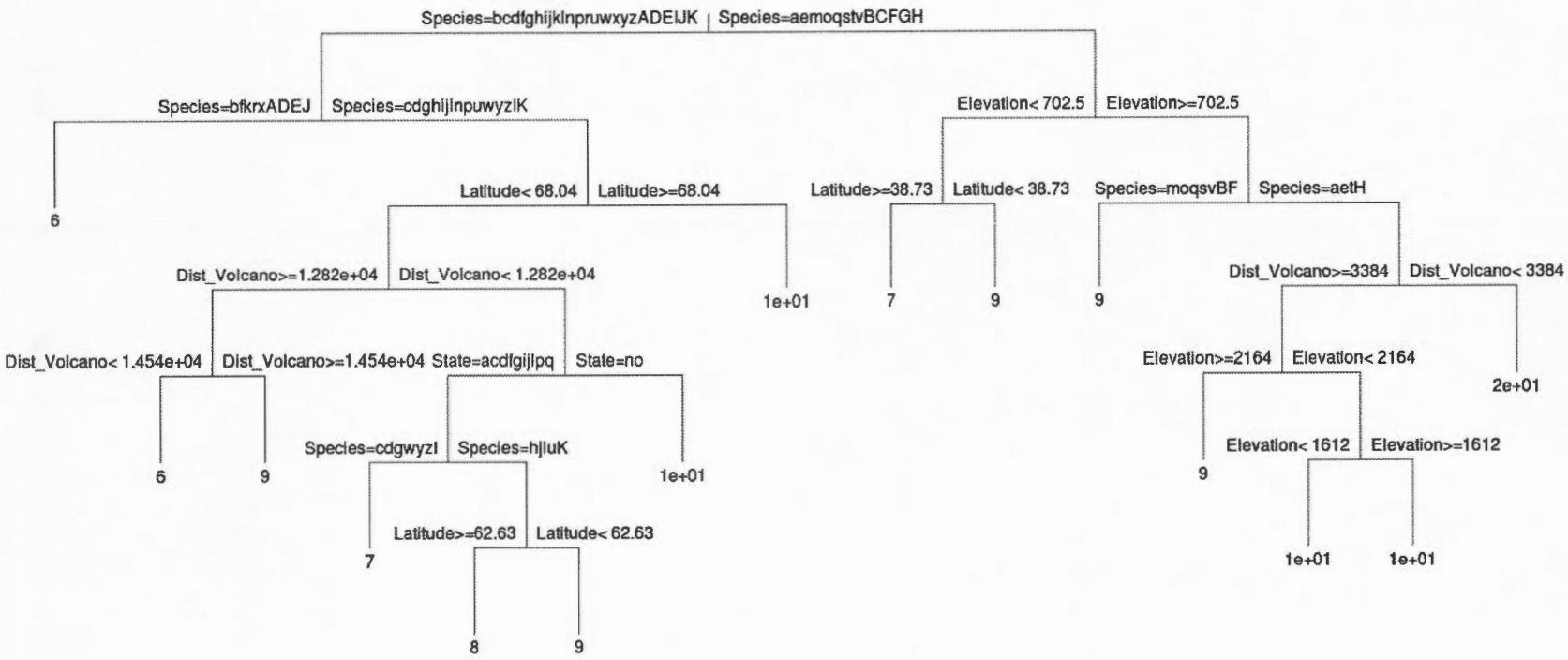

Figure 5.3 Regression tree classification of tree ring width response (intensity, duration and year of the maximum intensity) by data location, and species name (Species code are given in Table 5.2).

Tableau 5.2: Simplified table of species growth response to El Chichón (El C.) and Mount Pinatubo (Pina.) volcanic events and their respective Rpart and RDA groups. Species gives the common name, or, if in italic, the scientific name, # refers to the species code for the Rpart, Rpart and RDA refers to the group in which species were classified, then Int. and Dur. refers to the mean growth response of the considered species following the volcanic event considered for intensity, duration and the occurring year of intensity respectively.

				El C.		Pina.	
Species	#	Rpart	RDA	Int.	Dur.	Int.	Dur.
Armand's pine	a	2	+RDA2	-8.55	5	NA	NA
Austrian pine	b	1a	+RDA2	4.64	2	3.44	1.5
Black pine	c	1b	+RDA2	1.48	3	-3.48	1
Black spruce	d	1b	-RDA1	0.03	2	3.59	2
Blue oak	e	2	+RDA1	-1.2	1	-3.67	2
Calabrian pine	f	1a	+RDA1	-4.96	2	-0.54	1
Californian sycamore	g	1b	+RDA1	4.02	1	-4.96	2
Cedar of Lebanon	h	1b	+RDA2	-3.09	3	4.26	2.5
Chir pine	i	1b	+RDA2	NA	2	NA	NA
Cyprian cedar	j	1b	+RDA2	-6.81	2	NA	2
Dahurian larch	k	1a	-RDA1	NA	NA	1.67	1
Douglas fir	l	1b	+RDA2	-3.71	1	-2.52	1
Grecian juniper	m	2	+RDA2	-2.1	3.5	-2.48	2
Himalayan cedar	n	1b	+RDA2	NA	2.5	NA	NA
Himalayan fir	o	2	+RDA2	NA	3.5	NA	NA
Himalayan spruce	p	1b	+RDA2	NA	2	NA	NA
Jeffrey pine	q	2	+RDA2	-1.19	2	NA	2
Lenga	r	1a	+RDA1	NA	NA	0.34	1
Limber pine	s	2	+RDA2	4.05	7	-4.6	1.5

Continued on next page

Tableau 5.2: Simplified table of species growth response to El Chichón and Mount Pinatubo volcanic events (continued)

				El C.		Pina.	
Species	#	Rpart	RDA	Int.	Dur.	Int.	Dur.
Lodgepole pine	t	2	+RDA2	-5.17	7	1.68	3
Montezuma cypress	u	1b	+RDA1	-2.87	1.5	1.03	1
New Zealand cedar	v	2	+RDA1	-0.41	4	6.07	2
Norway spruce	w	1b	-RDA1	-8.52	1	-4.1	1
Pink pine	x	1a	+RDA1	3.21	1	4.18	2
Pinyon pine	y	1b	+RDA2	-1.99	1.5	-0.39	3.5
Ponderosa pine	z	1b	+RDA2	-3.37	3.5	NA	NA
Pterocarpus angolensis	A	1a	+RDA1	1.95	2	5.38	1
Qilianshan juniper	B	2	+RDA2	2.06	1	1.32	1
Scots pine	C	2	-RDA1	-0.79	3	-0.22	2
Sitka spruce	D	1a	-RDA1	NA	NA	5.14	1
Teak	E	1a	+RDA1	NA	NA	3.18	1
Umbrella pine	F	2	+RDA1	NA	NA	-0.26	4.5
Valley oak	G	2	+RDA1	4.39	2	-6.1	3
Western juniper	H	2	+RDA2	-0.91	5	-2.23	3.5
White oak	I	1a	-RDA1	2.47	3	NA	2
White spruce	J	1b	-RDA1	-0.12	1	-1.57	NA
Whitebark pine	K	1b	+RDA2	0.94	2	1.53	2

5.3.4 Latitude and Elevation Effect

We conducted a linear regression on the groups identified in both analyses. The variance explained is within the order of the RDA's inertia (< 10%, see figures in Appendix I). Species intensity at high elevations (from 1,500 to 3,500 m) seems to respond to

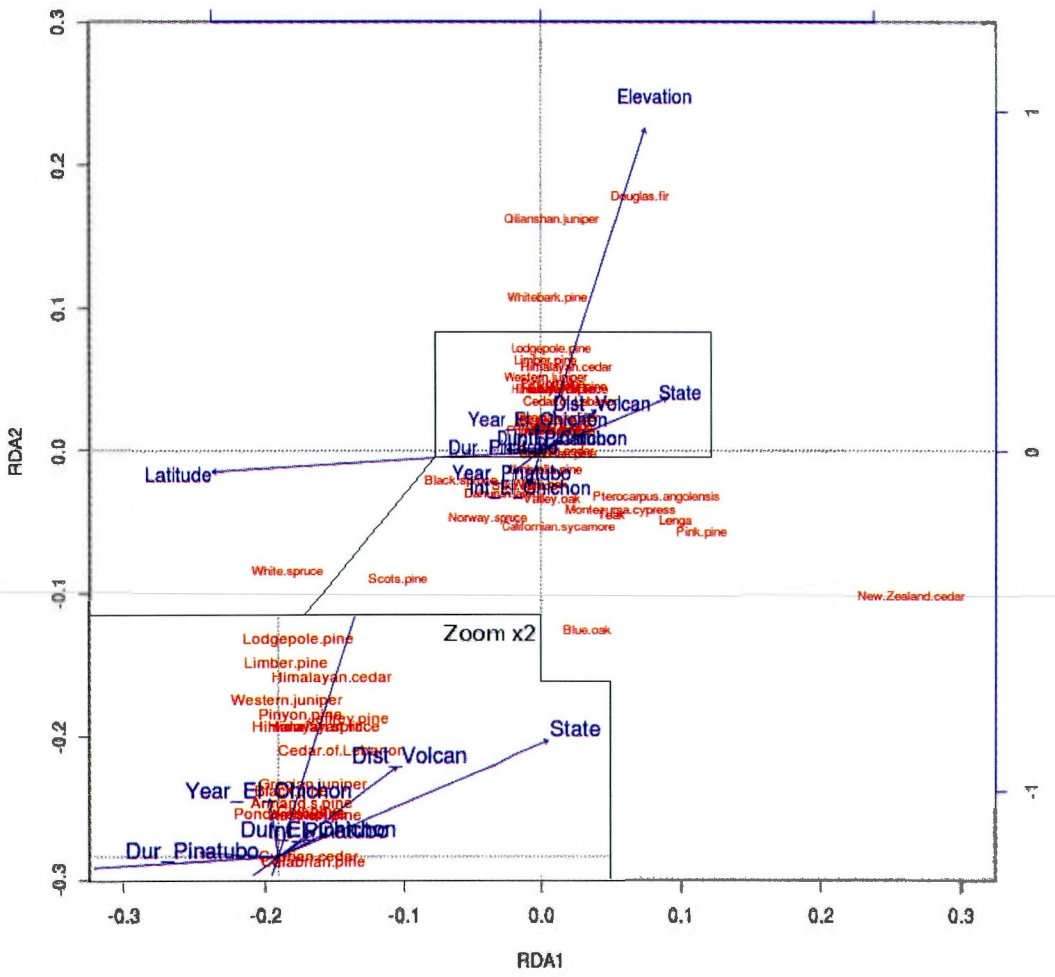

Figure 5.4 Species scores and biplot arrows representation for the redundancy analysis of tree growth response to volcanic events

Tableau 5.3 Comparison of Regression Tree and Redundancy Analysis groups for the mean intensity (Int.), duration (Dur.) and Year of species growth response to volcanic eruptions. Values in brackets give the standard deviation.

Volcano	Groups	Int.	Dur.	Year
El Chichón	2	-0.82 (5.44)	3.11 (2.05)	1.29 (1.13)
	1a	1.00 (4.32)	1.71 (0.95)	0.29 (0.49)
	1b	-1.57 (4.46)	2.48 (1.70)	1.01 (1.16)
	-RDA1	-0.47 (4.63)	2.87 (1.85)	1.19 (1.33)
	+RDA1	-0.80 (5.77)	2.00 (1.33)	0.77 (0.74)
	+RDA2	-2.21 (4.28)	2.94 (2.04)	1.18 (1.14)
Pinatubo	2	-1.49 (5.68)	2.24 (1.19)	1.00 (0.96)
	1a	1.83 (3.55)	1.27 (0.47)	0.64 (0.67)
	1b	-1.14 (4.55)	2.25 (1.47)	1.02 (0.98)
	-RDA1	-1.10 (4.7)	2.28 (1.44)	1.08 (1.02)
	+RDA1	-1.81 (5.71)	1.85 (1.10)	1.00 (0.98)
	+RDA2	-0.47 (4.73)	2.25 (1.37)	0.87 (0.84)

latitude during El Chichón only when growth increases (Figure 5.5 a). However, no direct relationships exist with elevation (Figure 5.5 b) ; a result independent of elevation values (Figure 5.5 c). We provide the other non-significant relationships in Appendix I. We evaluated a hyperbolic regression as suggested by the cloud of points observed in Figure 5.5. This relationship is consistent with our hypothesis expecting a latitudinal gradient starting from an absence in growth gain, followed by an increase and then a decrease in growth caused by excessive scattering. This regression (Figure 5.5 a) is significant for both orders, with a p-value of 0.0161 for the second order coefficient, and 0.0217 for the first order. The explained variance is 0.30 (Adjusted-R^2), which is higher than the RDA inertia.

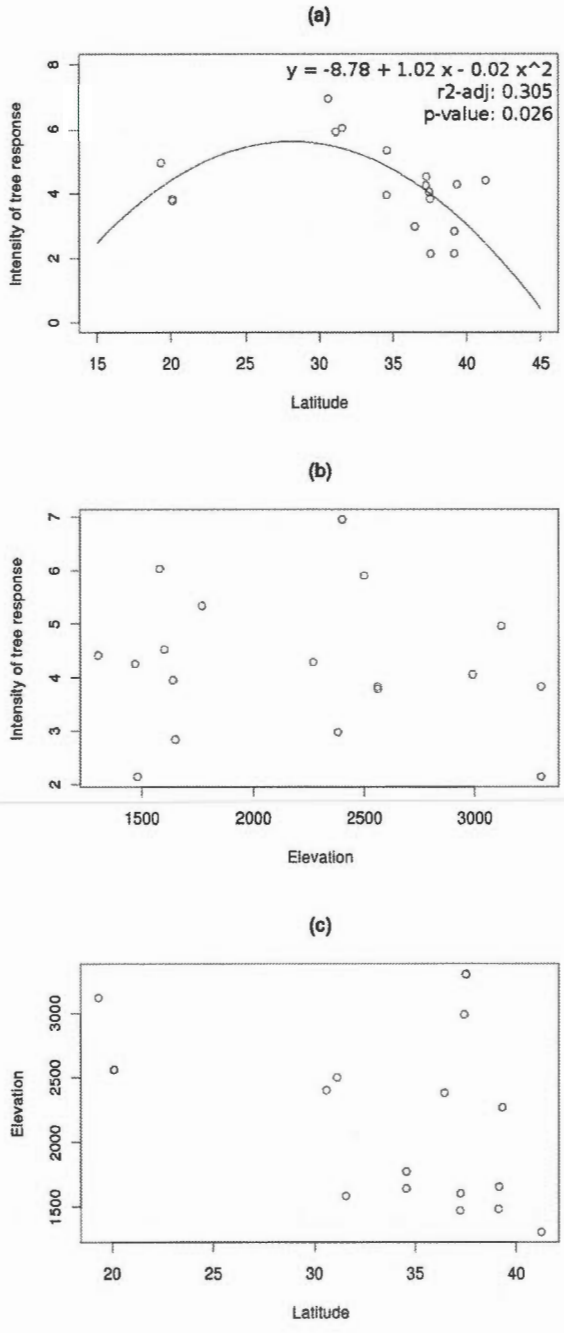

Figure 5.5 Effect of latitude on tree response at high elevation with curve of significant relationship with their coeficients, adjusted r^2 and p-value

5.4 DISCUSSION

Tree growth during the two volcanic episodes was very similar, although the effects of the eruptions on climate were pretty different. There were marked decreases in global temperatures after Pinatubo, while El Chichón did not affect climate due to a strong El Niño event (Handler, 1984; Hirono, 1988). This shows that, apart from direct effects of temperature, other volcanic driven factors, namely the optical depth of the atmosphere might drive tree growth. Robock (2005) discussed the global temperature reconstructions of Mann, Bradley & Hughes (1998), and show that during volcanic events, tree growth is higher than expected and does not poorly track the cooling induced by the eruptions. These errors have been attributed to diffuse light induced by the particles sent to the atmosphere by volcanoes. Moreover, during the Tambora eruption of 1815 (Robock, 2005), which is the biggest eruption of the last 1,000 years (according to the Smithsonian Global Volcanism Program and with a VEI of seven), the shape of the temperature reconstruction using tree ring was inverse to other proxies. This implies that tree growth actually increased during the global cooling. Robock (2005) suggested the proportion of diffuse light as a main driver of tree growth. This is corroborated by our observations of the El Chichón and Mount Pinatubo eruptions where, respectively, 29% and 34% of tree ring sites displayed an increase in growth. Therefore, globally there is a decrease in growth moderated by an increase in diffuse light, whereas locally there are some important increases due to the same phenomenon. Thus, the cooling effect is not itself responsible for the general decrease in NPP as observed by Krakauer & Randerson (2003). We do not suggest that cooling had no effect on trees since frost damage is a good proxy of volcanic eruptions (LaMarche & Hirschboeck, 1984). There were no differences in the mean reaction of trees to the eruption of Pinatubu and El Chichón.e. Moreover, larger and extreme positive values were found for species-specific responses to the Mount Pinatubo eruption. These affected the average intensity, whereas intensity of tree response quartiles are identical between the two eruptions (Table 5.1). This seems to reflect the higher amount of material sent to the atmosphere by Mount Pinatubo (VEI 6) compared with El Chichón (VEI 4 and 5), which would also be associated with

more diffuse light and confirm its global effect as shown in Chapter IV and Chapter III. Diffuse light appears to be the major moderator of tree growth during volcanic events. Moreover this effect follows the model proposed by Roderick (2006) in which a trade-off between direct light and diffuse light affects tree growth hyperbolically. We have hypothesized that this subtle effect would mostly benefit plants growing at intermediate latitude, or near 30^o. This effect was shown only for high elevation locations and for increases in growth (Figure 5.5). The question remains to understand why trees at high elevations follow the latitudinal model, whereas trees at much lower elevations do not. We suggest that the presence of anthropogenic particles, more abundant at low elevations, over increased diffuse light during volcanic eruptions and lead to the absence of any latitudinal effect.

CONCLUSION

L'évaluation de l'influence des changements globaux sur la croissance des arbres est un enjeu environnemental majeur. D'après les projections de l'IPCC (Solomon *et al.*, 2007), l'augmentation du CO_2 atmosphérique sera de 10,2 GtC.yr en 2070 et le puits terrestre résiduel devrait rester stable à 2 GtC.yr. Ce puits terrestre résiduel dépend grandement de l'état de santé de nos forêts subissant des changements climatiques importants et de la capacité des arbres à transformer le CO_2 en matière organique. Mais cette transformation physico-chimique du CO_2, par le biais de la photosynthèse, est également contrainte par les changements climatiques. Et comme nous l'avons montré dans cette thèse, l'augmentation de la lumière diffuse affecte la croissance des arbres.

Dans cette thèse, nous avons présenté une nouvelle méthode d'analyse des cernes de croissance ainsi que deux types d'applications de cette méthode. Ces applications sont d'une part la détection de perturbations qui affectent la croissance et d'autre part l'extraction de la partie de la croissance due au climat. Toutefois, cette dernière peut être plus difficile à mettre en œuvre. La méthode proposée, qui provient des sciences physiques, pourra ainsi être utilisées pour la recherche d'autres effets de l'environnement sur la croissance des arbres. Les sciences physiques, la médecine et les sciences économiques ont beaucoup à apporter à l'écologie : la physique, de part sa maturité, la médecine qui a su utiliser la physique avec l'essor des techniques modernes d'imagerie médicale, et les sciences économiques qui ont permis de faire des progrès énormes dans le traitement des données temporelles complexes. Or, il est rare de voir des publications d'écologie utiliser ce savoir alors que toutes ces sciences ont beaucoup en commun, du moins numériquement. De plus, nous pensons que cette méthode pourra être utilisée pour d'autres applications en écologie. L'utilisation d'une méthode aveugle de séparation des signaux sources, comme l'analyse en composants indépendants (ICA), évite certaines

suppositions qui, lorsqu'elles ne sont pas rencontrées, ne permettent pas d'utiliser les données à leur plein potentiel et ceci s'avère un problème souvent rencontré avec les méthodes traditionnelles.

Dans un premier temps, au cours de ce document, nous avons montré grâce à cette analyse, que la recherche de perturbations de la croissance ne dépend plus des chronologies d'espèces non-hôtes dans le cas des épidémies d'insectes. Ces espèces non-hôtes, comme nous l'avons montré dans le cas du pin ponderosa (*Pinus ponderosa*), peuvent elles aussi être affectées par les mêmes épidémies. C'est surtout important quand un insecte est relativement généraliste, telle la tordeuse des bourgeons de l'épinette, qui attaque aussi bien les sapins Douglass (*Pseudotsuga menziesi*), les épicéas (*Picea abies, Picea engelmannii, Picea glauca ...*) que les pins (*Pinus coulteri, Pinus jeffreyi, Pinus sylvestris ...*), les pins n'étant attaqués que lorsque les autres espèces ne sont plus disponibles. Avec cette méthode, on retrouve, en plus des événements de perturbation, la composante climatique de la croissance. De cette façon on évite des éléments qui peuvent fausser les résultats, surtout dans la recherche des tendances à long terme. En effet, les épidémies, les éruptions volcaniques et les autres perturbations affectent la croissance pendant plusieurs années, voire plusieurs dizaines années (l'épidémie de tordeuses de 1949 dans le Nord des rocheuses persista plus de trente ans) et induisent une tendance à court ou moyen terme. Il est donc difficile de faire la part des choses entre perturbations et effets de certaines composantes climatiques, comme le CO_2, qui peuvent "tendancer" la croissance. Le désavantage de cette analyse est qu'elle nécessite plus de travail après traitement, comparativement aux méthodes traditionnelles, puisqu'il est nécessaire de remettre les séries dans le bon sens (l'ICA fait faire des rotations aux données), et d'identifier quel composant correspond à quoi (perturbation, climat, ...). Mais les outils informatiques actuels permettent de réduire considérablement le durée de ces travaux.

Dans un second temps, ce nouvel outil analytique et sa mise en pratique furent appliqués à la recherche d'un effet de l'"assombrissement global" sur la croissance. Dans le premier chapitre traitant de ce sujet (Chapitre III) nous avons montré que la corrélation entre le cycle solaire et la croissance radiale des arbres n'est pas stable au Népal. Fait étonnant,

puisque le cycle solaire et la croissance sont stables dans le temps. De plus, la même analyse en Argentine et en Sibérie ne donne pas de changement à long terme dans cette corrélation. La seule explication dans le cas du Népal est que quelque chose, dans l'atmosphère, agit sur cette relation. Or, le Népal se situe directement aux frontières de la région la plus peuplée du monde (Uttar Pradesh, Inde : 167 millions d'habitants en 2001 sur 1/6 de la superficie du Québec). La pollution atmosphérique causée par les combustibles fossiles et les brûlages agricoles est une des explications possibles.

En poussant plus en avant sur cet effet de la pollution atmosphérique il est apparu que cette tendance devait être due à l'augmentation de lumière diffuse générée par la mise en suspension de poussières liées aux combustibles fossiles dans l'atmosphère. Cette augmentation de lumière diffuse est mesurée depuis plusieurs années, mais son effet sur la croissance n'était que théorique, ou du moins les études se limitaient aux phénomènes exceptionnels que sont les éruptions volcaniques qui la génèrent en libérant du SO_2. Notre contribution dans ce domaine a permis de montrer que la lumière diffuse agissait globalement et non pas uniquement lors des éruptions volcaniques dans les milieux ayant subi des stress hydriques importants comme en forêt Méditerranéenne ou en altitude sur des dépôts de surfaces minces.

Enfin une hypothèse sur l'effet de la lumière diffuse restait à être envisagée. Lorsque l'on augmente la lumière diffuse, la lumière directe diminue et la somme de l'énergie arrivant au sol diminue également. Il y a donc une diminution de la température, ce qui s'observe très bien durant les éruptions volcaniques. Or, cette diminution de température pourrait agir en sens inverse et contrebalancer le gain en croissance dû à la lumière diffuse. Ceci serait le cas dans les écosystèmes tempérés et boréaux. Pour vérifier cela nous avons étudié la réponse des arbres à la lumière diffuse durant les deux dernières éruptions volcaniques d'importance : celle d'El Chichón (Mexique) en 1982 et du Mont Pinatubo (Indonésie) en 1991. A la différence du Mont Pinatubo, l'éruption d'El Chichón a eu lieu pendant l'épisode d'El Niño le plus important du siècle dernier. Et au lieu d'avoir une chute de température globale, comme pendant l'éruption du Mont Pinatubo, la température a légèrement augmenté car les deux phénomènes se sont compensés. Au

final, aucune différence dans la réponse des arbres durant ces deux éruptions n'a été observée, et environ un tiers des sites a montré une augmentation de croissance. La lumière diffuse joue donc un rôle prépondérant dans la croissance des arbres qui annule l'effet de la baisse de température qui lui est associée.

Perspectives

Au vu de l'ensemble des résultats de cette thèse, la lumière diffuse semble être un phénomène agissant non marginalement sur la croissance des arbres. Des travaux ont montré que l'augmentation de lumière diffuse avait du affecter positivement le bilan de carbone (Mercado *et al.*, 2009) mais ces travaux ne se basent que sur des modèles, donc sans vérifications sur le terrain. Des travaux permettant de lier cette approche à des données de terrain utilisant la méthodologie de cette thèse pourraient être prometteurs pour analyser les effets du climat sur la croissance en détail. Parallèlement, la recherche d'un effet de la fertilisation au CO_2 sur la croissance des arbres va être encore plus difficile au vu des résultats de cette thèse. Cette difficulté supplémentaire est liée au problème de divergence (difference entre la reconstruction de la température par les cernes et les enregistrements issus des stations météorologiques) qui est lié à la lumière diffuse. Une recherche de l'effet du CO_2 sur la croissance nécessite donc de contrôler les données pour la lumière diffuse tout en séparant les deux effets. La difficulté de cet objectif réside dans la recherche de tendances qui ont la même origine : l'utilisation des combustibles fossiles. En effet, on peut supposer que ces tendances sont similaires et donc difficiles à distinguer l'une de l'autre. Cependant, ceci reste envisageable dans un cadre contrôlé, comme dans le projet FACE (Free air CO_2 enrichment) puisque dans ce cas-ci certaines conditions pourraient être ajustées pour faire ressortir l'une ou l'autre de ces tendances.

APPENDICE A

CHAPTER II : ICA SENSITIVITY

In this appendix we show how sensitive the ICA can be for spike detection. We ran the analysis on 100 series of 100 random values (normal distribution with mean of 0 and standard deviation of one), a new randomization was used for each simulation. Some of the series (Table A1) had one of their values increased by a fixed value at the same position in the series in order to simulate a spike/disturbance. Thus the resulting values deviate more and more from the initial distribution. An ANOVA test shows how far the spike values deviate from the other values for comparison (Table A2). We conducted 1000 ICA on the set of series for each case, with the number of series to be extracted being 2 : one for the noise and one for the spike. Results are shown in Table A1 and Figure A1. Overall, ICA detects spikes with ease when they are present in 50% of the data, reaching 100% of detection with spikes at 1.5. The detection ability decreases below these thresholds.

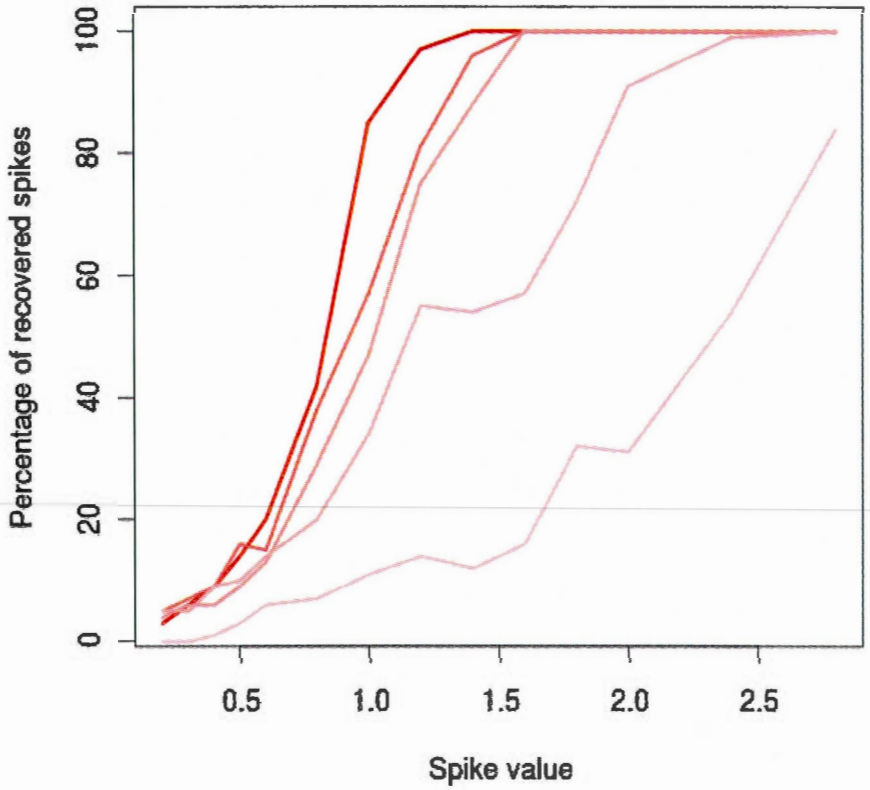

Figure A.1 Results of spike detection by ICA. Each curve represents table A1 data with a color ranging from dark red for 100 percent of spike in the data to light red for 10 percent of spikes.

Tableau A.1 Spike detection results by ICA. Each row gives different spike values which represents the value added and each column gives the percentage of series with spikes. Results give the percentage of detection based on 1000 tests.

Spikes	0.2	0.3	0.4	0.5	0.6	0.8	1	1.2	1.4	1.6	1.8	2	2.4	2.8
100	3	6	9	14	20	42	85	97	100	100	100	100	100	100
75	5	7	9	16	15	38	57	81	96	100	100	100	100	100
50	4	6	6	9	13	29	47	75	88	100	100	100	100	100
25	5	5	9	10	14	20	34	55	54	57	72	91	99	100
10	0	0	1	3	6	7	11	14	12	16	32	31	54	84

APPENDICE B

CHAPTER III : MAPS WITH SITE LOCATIONS

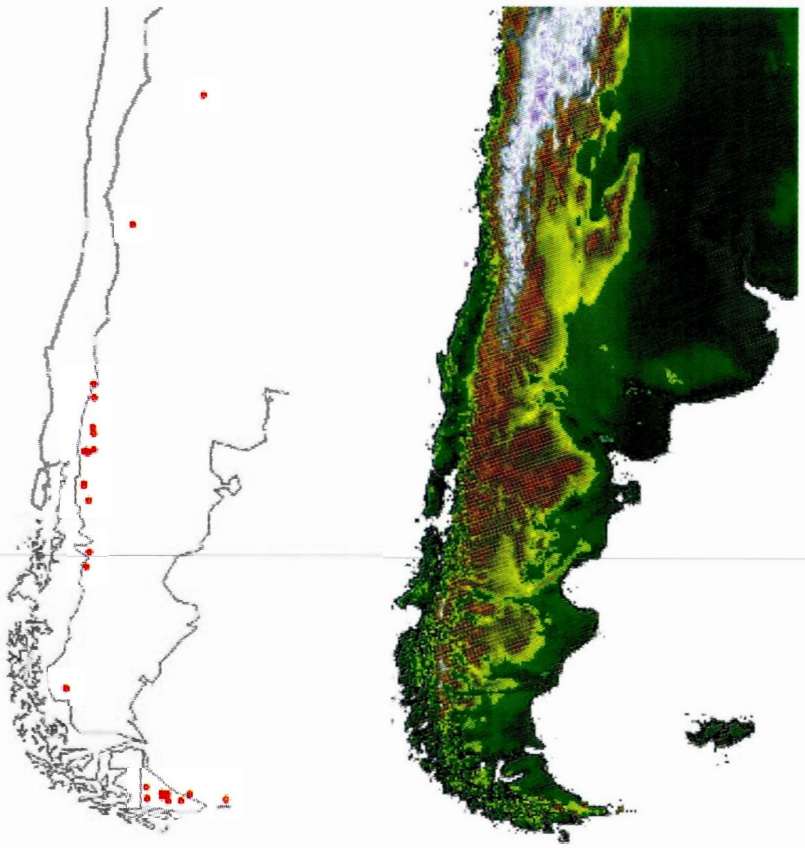

Figure B.1 Argentina tree ring width site locations map highlighted in red and elevation map from the NOAA National Geophysical Data Center

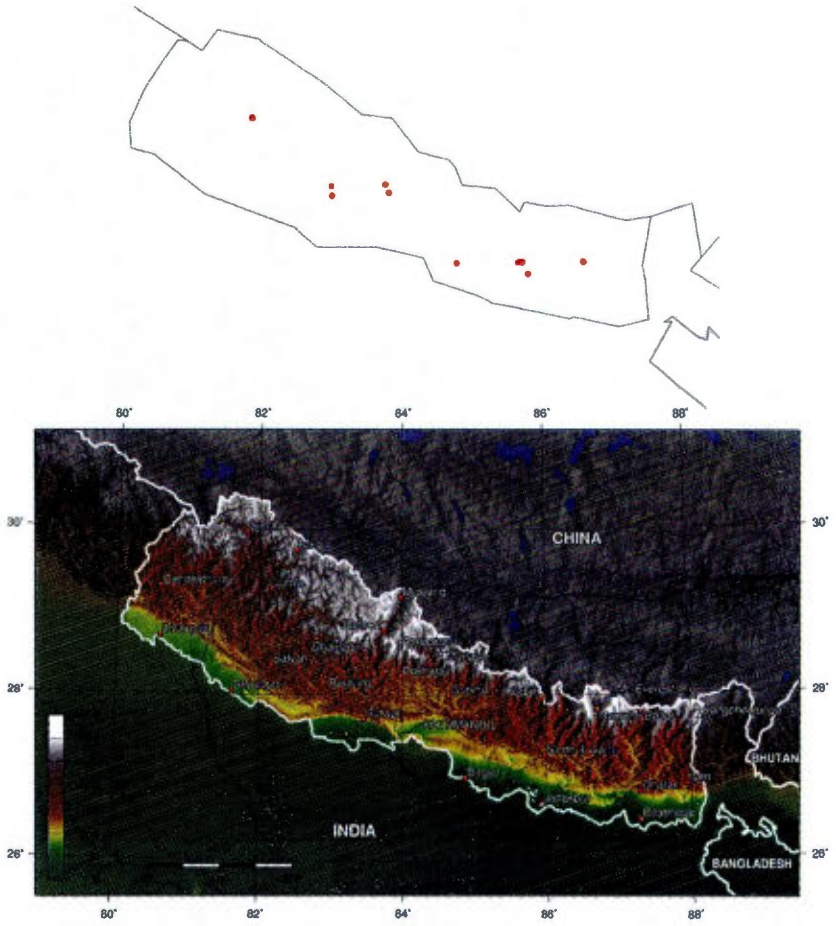

Figure B.2 Nepal tree ring width site locations map highlighted in red and topographic map build with data from the NOAA National Geophysical Data Center

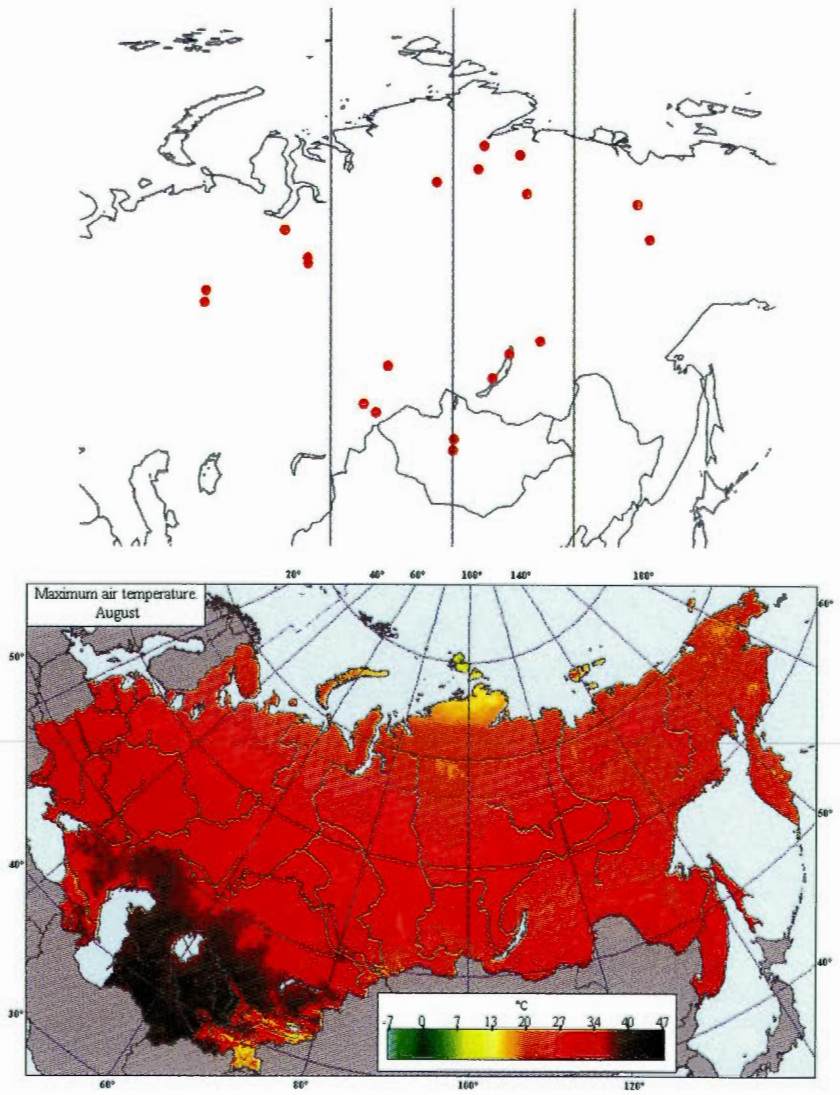

Figure B.3 Russia tree ring width site locations map highlighted in red and averaged values of mean annual maximum air temperature in August from the Interactive Agricultural Ecological Atlas of Russia and Neighboring Countries. Economic Plants and their Diseases, Pests and Weed

APPENDICE C

CHAPTER III : SPECTRUM ANALYSIS OF SIBERIA'S TEMPERATURE AND PRECIPITATION DATA

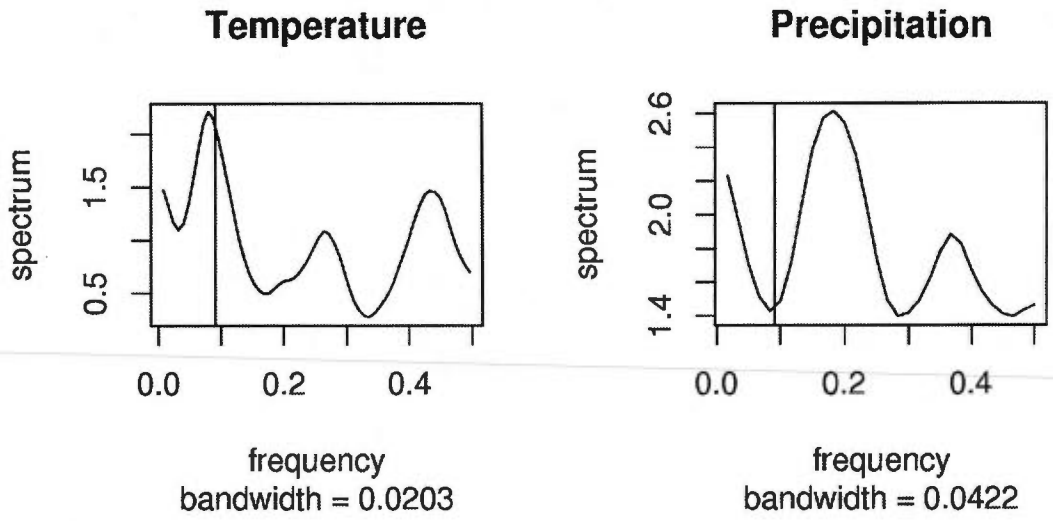

Figure C.1 Spectrum analysis of Siberia's temperature and precipitation data. The y axis shows the spectrum amplitude and the x axis its frequency.

APPENDICE D

CHAPTER III : RESULT OF ENGEL-GRANGER COINTEGRATION TEST

Tableau D.1 partie a : Chapter III results for Engel-Granger cointegration test. Site refers to the name of the site in the International Tree Ring Databank. With S the solar cycle, G tree radial growth, T temperature, P precipitations and the arrow refers to the direction of the test : S $\rightarrow$ G is solar cycle Granger causing growth and S $\leftarrow$ G is growth Granger causing the solar cycle; and the number in these columns is the error correction model which give the speed of adjustment between the two variables considered, and when taken as absolute value a lower value indicate a lower speed of adjustment. And p refers to the p value of the test.

Site	S $\leftarrow$ G	p	S $\rightarrow$ G	p	S $\leftarrow$ T	p	S $\rightarrow$ T	p	S $\leftarrow$ P	p	S $\rightarrow$ P	p
Arg040	-0.329	0.000	-0.735	0.000	-0.321	0.000	-0.577	0.000	0.110	0.049	0.018	0.533
Arg060	-0.305	0.000	-0.525	0.000	-0.317	0.000	-0.555	0.000	-0.033	0.520	-0.019	0.497
Arg051	-0.305	0.000	-0.436	0.000	-0.321	0.000	-0.577	0.000	0.110	0.049	0.018	0.533
Arg061	-0.293	0.000	-0.500	0.000	0.124	0.003	-0.065	0.430	0.001	0.981	0.016	0.570
Arg038	-0.285	0.000	-0.547	0.000	-0.188	0.000	-0.050	0.535	-0.006	0.904	-0.013	0.650
Arg066	-0.295	0.000	-0.408	0.000	-0.259	0.000	0.066	0.424	-0.006	0.900	0.010	0.724
Arg059	-0.304	0.000	-0.413	0.000	-0.320	0.000	-0.558	0.000	0.095	0.066	0.008	0.768
Arg022	-0.305	0.000	-0.627	0.000	-0.317	0.000	-0.577	0.000	0.124	0.022	0.050	0.101
Arg055	-0.306	0.000	-0.639	0.000	-0.320	0.000	-0.558	0.000	0.095	0.066	0.008	0.768
Arg033	-0.305	0.000	-0.907	0.000	-0.322	0.000	-0.548	0.000	0.038	0.458	-0.015	0.622
Arg034	-0.315	0.000	-0.890	0.000	-0.330	0.000	-0.553	0.000	0.030	0.561	0.024	0.404
Arg028	-0.316	0.000	-0.724	0.000	-0.317	0.000	-0.586	0.000	-0.218	0.000	0.094	0.003

Continued on next page

Tableau D.1: Chapter III results for Engel-Granger cointegration test (continued)

Site	S ← G	p	S → G	p	S ← T	p	S → T	p	S ← P	p	S → P	p
Arg063	-0.298	0.000	-1.013	0.000	-0.310	0.000	-0.526	0.000	-0.320	0.000	-0.086	0.016
Arg023	-0.293	0.000	-0.630	0.000	-0.306	0.000	-0.563	0.000	-0.309	0.000	-0.092	0.008
Arg037	-0.308	0.000	-0.422	0.000	-0.099	0.025	0.011	0.892	-0.064	0.251	0.030	0.290
Arg085	-0.297	0.000	-0.929	0.000	-0.296	0.000	-0.578	0.000	-0.299	0.000	-0.095	0.002
Arg093	-0.323	0.000	-0.437	0.000	-0.320	0.000	-0.558	0.000	0.095	0.066	0.008	0.768
Arg094	-0.310	0.000	-0.506	0.000	-0.321	0.000	-0.577	0.000	0.110	0.049	0.018	0.533
Arg095	-0.379	0.000	-1.087	0.000	-0.381	0.000	-0.438	0.019	-0.384	0.000	-0.118	0.182
Arg027	-0.321	0.000	-0.220	0.000	-0.331	0.000	-0.548	0.000	-0.020	0.705	0.028	0.322
Arg039	-0.310	0.000	-0.563	0.000	-0.310	0.000	-0.563	0.000	0.039	0.443	-0.012	0.674
Arg0107	-0.306	0.000	-0.536	0.000	-0.317	0.000	-0.563	0.000	0.031	0.550	-0.005	0.857
Arg104	-0.319	0.000	-0.749	0.000	-0.316	0.000	-0.549	0.000	-0.323	0.000	-0.120	0.002
Arg103	-0.336	0.000	-0.519	0.000	-0.332	0.000	-0.583	0.000	-0.339	0.000	-0.134	0.045
Arg075	-0.280	0.000	-0.428	0.000	0.141	0.001	-0.091	0.275	0.015	0.781	0.019	0.505
Arg068	-0.312	0.000	-0.687	0.000	-0.317	0.000	-0.577	0.000	0.124	0.022	0.050	0.101
Arg029	-0.326	0.000	-0.900	0.000	-0.315	0.000	-0.543	0.000	-0.034	0.535	0.000	0.997
Arg079	-0.327	0.000	-0.724	0.000	-0.326	0.000	-0.556	0.000	-0.008	0.883	0.031	0.291
Arg012	-0.330	0.000	-0.364	0.001	-0.302	0.000	-0.530	0.000	-0.322	0.000	-0.271	0.000

Continued on next page

Tableau D.1: Chapter III results for Engel-Granger cointegration test (continued)

Site	S ← G	p	S → G	p	S ← T	p	S → T	p	S ← P	p	S → P	p
Arg025	-0.418	0.000	-0.847	0.001	-0.385	0.000	-0.417	0.037	-0.387	0.000	-0.114	0.222
Arg035	-0.308	0.000	-0.631	0.000	-0.312	0.000	-0.541	0.000	-0.326	0.000	-0.256	0.000
Nepa3	-0.299	0.000	-0.732	0.000	0.159	0.001	-0.151	0.205	0.202	0.000	-0.072	0.558
Nepa4	-0.354	0.000	-0.272	0.002	-0.301	0.000	-0.853	0.000	-0.156	0.010	0.081	0.555
Nepa5	-0.324	0.000	-0.443	0.000	-0.100	0.060	-0.076	0.537	-0.139	0.025	0.077	0.578
Nepa6	-0.283	0.000	-0.414	0.000	-0.092	0.094	-0.056	0.631	-0.212	0.000	-0.147	0.229
Nepa7	-0.340	0.000	-0.679	0.000	0.132	0.005	0.189	0.116	0.076	0.172	0.245	0.047
Nepa8	-0.295	0.000	-0.430	0.000	0.100	0.072	0.009	0.943	0.202	0.001	0.023	0.854
Nepa9	-0.305	0.000	-0.630	0.000	-0.180	0.002	-0.063	0.596	-0.220	0.000	0.088	0.476
Nepa10	-0.315	0.000	-0.669	0.000	0.107	0.029	-0.140	0.229	-0.056	0.345	0.045	0.719
Nepa11	-0.320	0.000	-0.469	0.000	-0.188	0.000	0.113	0.344	-0.205	0.000	-0.012	0.924
Nepa12	-0.312	0.000	-0.394	0.000	-0.306	0.000	-0.852	0.000	-0.010	0.885	-0.052	0.710
Nepa13	-0.327	0.000	-0.281	0.000	0.149	0.003	0.021	0.854	0.202	0.000	-0.201	0.101
Nepa14	-0.313	0.000	-0.335	0.000	0.185	0.000	-0.044	0.707	0.127	0.019	0.050	0.687
Nepa15	-0.329	0.000	-0.355	0.000	-0.294	0.000	-0.628	0.000	-0.112	0.088	0.158	0.211
Nepa16	-0.317	0.000	-0.654	0.000	0.011	0.836	-0.049	0.685	0.001	0.985	0.024	0.855
Nepa17	-0.314	0.000	-0.291	0.000	-0.165	0.001	-0.003	0.982	-0.109	0.043	0.175	0.164

Continued on next page

Tableau D.1: Chapter III results for Engel-Granger cointegration test (continued)

Site	S ← G	p	S → G	p	S ← T	p	S → T	p	S ← P	p	S → P	p
Nepa18	-0.311	0.000	-0.751	0.000	0.107	0.029	-0.140	0.229	-0.055	0.348	0.045	0.719
Nepa19	-0.339	0.000	-0.303	0.002	-0.324	0.000	-0.565	0.002	-0.343	0.000	-0.852	0.000
Nepa20	-0.326	0.000	-0.946	0.000	-0.324	0.000	-0.870	0.000	-0.323	0.000	-0.807	0.000
mg010	0.012	0.718	-0.022	0.748	-0.241	0.000	-0.063	0.520	-0.272	0.000	0.174	0.160
mg011	-0.048	0.136	-0.009	0.873	-0.241	0.000	-0.063	0.520	-0.272	0.000	0.174	0.160
ru003	0.118	0.006	-0.023	0.818	-0.002	0.974	-0.029	0.793	-0.028	0.721	0.014	0.927
ru019	0.260	0.000	-0.017	0.854	-0.241	0.000	-0.063	0.520	-0.174	0.007	-0.056	0.650
ru037	0.195	0.000	-0.048	0.608	0.197	0.000	0.019	0.850	-0.105	0.091	-0.123	0.349
ru048	-0.062	0.078	0.040	0.567	0.197	0.000	0.019	0.850	-0.105	0.091	-0.123	0.349
ru076	0.262	0.000	0.032	0.728	0.092	0.083	-0.027	0.785	-0.212	0.001	-0.099	0.453
ru094	-0.337	0.000	-0.455	0.000	0.092	0.083	-0.027	0.785	-0.212	0.001	-0.099	0.453
ru103	0.044	0.371	-0.079	0.499	-0.142	0.002	0.061	0.533	-0.052	0.458	0.087	0.514
ru099	0.060	0.276	-0.005	0.957	0.092	0.083	-0.027	0.785	-0.212	0.001	-0.099	0.453
ru110	0.204	0.000	0.097	0.349	0.198	0.000	0.060	0.541	0.116	0.089	-0.080	0.533
ru129	0.002	0.950	-0.008	0.916	-0.205	0.000	0.193	0.064	0.250	0.000	0.063	0.641
ru131	0.127	0.005	0.106	0.229	-0.241	0.000	-0.063	0.520	0.245	0.000	-0.026	0.837
ru137	0.220	0.000	0.020	0.804	-0.241	0.000	-0.063	0.520	-0.174	0.007	-0.056	0.650

Continued on next page

Tableau D.1: Chapter III results for Engel-Granger cointegration test (continued)

Site	S ← G	p	S → G	p	S ← T	p	S → T	p	S ← P	p	S → P	p
ru155	0.289	0.000	-0.029	0.642	-0.241	0.000	-0.063	0.520	0.299	0.000	-0.072	0.565
ru158	-0.160	0.001	0.044	0.650	-0.241	0.000	-0.063	0.520	0.299	0.000	-0.072	0.565
ru159	-0.086	0.147	0.055	0.560	0.198	0.000	0.060	0.541	0.116	0.089	-0.080	0.533
ru165	-0.051	0.234	0.089	0.125	-0.241	0.000	-0.063	0.520	-0.272	0.000	0.174	0.160
ru167	0.085	0.311	0.013	0.949	-0.241	0.000	-0.063	0.520	-0.272	0.000	0.174	0.160
ru171	0.098	0.028	-0.078	0.447	-0.241	0.000	-0.063	0.520	-0.174	0.007	-0.056	0.650

Tableau D.2 partie b du tableau D.1 : Chapter III results for Engel-Granger cointegration test (continued)

Site	G ← T	p	G → T	p	G ← P	p	G → P	p
Arg040	-0.659	0.000	-0.586	0.000	-0.034	0.742	0.024	0.411
Arg060	-0.536	0.000	-0.545	0.000	0.029	0.735	-0.013	0.642
Arg051	-0.448	0.000	-0.583	0.000	0.086	0.355	0.024	0.396
Arg061	-0.107	0.169	-0.074	0.371	-0.029	0.736	0.019	0.501
Arg038	0.149	0.048	-0.062	0.447	-0.099	0.262	-0.011	0.689
Arg066	0.100	0.141	0.065	0.434	-0.033	0.700	0.004	0.894
Arg059	-0.419	0.000	-0.572	0.000	0.110	0.237	0.005	0.848
Arg022	-0.615	0.000	-0.559	0.000	0.082	0.445	0.037	0.227
Arg055	-0.637	0.000	-0.557	0.000	0.104	0.355	0.008	0.783
Arg033	-0.879	0.000	-0.538	0.000	-0.194	0.089	-0.015	0.620
Arg034	-0.892	0.000	-0.556	0.000	0.001	0.990	0.024	0.387
Arg028	-0.715	0.000	-0.588	0.000	-0.002	0.984	0.091	0.003
Arg063	-0.994	0.000	-0.521	0.000	-1.020	0.000	-0.080	0.024
Arg023	-0.612	0.000	-0.550	0.000	-0.636	0.000	-0.092	0.008
Arg037	0.004	0.959	0.028	0.737	0.002	0.986	0.028	0.326
Arg085	-0.939	0.000	-0.575	0.000	-0.914	0.000	-0.092	0.002
Arg093	-0.417	0.000	-0.561	0.000	-0.024	0.794	0.006	0.840
Arg094	-0.455	0.000	-0.609	0.000	0.160	0.090	0.020	0.496
Arg095	-0.956	0.000	-0.369	0.041	-1.063	0.000	-0.111	0.210
Arg027	-0.220	0.000	-0.550	0.000	0.005	0.944	0.017	0.567
Arg039	NA	0.329	NA	0.329	-0.170	0.089	-0.012	0.662
Arg0107	-0.526	0.000	-0.562	0.000	0.015	0.874	0.001	0.965
Arg104	-0.763	0.000	-0.504	0.000	-0.764	0.000	-0.117	0.003
Arg103	-0.438	0.001	-0.575	0.000	-0.501	0.000	-0.124	0.059
Arg075	-0.039	0.596	-0.072	0.386	-0.005	0.961	0.016	0.578

Continued on next page

Tableau D.2: Chapter III results for Engel-Granger cointegration test (continued)

Site	G ← T	p	G → T	p	G ← P	p	G → P	p
Arg068	-0.709	0.000	-0.588	0.000	-0.062	0.554	0.047	0.113
Arg029	-0.898	0.000	-0.560	0.000	0.123	0.281	0.000	0.986
Arg079	-0.706	0.000	-0.567	0.000	-0.068	0.537	0.033	0.254
Arg012	-0.326	0.002	-0.529	0.000	-0.398	0.000	-0.273	0.000
Arg025	-0.690	0.005	-0.545	0.008	-0.671	0.003	-0.116	0.210
Arg035	-0.723	0.000	-0.550	0.000	-0.625	0.000	-0.236	0.000
Nepa3	0.020	0.849	-0.151	0.200	0.080	0.480	-0.019	0.880
Nepa4	-0.242	0.002	-0.824	0.000	-0.036	0.639	0.040	0.766
Nepa5	-0.036	0.721	-0.056	0.647	0.219	0.070	0.058	0.666
Nepa6	-0.034	0.735	-0.060	0.623	0.007	0.943	-0.147	0.226
Nepa7	0.082	0.409	0.191	0.114	0.024	0.842	0.212	0.102
Nepa8	0.000	0.998	-0.001	0.994	-0.006	0.947	0.035	0.779
Nepa9	0.038	0.693	-0.061	0.606	-0.129	0.257	0.092	0.449
Nepa10	-0.134	0.214	-0.110	0.334	0.095	0.436	0.044	0.720
Nepa11	-0.006	0.948	0.119	0.344	0.081	0.407	-0.014	0.912
Nepa12	-0.373	0.000	-0.841	0.000	-0.067	0.510	-0.053	0.700
Nepa13	0.013	0.862	0.056	0.625	0.179	0.078	-0.199	0.105
Nepa14	-0.084	0.273	-0.050	0.670	-0.013	0.890	0.048	0.704
Nepa15	-0.351	0.000	-0.601	0.000	0.021	0.850	0.154	0.224
Nepa16	0.024	0.830	-0.041	0.731	-0.080	0.535	0.038	0.771
Nepa17	0.059	0.350	-0.004	0.974	0.020	0.772	0.150	0.234
Nepa18	0.089	0.384	-0.138	0.236	0.143	0.225	0.044	0.720
Nepa19	-0.047	0.674	-0.572	0.001	-0.304	0.002	-0.806	0.000
Nepa20	-0.981	0.000	-0.852	0.000	-0.970	0.000	-0.802	0.000
mg010	0.065	0.453	-0.089	0.350	-0.200	0.078	0.019	0.869
mg011	-0.025	0.772	-0.071	0.466	0.143	0.167	-0.033	0.780

Continued on next page

Tableau D.2: Chapter III results for Engel-Granger cointegration test (continued)

Site	G ← T	p	G → T	p	G ← P	p	G → P	p
ru003	-0.015	0.887	0.022	0.836	-0.045	0.749	0.116	0.384
ru019	-0.114	0.214	-0.094	0.336	-0.018	0.878	-0.017	0.883
ru037	0.001	0.992	0.045	0.641	0.002	0.988	-0.132	0.263
ru048	-0.009	0.917	0.039	0.696	-0.012	0.916	-0.149	0.197
ru076	0.037	0.686	-0.016	0.872	0.010	0.928	-0.131	0.262
ru094	-0.011	0.887	-0.016	0.867	0.142	0.179	-0.153	0.198
ru103	-0.052	0.654	0.043	0.677	-0.064	0.636	0.006	0.956
ru099	-0.017	0.857	0.278	0.010	0.104	0.332	-0.117	0.321
ru110	-0.180	0.089	0.050	0.621	0.026	0.843	-0.025	0.822
ru129	0.033	0.698	0.168	0.111	0.017	0.865	0.149	0.219
ru131	0.125	0.154	-0.138	0.129	0.177	0.097	0.025	0.826
ru137	0.158	0.059	-0.049	0.617	-0.080	0.482	-0.048	0.682
ru155	-0.042	0.476	-0.082	0.405	0.098	0.101	-0.008	0.943
ru158	0.096	0.310	0.086	0.356	-0.135	0.224	0.051	0.658
ru159	0.047	0.620	0.122	0.351	0.019	0.843	-0.005	0.963
ru165	-0.032	0.582	-0.065	0.510	-0.106	0.254	0.040	0.745
ru167	-0.169	0.374	0.448	0.005	0.119	0.516	-0.256	0.164
ru171	0.114	0.264	0.009	0.927	-0.043	0.726	0.044	0.712

APPENDICE E

CHAPTER IV : TREE RING WIDTH SERIES AVAILABLE FOR EACH YEAR

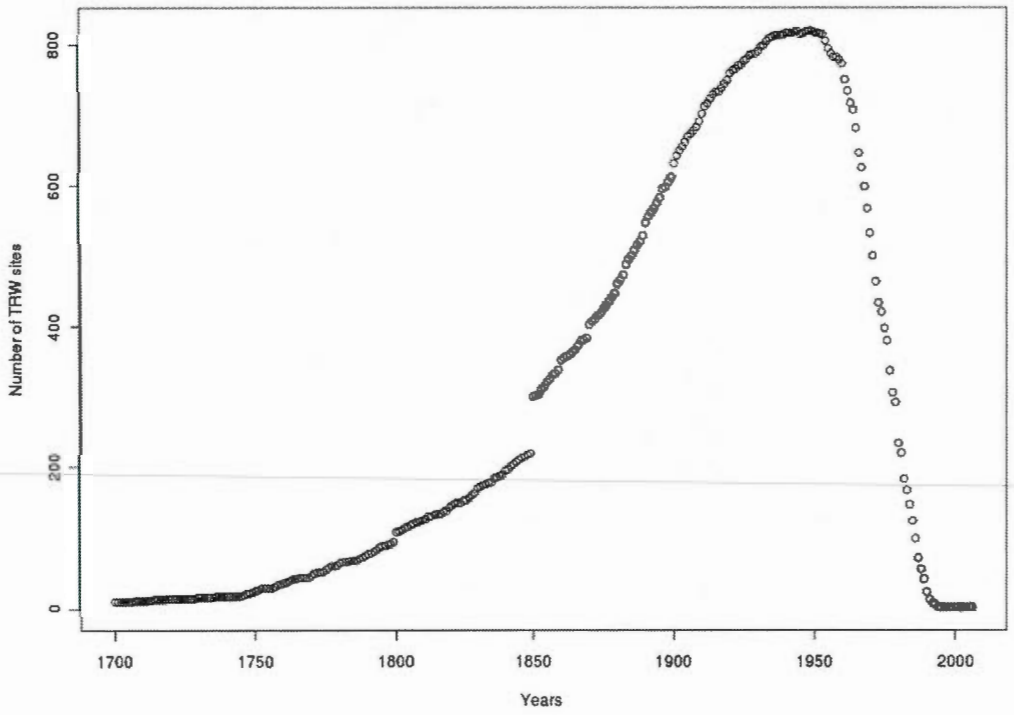

Figure E.1 Number of tree ring width sites (TRW, for a total of 841) with data for each year over the 1700–2005 period.

APPENDICE F

CHAPTER IV : DATA SUMMARY

Tableau F.1 : Chapter IV data summary. Summary of tree ring width data used in this study. Only the first rows are presented here. Location refers to site name, Long to the longitude, Lat to the latitude, Elev to the elevation, Precip to the annual precipitations, Temp to the annual mean temperature, AOD 440 to the mean atmospheric optical depth at 440 nm for the 1998–2005 period, TRW 150 km to the number of tree ring width site in a 150-km radius from the site, ICA 150 km the number of independent component successfully extracted within a range of 150 km from the site.

Location	Long	Lat	Elev	Precip	Temp	AOD 440	TRW 150km	ICA 150km
Chapais	-75.98	49.82	381	693.19	-1.73	0.12	1	0
Clermont Ferrand	2.96	45.76	1464	726.59	11.53	0.12	1	1
Dunkerque	2.37	51.04	0	749.07	9.89	0.22	1	1
El Arenosillo	-6.73	37.11	0	656.11	14.13	0.18	1	1
Flin Flon	-101.69	54.67	305	482.44	-1.9	0.3	1	1
Halifax	-63.59	44.64	65	1152.62	4.4	0.13	1	1
Helsinki Lighthouse	24.93	59.95	0	497.21	4.78	NA	1	1
Thompson	-97.85	55.8	218	455.87	-4.39	0.19	1	0
Hermosillo	-110.96	29.08	237	177.5	17.69	0.11	1	1
Kejimkujik	-65.28	44.38	154	1190.59	4.01	0.15	1	1
Kellogg LTER	-85.37	42.41	293	784.88	6.87	0.26	1	0
Kolimbari	23.78	35.53	0	676.5	11.51	0.33	1	0
Oostende	2.93	51.23	23	689.7	10.58	0.23	1	1

Continued on next page

Tableau F.1: Chapter IV data summary (continued)

Location	Long.	Lat.	Elev.	Prec.	Temp.	AOD 440	TRW 150km	ICA 150km
SEDE BOKER	34.78	30.86	480	1323.48	12.18	0.21	1	0
Yakutsk	129.37	61.66	118	288.13	-10.19	0.14	1	1
Tamihua	-97.44	21.26	10	440.3	20.23	0.4	1	2
Stennis	-89.62	30.37	20	1426.23	18.29	0.22	1	1
Windsor B	-83.08	42.28	200	744.86	6.8	0.16	1	1
Brookhaven	-72.89	40.87	33	1050.65	7.75	0.25	2	2
Ulaangom	92.08	49.97	1363	526.63	-4.13	0.2	2	0
Trinidad Head	-124.15	41.05	105	2444.46	7.58	0.11	2	1
Kolfield	-74.48	39.8	50	1085.89	7.92	0.56	2	2
Belsk	20.79	51.84	190	623.26	7.87	0.28	2	2
Nairobi	36.87	-1.34	1650	1216.32	20.72	0.19	2	2
T0 MAX MEX	-99.15	19.49	2257	696.36	19.83	0.38	2	3
Mexico City	-99.18	19.33	2268	696.36	19.83	0.43	2	3
KONZA EDC	-96.61	39.1	341	612.77	10.15	0.17	2	1
Helgoland	7.89	54.18	33	NA	NA	0.23	2	0
San Nicolas	-119.49	33.26	133	627.34	11.77	0.09	2	1
Candle Lake	-105.27	53.73	503	427.29	-0.06	0.07	3	2

Continued on next page

Tableau F.1: Chapter IV data summary (continued)

Location	Long.	Lat.	Elev.	Prec.	Temp.	AOD 440	TRW 150km	ICA 150km
Pickle Lake	-90.22	51.45	393	601.36	-1.1	0.12	3	3
Nes Ziona	34.79	31.92	40	NA	NA	0.27	3	1
T1 MAX MEX	-98.98	19.7	2272	699.38	19.83	0.32	3	4
Dead Sea	35.45	31.1	-410	1322.7	12.11	0.36	3	1
Osaka	135.59	34.65	50	2766.36	19.84	0.44	3	0
Rame Head	-4.15	50.37	0	1332.52	9.88	0.2	3	1
Mont Joli	-68.16	48.64	30	1009.14	-0.9	0.18	3	1
Paddockwood	-105.5	53.5	503	427.29	-0.06	0.31	3	2
Rome Tor Vergata	12.65	41.84	130	795.36	11.23	0.24	3	2
IMAA Potenza	15.72	40.6	820	815.35	14.75	0.15	3	3
Cart Site 1	-97.49	36.61	318	554.21	12.25	0.18	4	4
Ahi De Cara	-3.23	37.12	2103	568.65	16.12	0.05	4	4
Armilla	-3.24	37.13	691	568.65	16.12	0.17	4	4
Andenes	16.01	69.28	379	NA	NA	0.12	4	4
Cart Site 2	-97.49	36.61	318	554.21	12.25	0.18	4	4
Sioux Falls 1	-96.63	43.74	500	463.55	6.65	0.14	4	3
Chequamegon	-90.25	45.93	0	685.54	3.43	0.13	4	3

Continued on next page

Tableau F.1: Chapter IV data summary (continued)

Location	Long.	Lat.	Elev.	Prec.	Temp.	AOD 440	TRW 150km	ICA 150km
Granada	-3.61	37.16	680	605.69	16.22	0.19	4	4
Sioux Falls 2	-96.63	43.74	500	463.55	6.65	0.15	4	3
Univ of Houston	-95.34	29.72	65	840.69	18.75	0.19	4	4
Mace Head	-9.9	53.33	20	NA	NA	0.08	4	2
IMS-METU-ERDEMLI	34.26	36.57	3	459.86	11.56	0.29	5	4
Albany Oregon	-123.07	44.58	67	2608.1	5.71	0.39	5	4
Pitres	-3.22	36.93	1252	568.65	16.12	0.17	5	4
Barcelona	2.12	41.39	125	958.55	12.76	0.24	6	6
Bondville	-88.37	40.05	212	929.07	9.53	0.24	6	5
Cheritan	-75.97	37.29	5	1113.58	11.59	0.7	6	3
Cove	-75.71	36.9	37	1127.7	12.02	0.24	6	3
Egbert 1	-79.75	44.23	264	861.13	4.93	0.17	6	3
Cove Seaprism	-75.71	36.9	37	1127.7	12.02	0.34	6	3
Egbert 2	-79.75	44.23	264	861.13	4.93	0.14	6	3
EOPACE1	-75.75	36.18	0	1079.75	13.23	0.15	6	3
EOPACE2	-75.75	36.18	0	1079.75	13.23	0.15	6	3
Gustav Dalen Tower	17.47	58.59	25	719.7	4.15	0.12	6	3

Continued on next page

Tableau F.1: Chapter IV data summary (continued)

Location	Long.	Lat.	Elev.	Prec.	Temp.	AOD 440	TRW 150km	ICA 150km
Hog Island	-75.7	37.42	50	1113.58	11.59	0.56	6	3
Missoula	-114.08	46.92	1028	633.19	4.46	0.15	6	5
Oyster	-75.93	37.3	8	1113.58	11.59	0.32	6	3
Rochester	-77.59	44.23	0	893.18	4.82	0.19	6	3
Toronto	-79.47	43.97	300	846.86	4.95	0.22	6	3
Wallops	-75.48	37.94	10	1069.82	11.23	0.26	6	3
Columbia SC	-81.04	34.02	104	1360.25	13.66	0.28	7	6
Sandy Hook	-73.99	40.45	0	1076.53	7.48	0.58	7	7
GISS	-73.96	40.8	50	1044.18	7.84	0.26	7	7
Lille	3.14	50.61	60	656.41	11.26	0.28	7	4
CCNY	-73.95	40.82	100	1044.18	7.84	0.24	7	7
Carlsbad	-104.23	32.37	942	344.81	10.71	0.16	8	7
SERC	-76.5	38.88	10	1054.6	9.75	0.27	8	6
Hamburg	9.97	53.57	105	606.03	2.96	0.21	8	2
La Crau	4.82	43.58	32	931.53	10.77	0.23	8	6
Jug Bay	-76.78	38.77	10	1039.65	9.7	0.19	8	7
GSFC	-76.84	38.99	87	1039.65	9.7	0.27	8	7

Continued on next page

Tableau F.1: Chapter IV data summary (continued)

Location	Long.	Lat.	Elev.	Prec.	Temp.	AOD 440	TRW 150km	ICA 150km
Avignon	4.88	43.93	32	895.04	10.59	0.21	8	6
Toulouse	1.37	43.58	150	806.32	10.5	0.2	9	8
NASA Ames	-122.06	37.42	10	1626.14	8.92	0.12	9	6
Biarritz	-1.55	43.48	0	NA	NA	0.17	9	8
Toulouse	1.48	43.56	150	806.32	10.5	0.19	9	8
Aire Adour	0.25	43.7	80	871.88	8.32	0.27	10	7
Tarbes	0.08	43.25	350	871.88	8.32	0.17	10	7
Penn State Univ	-78.08	40.74	401	926.56	8.48	0.39	11	8
MVCO	-70.55	41.3	10	1123.52	7.29	0.24	11	0
Cartel 1	-71.93	45.38	300	1024.76	2.37	0.15	12	12
Bordman	-119.67	45.82	200	1343.27	8.6	0.19	12	10
Cartel 2	-71.93	45.38	300	1024.76	2.37	0.13	12	12
Karlsruhe	8.43	49.09	140	823.69	9.69	0.3	13	8
Philadelphia	-75.01	40.04	20	1067.9	8.05	0.51	13	13
Mainz	8.3	50	150	752.7	10.63	0.23	13	8
Nicelli Airport	12.38	45.43	13	1441.6	5.97	0.27	14	7
Venise	12.51	45.31	10	1455.27	5.45	0.32	14	7

Continued on next page

Tableau F.1: Chapter IV data summary (continued)

Location	Long.	Lat.	Elev.	Prec.	Temp.	AOD 440	TRW 150km	ICA 150km
Spokane	-117.53	47.62	360	1361.96	5.19	0.14	14	12
ISDGM CNR	12.33	45.44	20	1441.6	5.97	0.36	14	7
Palencia	-4.52	41.99	750	763.57	13.98	0.16	16	10
Richland	-119.28	46.34	123	1459.7	7	0.14	16	11
Railroad Valley	-115.96	38.5	1435	469.85	9.38	0.07	17	13
MISR-JPL	-118.25	34.25	450	457.65	12.75	0.27	17	15
UCLA	-118.45	34.07	131	381.26	13.27	0.19	17	15
Lunar Lake	-115.99	38.39	1908	469.85	9.38	0.14	17	13
Toulon	6.01	43.14	50	1038.43	9.52	0.18	18	10
Lochiel	-122.6	49.03	0	1783.83	4.84	0.1	29	19
HJAndrews	-122.22	44.24	830	2185.21	5.5	0.09	30	18
Angiola	-119.54	35.95	210	758.46	12.37	0.28	36	30
Owens Lake	-117.87	36.49	1167	586.45	11.78	0.03	40	31
China Lake	-117.75	35.67	800	420.16	13.08	0.04	52	45
Ispra	8.63	45.8	235	871.41	9.8	0.37	62	49
Corcoran	-119.57	36.1	110	758.46	12.37	0.21	76	59
Fresno 2	-119.77	36.78	0	781.69	13.12	0.16	76	59

Continued on next page

Tableau F.1: Chapter IV data summary (continued)

Location	Long.	Lat.	Elev.	Prec.	Temp.	AOD 440	TRW 150km	ICA 150km
Fresno 1	-119.77	36.78	0	781.69	13.12	0.2	76	59
SSA YJP BOREAS	-104.65	53.68	490	438.74	-0.13	0.29	1	0
NSA YJP BOREAS	-98.29	55.9	290	458.88	-4.26	0.22	1	0
SS OJP BOREAS	-104.69	53.92	500	447.88	-0.38	0.23	1	0
Madison	-89.41	43.07	326	755.76	6.56	0.3	1	1
ETNA	15.02	37.61	736	1089.12	11.43	0.2	1	1
SMHI	16.15	58.58	0	730.58	4.08	0.13	2	1
Sopot	18.57	54.45	0	748.29	10.34	0.25	2	0
Dunedin	170.51	-45.86	43	2527.91	8.86	0.06	2	1
Creteil	2.44	48.79	57	813.58	10.56	0.22	4	3
Paris	2.33	48.87	50	813.58	10.56	0.24	4	3
Messina	15.57	38.2	15	915.02	9.77	0.26	4	4
Fontainebleau	2.68	48.41	85	638.36	5.84	0.25	4	3
Palaiseau	2.21	48.7	156	660.57	5.08	0.22	4	3
Epanomi	22.98	40.38	20	801.78	11.47	0.28	5	4
Kuujjuarapik	-77.8	55.3	0	NA	NA	0.09	6	6
UCSB	-119.85	34.42	33	737.09	10.41	0.14	6	4

Continued on next page

Tableau F.1: Chapter IV data summary (continued)

Location	Long.	Lat.	Elev.	Prec.	Temp.	AOD 440	TRW 150km	ICA 150km
OceolaNF	-82.44	30.21	0	1319.87	18.54	0.27	7	7
OkefenokeeNWR	-82.13	30.74	0	1268.93	18.36	0.17	7	7
Ames	-93.78	42.02	338	618.74	7.51	0.16	7	4
Bonanza Creek	-148.32	64.74	150	279.13	-5.16	0.15	9	7
USDA	-76.88	39.03	50	1039.65	9.7	0.25	9	8
MD Science Center	-76.62	39.28	15	1052.99	9.05	0.27	9	8
Burtonsville	-76.95	39.09	140	1039.65	9.7	0.14	9	8
USDA-BARC	-76.93	39.03	46	1039.65	9.7	0.22	9	8
La Jolla	-117.25	32.87	115	480.8	12.48	0.14	10	10
Tonopah Airport	-117.09	38.05	1580	448.08	10.95	0.06	11	6
Gerlitzen	13.91	46.68	1900	872.89	8.65	0.04	12	5
Red Bluff	-122.25	40.15	40	1102.16	5.54	0.18	13	9
Hagerstown	-77.73	39.71	200	999.52	9.12	0.46	16	14
Rimrock	-116.99	46.49	824	968.5	6.69	0.11	16	12
Gaithersburg	-77.21	39.13	50	1011.4	9.66	0.28	16	14
Walker Branch	-84.29	35.96	365	1147.09	13.47	0.26	31	22
Maricopa	-111.97	33.07	360	303.5	17.19	0.1	32	22

Continued on next page

Tableau F.1: Chapter IV data summary (continued)

Location	Long.	Lat.	Elev.	Prec.	Temp.	AOD 440	TRW 150km	ICA 150km
Rottnest Island	115.5	-32	70	118.76	24.44	0.06	2	2
Waskesiu	-106.08	53.92	550	433.34	-0.19	0.14	2	2
Perth	115.89	-32.01	0	118.76	24.44	0.07	2	2
Churchill	-93.82	58.74	10	396.45	-4.68	0.11	3	2
LW-SCAN	-97.98	34.96	358	599.38	14.24	0.22	5	5
Niabrara	-100.02	42.77	730	432.52	7.27	0.19	5	2
Monterey	-121.86	36.59	50	1328.87	10.56	0.11	9	6
Moss Landing	-121.79	36.79	20	1233.83	10.6	0.08	9	6
NASA LaRC	-76.38	37.11	5	1132.19	11.87	0.12	11	7
Munich University	11.57	48.15	533	706.98	8.97	0.15	22	15
Munich Maisach	11.26	48.21	520	757.37	9.14	0.24	22	15
Sevilleta	-106.89	34.36	1477	303.66	10.47	0.09	30	21
Kelowna	-119.37	49.96	344	734.12	3.18	0.13	47	42
SMEX	-93.66	41.94	316	618.74	7.51	0.38	8	5
Villefranche	7.33	43.68	130	1151.03	8.65	0.26	10	4
Harvard Forest	-72.19	42.53	322	1010.01	6.11	0.19	13	5
Modena	10.95	44.63	56	1696.33	3.83	0.37	13	10

Continued on next page

Tableau F.1: Chapter IV data summary (continued)

Location	Long.	Lat.	Elev.	Prec.	Temp.	AOD 440	TRW 150km	ICA 150km
Jornada	-106.52	32.35	1288	394.31	11.21	0.1	14	9
Rossfeld	7.63	48.34	167	846.84	9.59	0.4	46	41
JonesERC	-84.47	31.23	50	1380.11	17.53	0.14	6	3
Norfolk State Univ	-76.26	36.85	20	1132.19	11.87	0.36	7	4
Hampton Roads	-76.45	36.78	10	1132.19	11.87	0.54	7	4
Chilbolton	-1.44	51.14	88	1015.47	8.65	0.19	12	3
Realtor	5.38	43.49	208	947.5	10.56	0.24	13	8
Vinon	5.76	43.71	304	969.45	10.41	0.22	13	8
OHP Observatoire	5.71	43.94	680	947.12	10.33	0.14	13	8
Marseille	5.38	43.28	100	947.5	10.56	0.26	13	8
Sterling	-77.47	38.98	50	1011.4	9.66	0.35	15	13
Carpentras	5.06	44.08	100	915.32	10.49	0.21	19	11
Ukiah	-118.92	45.13	1100	1007.53	9.4	0.18	21	16
Tombstone	-110.05	31.74	1408	226.76	20.48	0.07	35	25
Red Mountain Pass	-107.73	37.91	3368	382.68	6.61	0.07	49	41
The Hague	4.33	52.11	18	775.24	8.64	0.22	22	2
Cabauw	4.93	51.97	-1	792.83	7.18	0.34	28	2

Continued on next page

Tableau F.1: Chapter IV data summary (continued)

Location	Long.	Lat.	Elev.	Prec.	Temp.	AOD 440	TRW 150km	ICA 150km
Laegeren	8.35	47.48	735	709.22	10.09	0.19	103	82
Howland	-68.73	45.2	100	1088.92	3.16	0.14	18	16
Big Meadows	-78.44	38.52	1082	1061.59	10.14	0.09	22	18
Davos	9.84	46.81	1596	766.72	9.7	0.11	28	18
Billerica	-71.27	42.53	82	1152.77	5.63	0.16	14	2
Saturn Island	-123.13	48.78	200	1696.24	5.58	0.08	36	25
Los Alamos	-106.33	35.87	2350	351.47	5.75	0.07	47	36
EVK2-CNR	86.81	27.96	5050	740.01	-1.3	0.07	26	21
Rogers Dry Lake	-117.89	34.93	680	414.27	13.92	0.09	30	27
Table Mountain CA	-117.68	34.38	2200	428.05	13.36	0.05	30	27
Tucson	-110.95	32.23	779	267.96	19.53	0.08	48	38
BSRN BAO Boulder	-105.01	40.05	1604	272.9	5.26	0.11	82	62
Table Mountain	-105.24	40.13	1689	272.9	5.26	0.09	82	62
Boulder	-105.25	40.02	1600	272.9	5.26	0.1	82	62

APPENDICE G

CHAPTER IV : AVERAGING OF ANOMALIES AND CHANGE OF THE DOWNWELLING SHORTWAVE RADIATION AT SURFACE FROM 9 MODELS

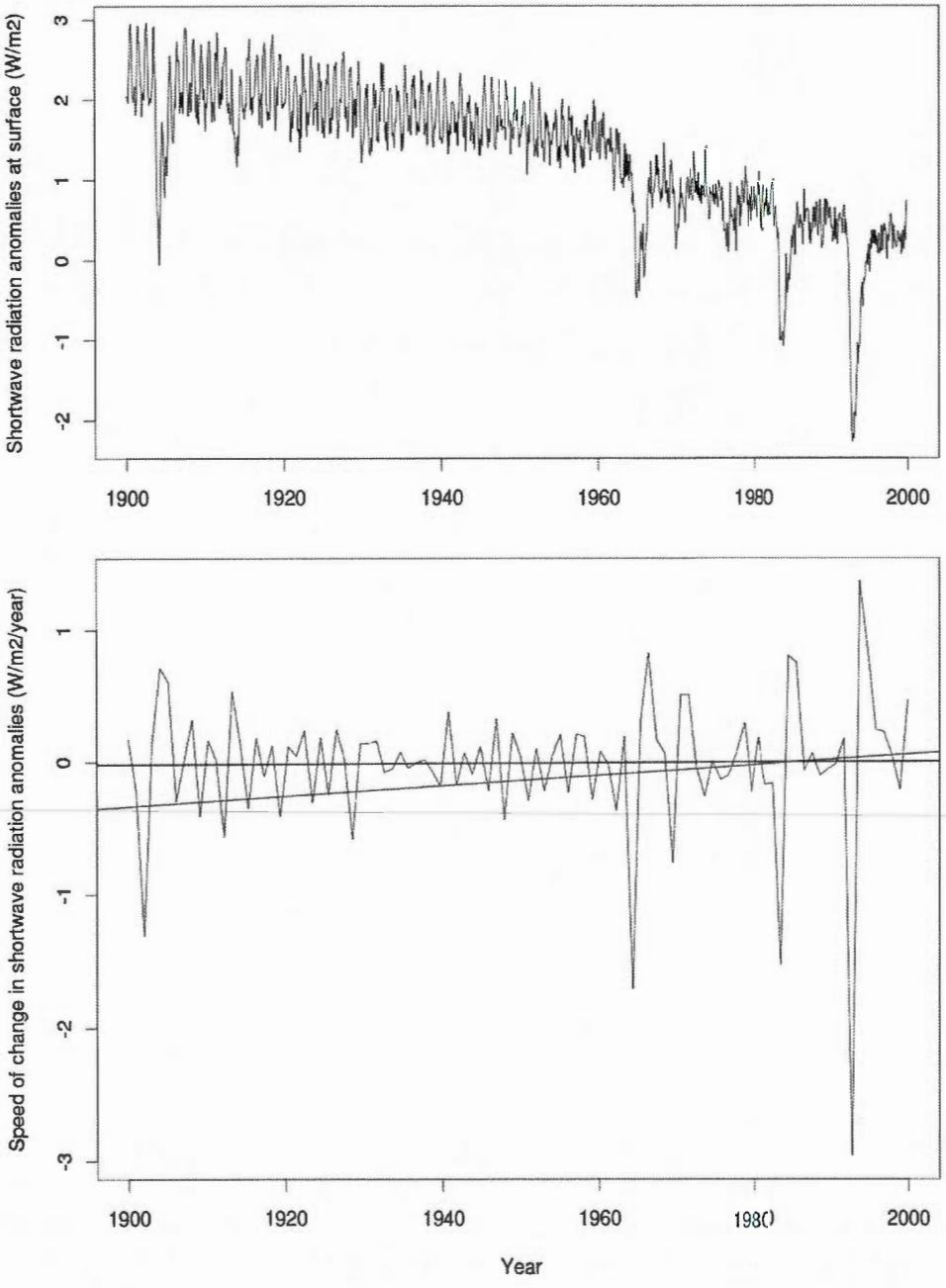

Figure G.1 Anomalies and change of the downwelling shortwave radiation at surface from 9 models (GFDL, CCSM, PCM, GISSAOM, GISSER, GISSEH, HADCM, MIROC, ECHAM). Upper panel show anomalies (W/m2) adapted from Romanou et al. (2007) and the lower panel show the speed of change (differential of the above de-seasonalized data) with the estimated trend before 1960 in blue and after 1960 in red (volcanic eruptions removed). Data courtesy of Anastasia Romanou.

APPENDICE H

CHAPTER V : SPECIES GROWTH RESPONSE FOLLOWING EL CHICHÓN AND MOUNT PINATUBO VOLCANIC EVENTS (FULL TABLE)

Tableau H.1 : Chapter V Species growth response following El Chichón volcanic event. Rpart gives the regression partitionning tree group name, RDA the redundancy analysis groups following the ordination axis, Int m gives the average intensity, Int sdt its standard deviation, Min its minimum, Max its maxiumum, Dur m gives the duration average in year, Dur std its standard deviation, Year m gives the average year of the intensity and Year std its standard deviation.

Species	Rpart	RDA	Int m	Int std	Min	Max	Dur m	Dur std	Year m	Year std
Armand's pine	2	+RDA2	-8.55	NA	NA	NA	5	0	1985	0
Austrian pine	1a	+RDA2	4.64	0.98	3.95	5.33	2	2	1982	0
Black pine	1b	+RDA2	1.48	3.52	-3.58	4.52	3	3	1982.5	2.5
Black spruce	1b	-RDA1	0.03	4.44	-4.46	6.78	2	3	1983	1.5
Blue oak	2	+RDA1	-1.2	6.51	-8.28	9.29	1	1	1983	1
Calabrian pine	1a	+RDA1	-4.96	2.4	-6.65	-3.26	2	2	1982.5	1
Californian sycamore	1b	+RDA1	4.02	0.93	3.36	4.67	1	0	1982.5	1
Cedar of Lebanon	1b	+RDA2	-3.09	3.43	-6.6	4.25	3	3	1982	1
Chir pine	1b	+RDA2	NA	NA	NA	NA	2	0	1982	0
Cyprian cedar	1b	+RDA2	-6.81	0.6	-7.23	-6.38	2	0	1982	0
Dahurian larch	1a	-RDA1	NA	NA	NA	NA	NA	NA	NA	NA
Douglas fir	1b	+RDA2	-3.71	3.63	-7.68	4.95	1	2	1983	1
Grecian juniper	2	+RDA2	-2.1	4.81	-6.27	4.8	3.5	2	1983.5	2
Himalayan cedar	1b	+RDA2	NA	NA	NA	NA	2.5	1	1982.5	1.5

Continued on next page

Tableau H.1: Chapter V Species growth response following El Chichón volcanic event (continued)

Species	Rpart	RDA	Int.m	Int.std	Min	Max	Dur. m	Dur std	Year m	Year std
Himalayan fir	2	+RDA2	NA	NA	NA	NA	3.5	1	1983	0
Himalayan spruce	1b	+RDA2	NA	NA	NA	NA	2	2	1983	0
Jeffrey pine	2	+RDA2	-1.19	5.02	-7.13	6.94	2	1	1984	1
Lenga	1a	+RDA1	NA	NA	NA	NA	NA	NA	NA	NA
Limber pine	2	+RDA2	4.05	NA	NA	NA	7	0	1982	0
Lodgepole pine	2	+RDA2	-5.17	0.93	-6.17	-4.32	7	2	1984	1
Montezuma cypress	1b	+RDA1	-2.87	6.34	-7.39	6.23	1.5	1	1983	1
New Zealand cedar	2	+RDA1	-0.41	4.92	-6.2	6.79	4	1	1983	1
Norway spruce	1b	-RDA1	-8.52	0.34	-8.76	-8.28	1	0	1982.5	1
Pink pine	1a	+RDA1	3.21	NA	NA	NA	1	0	1983	0
Pinyon pine	1b	+RDA2	-1.99	3.45	-4.83	2.97	1.5	1	1983	1
Ponderosa pine	1b	+RDA2	-3.37	1.69	-4.56	-2.17	3.5	3	1982.5	1
Pterocarpus angolensis	1a	+RDA1	1.95	NA	NA	NA	2	0	1982	0
Qilianshan juniper	2	+RDA2	2.06	7.32	-6.25	9.48	1	0	1983	1
Scots pine	2	-RDA1	-0.79	4.59	-6.38	5.67	3	3	1984	2
Sitka spruce	1a	-RDA1	NA	NA	NA	NA	NA	NA	NA	NA

Continued on next page

Tableau H.1: Chapter V Species growth response following El Chichón volcanic event (continued)

Species	Rpart	RDA	Int.m	Int.std	Min	Max	Dur. m	Dur std	Year m	Year std
Teak	1a	+RDA1	NA	NA	NA	NA	NA	NA	NA	NA
Umbrella pine	2	+RDA1	NA	NA	NA	NA	NA	NA	NA	NA
Valley oak	2	+RDA1	4.39	NA	NA	NA	2	0	1983	0
Western juniper	2	+RDA2	-0.91	4.83	-4.98	4.41	5	3	1983	2
White oak	1a	-RDA1	2.47	NA	NA	NA	3	1	1984	0.5
White spruce	1b	-RDA1	-0.12	4.56	-8.22	6.46	1	0	1982	0
Whitebark pine	1b	+RDA2	0.94	3.64	-3.14	3.83	2	3	1982.5	2

Tableau H.2 : Chapter V Species growth response following Mount Pinatubo volcanic event. Rpart gives the regression partitionning tree group name, RDA the redundancy analysis groups following the ordination axis, Int m gives the average intensity, Int sdt its standard deviation, Min its minimum, Max its maxiumum, Dur m gives the duration average in year, Dur std its standard deviation, Year m gives the average year of the intensity and Year std its standard deviation.

Species	Rpart	RDA	Int m	Int std	Min	Max	Dur m	Dur std	Year m	Year std
Armand's pine	NA	NA	NA	NA	NA	NA	NA	NA	1985	0
Austrian pine	3.44	1.22	2.57	4.3	1.5	1	1991.5	1	1982	0
Black pine	-3.48	0.71	-4.44	-2.89	1	1.5	1992	0.5	1982.5	2.5
Black spruce	3.59	NA	NA	NA	2	0	1992	0	1983	1.5
Blue oak	-3.67	6.28	-8.79	7.9	2	1	1992	2	1983	1
Calabrian pine	-0.54	4	-4.23	3.27	1	0.5	1991.5	1	1982.5	1
Californian sycamore	-4.96	1.58	-6.08	-3.84	2	2	1993	0	1982.5	1
Cedar of Lebanon	4.26	1.24	2.25	6.06	2.5	2	1992	1	1982	1
Chir pine	NA	NA	NA	NA	NA	NA	NA	NA	1982	0
Cyprian cedar	NA	NA	NA	NA	2	0	1992	0	1982	0
Dahurian larch	1.67	4.57	-3.6	4.45	1	0	1991.5	1	NA	NA
Douglas fir	-2.52	3.95	-6.69	6.33	1	2	1991	1	1983	1
Grecian juniper	-2.48	6.63	-8.43	6.75	2	3	1992	2	1983.5	2
Himalayan cedar	NA	NA	NA	NA	NA	NA	NA	NA	1982.5	1.5

Continued on next page

Tableau H.2: Chapter V Species growth response following Mount Pinatubo volcanic event (continued)

Species	Rpart	RDA	Int.m	Int.std	Min	Max	Dur. m	Dur std	Year m	Year std
Himalayan fir	NA	NA	NA	NA	NA	NA	NA	NA	1983	0
Himalayan spruce	NA	NA	NA	NA	NA	NA	NA	NA	1983	0
Jeffrey pine	NA	NA	NA	NA	2	0.5	1992	1.5	1984	1
Lenga	0.34	7.03	-7.81	8.48	1	0	1993	0	NA	NA
Limber pine	-4.6	0.36	-4.85	-4.34	1.5	1	1992	0	1982	0
Lodgepole pine	1.68	5.41	-4.32	6.18	3	1	1992	0.5	1984	1
Montezuma cypress	1.03	5.88	-5.73	4.91	1	0.5	1992	0.5	1983	1
New Zealand cedar	6.07	NA	NA	NA	2	0	1991	0	1983	1
Norway spruce	-4.1	1.54	-5.86	-2.98	1	0	1991	0.5	1982.5	1
Pink pine	4.18	NA	NA	NA	2	0	1992	0	1983	0
Pinyon pine	-0.39	4	-3.21	2.44	3.5	1	1993.5	1	1983	1
Ponderosa pine	NA	NA	NA	NA	NA	NA	NA	NA	1982.5	1
Pterocarpus angolensis	5.38	NA	NA	NA	1	0	1991	0	1982	0
Qilianshan juniper	1.32	8.95	-8.72	8.48	1	0	1992	0.5	1983	1
Scots pine	-0.22	4.56	-7.32	5.02	2	2	1992	2	1984	2
Sitka spruce	5.14	NA	NA	NA	1	0	1991	0	NA	NA

Continued on next page

Tableau H.2: Chapter V Species growth response following Mount Pinatubo volcanic event (continued)

Species	Rpart	RDA	Int.m	Int.std	Min	Max	Dur. m	Dur std	Year m	Year std
Teak	3.18	NA	NA	NA	1	0	1992	0	NA	NA
Umbrella pine	-0.26	4.36	-3.34	-0.26	4.5	1	1993	0	NA	NA
Valley oak	-6.1	NA	NA	NA	3	0	1993	0	1983	0
Western juniper	-2.23	6.97	-7.41	8.03	3.5	2	1992	0.5	1983	2
White oak	NA	NA	NA	NA	2	1.5	1992	1	1984	0.5
White spruce	-1.57	4.82	-8.96	7.89	NA	NA	NA	NA	1982	0
Whitebark pine	1.53	4.26	-3.18	5.12	2	2	1992	2	1982.5	2

APPENDICE I

CHAPTER V : EFFECT OF LATITUDE AND ELEVATION ON TREE RESPONSE FOLLOWING EL CHICHÓN AND MOUNT PINATUBO VOLCANIC EVENTS

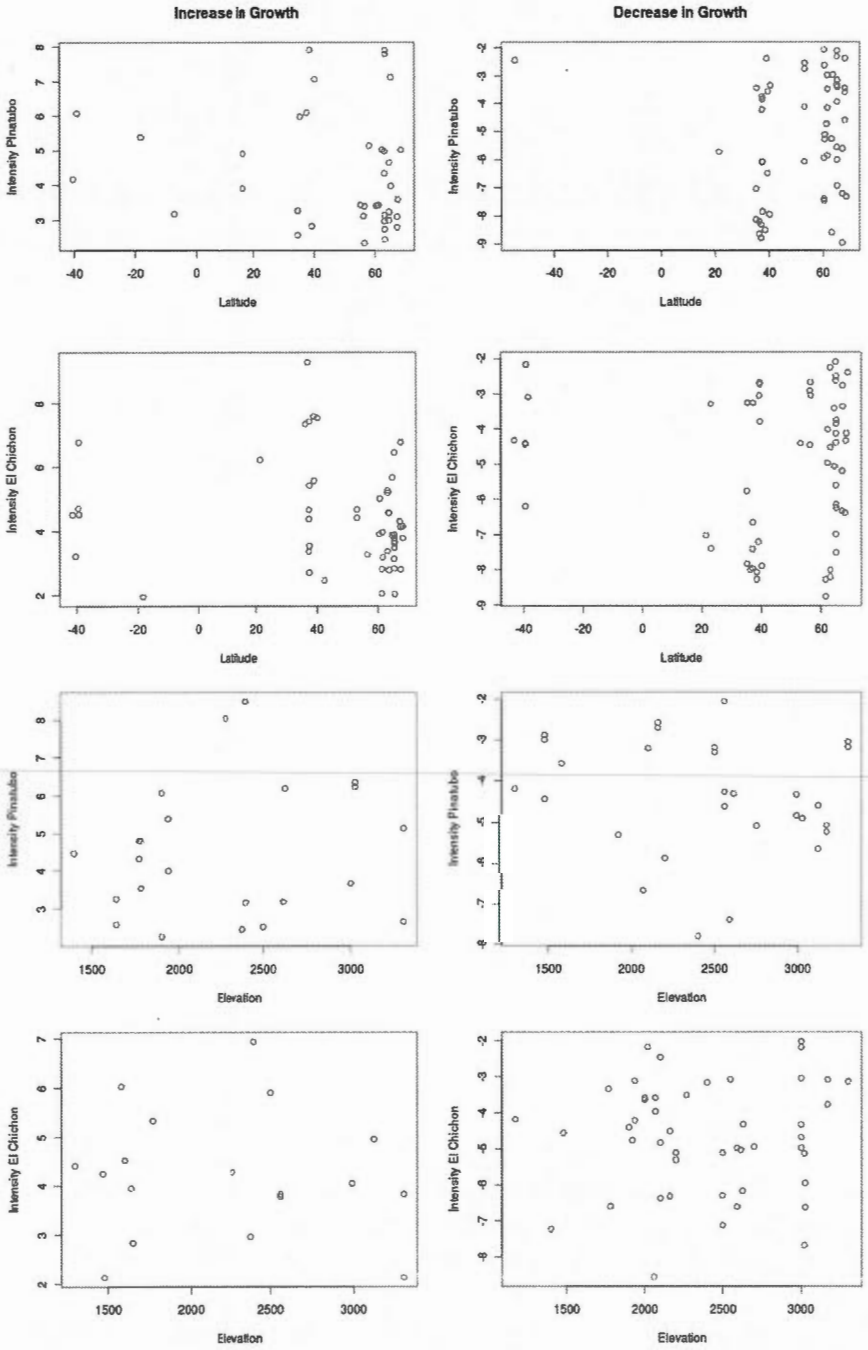

Figure I.1 Effect of latitude and elevation on tree response for Rpart groups

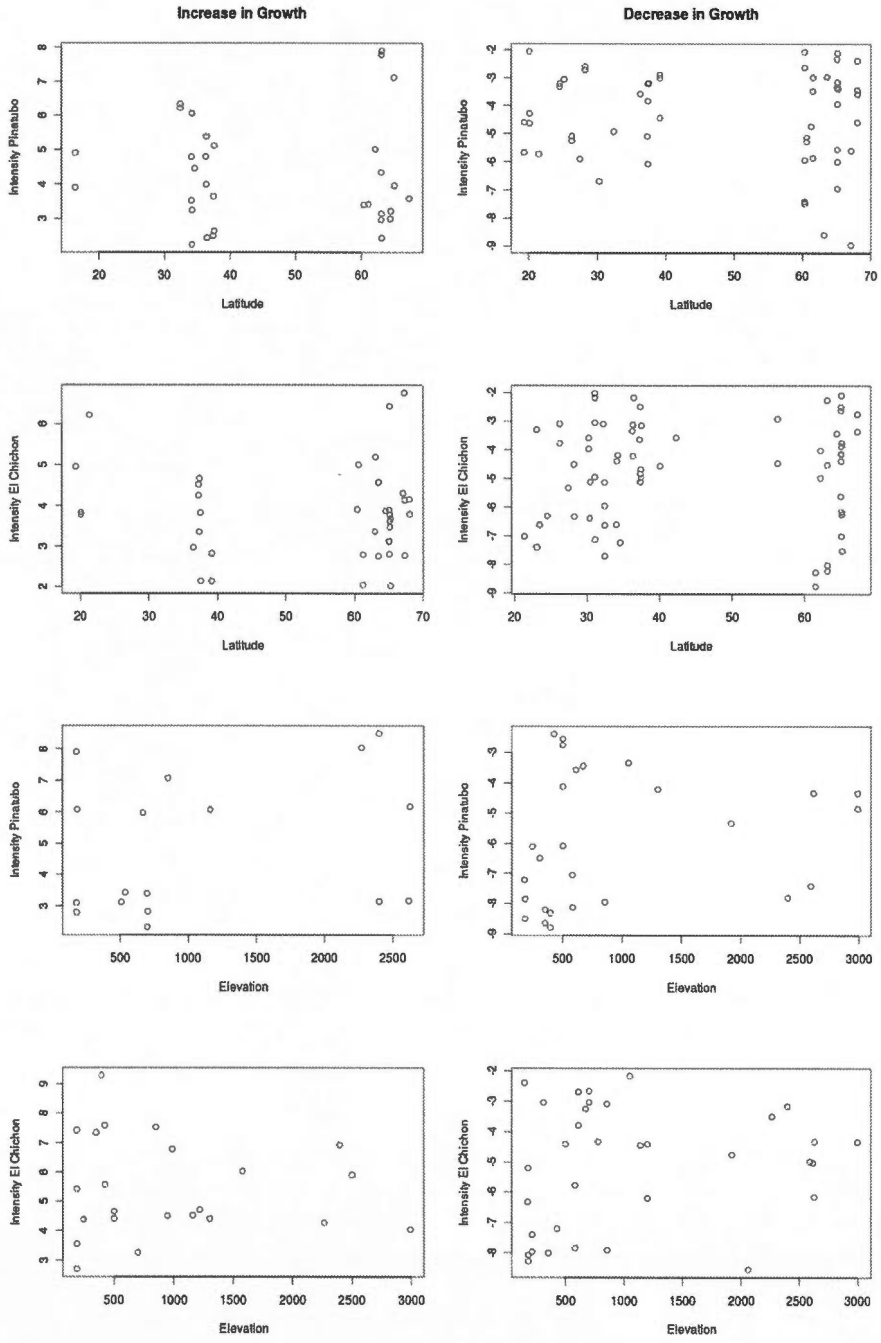

Figure I.2 Effect of latitude and elevation on tree response for RDA groups

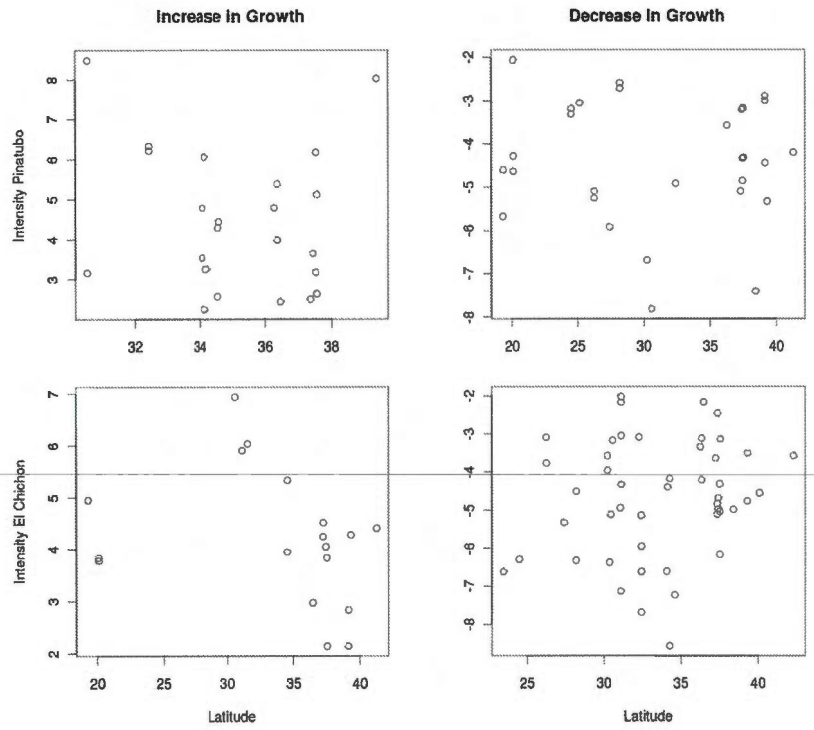

Figure I.3 Effect of latitude on tree response at high elevation

Bibliographie

Ackerman, A., O. Toon, D. Stevens, A. Heymsfield, V. Ramanathan, & E. Welton. 2000. « Reduction of tropical cloudiness by soot », *Science*, vol. 288, no. 5468, p. 1042–1047.

Ainsworth, E. & S. Long. 2005. « What have we learned from 15 years of free-air CO_2 enrichment (FACE) ? A meta-analytic review of the responses of photosynthesis, canopy properties and plant production to rising CO_2 », *New Phytologist*, vol. 165, no. 2, p. 351–372.

Bacastow, R., C. Keeling, G. Woodwell, & E. Pecan. 1973. « Carbon and the Biosphere ». In *USAEC CONF-720510*. US Atomic Energy Commission, Springfield, VA.

Back, A. & A. Weigend. 1997. « A first application of independent component analysis to exctracting structure from stock returns », *International Journal on Neural Systems*, vol. 8, p. 473–484.

Baker, T., O. Phillips, Y. Malhi, S. Almeida, L. Arroyo, A. Di Fiore, T. Erwin, N. Higuchi, T. Killeen, S. Laurance, W. Laurance, S. Lewis, A. Monteagudo, D. Neill, P. Núñez Vargas, N. Pitman, J. Natalino, M. Silva, et R. Vásquez Martínez. 2004. « Increasing biomass in amazonian forest plots », *Philosophical Transactions : Biological Sciences*, vol. 359, no. 1443, p. 353–365.

Bandeen, W. & R. Fraser. 1982. « Radiative Effects of the El Chichon volcanic eruption », *Preliminary results concerning remote sensing, NASA TM-84959.*

Battle, M., M. Bender, P. Tans, J. White, J. Ellis, T. Conway, & R. Francey. 2000. « Global carbon sinks and their variability inferred from atmospheric o_2 and delta ^{13}c », *Science*, vol. 287, no. 5462, p. 2467–2470.

Bergeron, Y., A. Leduc, B. Harvey, & S. Gauthier. 2002. « Natural fire regime : a guide for sustainable management of the Canadian boreal forest », *Silva Fennica*, vol. 36, no. 1, p. 81–95.

Beyschlag, W. & R. Ryel. 2007. *Functional Plant Ecology*, chapitre Canopy Photosynthesis Modeling, p. 627–653. CRC Press.

Bouchard, M., D. Kneeshaw, & Y. Bergeron. 2005. « Mortality and stand renewal patterns following the last spruce budworm outbreak in mixed forests of western Quebec », *Forest Ecology and Management*, vol. 204, no. 2-3, p. 297–313.

———. 2006. « Forest dynamics after successive spruce budworm outbreaks in mixedwood forests », *Ecology*, vol. 87, no. 9, p. 2319–2329.

Bousquet, P., P. Peylin, P. Ciais, C. Le Quéré, P. Friedlingstein, et P. Tans. 2000. « Regional changes in carbon dioxide fluxes of land and oceans since 1980 », *Science*, vol. 290, no. 5495, p. 1342–1346.

Breiman, L., J. Friedman, R. Olshen, & C. Stone. 1984. *Classification and Regression Trees*. Belmont, California : Wadsworth. 358 pp.

British Petroleum. 2006. *Quantifying Energy : BP Statistical Review of World Energy*. BP p.l.c., London, U.K. 45 pp.

Broecker, W. & T.-H. Peng. 1998. *Greenhouse Puzzles*. Palisades, New York : Observatory of Columbia University, Eldigio Press, Lamont-Doherty Earth édition. 277 pp.

Bryden, H., H. Longworth, & S. Cunningham. 2005. « Slowing of the atlantic meridional overturning circulation at $25°n$ », *Nature*, vol. 438, no. 7068, p. 655–657.

Burke, I., J. Kaye, S. Bird, S. Hall, R. McCulley, & G. Sommerville. 2003. *Models in Ecosystem Science*, chapitre Evaluating and testing models of terrestrial biogeochemistry : the role of temperature in controlling decomposition, p. 225–253. Princeton University Press.

Burkhardt, U., B. Kärcher, H. Mannstein, & U. Schumann. 2008. « Climate impact of contrails and contrail cirrus », *U.S. Department of Transportation, Federal Aviation Administration, Aviation-Climate Change Research Initiative, SSWP IV*, p. 58.

Burton, P., C. Messier, D. Smith, & W. Adamowicz. 2003. *Towards sustainable management of the boreal forest.* NRC Research Press. 1039 pp.

Cao, M. & F. Woodward. 1998. « Dynamic responses of terrestrial ecosystem carbon cycling to global climate change », *Nature*, vol. 393, no. 6682, p. 249–252.

Cardoso, J.-F. 1989. « Source separation using higher order moments. ». In *Intl. Conf. on Acoustics, Speech, and Signal Processing (ICASSP '89).* T. 4, p. 2109–2112, Glasgow, England.

Carolin, V. & J. Knopf. 1968. « The pandora moth », *Forest Pest Leaflet, USDA Forest Service*, vol. 114, p. 7.

Caron, M., D. Kneeshaw, L. De Grandpré, H. Kauhanen, & T. Kuuluvainen. 2009. « Canopy gap characteristics and disturbance dynamics in old-growth Picea abies stands in northern Fennoscandia : Is the forest in quasi-equilibrium ? », *Annales Botanici Fennici*, vol. 46, no. 4, p. 251–262.

Carrer, M. & C. Urbinati. 2006. « Long-term change in the sensitivity of tree-ring growth to climate forcing in Larix decidua », *New Phytologist*, vol. 170, no. 4, p. 861–872.

Carslaw, K., O. Boucher, D. Spracklen, G. Mann, J. Rae, S. Woodward, et M. Kulmala. 2009. « Atmospheric aerosols in the earth system : a review of interactions and feedbacks », *Atmospheric Chemistry and Physics Discussions*, vol. 9, no. 3, p. 11087–11183.

Chapin, F., E. Zavaleta, V. Eviner, R. Naylor, P. Vitousek, H. Reynolds, D. Hooper, S. Lavorel, O. Sala, S. Hobbie, M. Mack, & S. Diaz. 2000. « Consequences of changing biodiversity », *Nature*, vol. 405, no. 6783, p. 234–242.

Chattopadhyay, N. & M. Hulme. 1997. « Evaporation and potential evapotranspiration in India under conditions of recent and future climate change », *Agricultural and Forest Meteorology*, vol. 87, no. 1, p. 55–73.

Cohan, D., J. Xu, R. Greenwald, M. Bergin, & W. Chameides. 2002. « Impact of atmospheric aerosol light scattering and absorption on terrestrial net primary productivity », *Global Biogeochemical Cycles*, vol. 16, no. 4, p. 1090.

Comon, P. 1994. « Independent component analysis, a new concept ? », *Signal Processing*, vol. 36, no. 3, p. 287–314.

Cook, E. 1987. « The decomposition of tree-ring series for environmental studies », *Tree-ring bulletin*, vol. 47, p. 37–59.

Cook, E. & L. Kairiukstis, éditeurs. 1990. *Methods of Dendrochronology - Applications in the Environmental Sciences*. Dordrecht, The Netherlands : Kluwer Academic Publishers and International Institute for Applied Systems Analysis. 394 pp.

D'Arrigo, R., R. Wilson, B. Liepert, & P. Cherubini. 2008. « On the 'divergence problem' in northern forests : A review of the tree-ring evidence and possible causes », *Global and Planetary Change*, vol. 60, no. 3-4, p. 289–305.

De Pury, D. & G. Farquhar. 1997. « Simple scaling of photosynthesis from leaves to canopies without the errors of big-leaf models », *Plant Cell and Environment*, vol. 20, no. 5, p. 537–557.

De'ath, G. 2002. « Multivariate regression trees : a new technique for modeling species-environment relationships », *Ecology*, vol. 83, no. 4, p. 1105–1117.

De'ath, G. & K. Fabricius. 2000. « Classification and regression trees : a powerful yet simple technique for ecological data analysis », *Ecology*, vol. 81, no. 11, p. 3178–3192.

Degens, E. & B. Buch. 1989. « Sedimentological events in saleh Bay, off Mount Tambora », *Netherlands journal of sea research*, vol. 24, no. 4, p. 399–404.

Del Giorgio, P. & C. Duante. 2002. « Respiration in the open ocean », *Nature*, vol. 420, no. 6914, p. 379–384.

Dengel, S., D. Aeby, & J. Grace. 2009. « A relationship between galactic cosmic radiation and tree rings », *New Phytologist*, vol. 184, no. 3, p. 545–551.

Dickinson, R. 1975. « Solar variability and the lower atmosphere », *Bulletin of the American Meteorological Society*, vol. 56, no. 12, p. 1240–1248.

Douglass, A. 1927. « Solar records in tree growth », *Science*, vol. 21, p. 220–221.

Dutton, E. & B. Bodhaine. 2001. « Solar irradiance anomalies caused by clear-sky transmission variations above Mauna Loa : 1958–99 », *Journal of Climate*, vol. 14, no. 15, p. 3255–3262.

Edenius, L. & K. Danell. 1993. « Impact of herbivory and competition on compensatory growth in woody plants : winter browsing by moose on Scots pine », *Oikos*, vol. 66, no. 2, p. 286–292.

Ehleringer, J. & I. Forseth. 1980. « Solar tracking by plants », *Science*, vol. 210, no. 4474, p. 1094–1098.

Eischeid, J., C. Bruce Baker, T. Karl, & H. Diaz. 1995. « The quality control of long-term climatological data using objective data analysis », *Journal of Applied Meteorology*, vol. 34, no. 12, p. 2787–2795.

Ellis, J. & D. Schneider. 1997. « Evaluation of a gradient sampling design for environmental impact assessment », *Environmental Monitoring and Assessment*, vol. 48, no. 2, p. 157–172.

Ellsworth, D. & P. Reich. 1993. « Canopy structure and vertical patterns of photosynthesis and related leaf traits in a deciduous forest », *Oecologia*, vol. 96, no. 2, p. 169–178.

Engle, R. & C. Granger. 1987. « Co-integration and error-correction : Representation, estimation and testing », *Econometrica*, vol. 55, no. 2, p. 251–276.

Falkowski, P., R. J. Scholes, E. Boyle, J. Canadell, D. Canfield, J. Elser, N. Gruber, K. Hibbard, P. Hogberg, S. Linder, F. T. Mackenzie, I. Moore, B., T. Pedersen, Y. Rosenthal, S. Seitzinger, V. Smetacek, & W. Steffen. 2000. « The Global Carbon Cycle : A Test of Our Knowledge of Earth as a System », *Science*, vol. 290, no. 5490, p. 291–296.

Falster, D. & M. Westoby. 2003. « Leaf size and angle vary widely across species : what consequences for light interception ? », *New Phytologist*, vol. 158, no. 3, p. 509–525.

Farquhar, G. & M. Roderick. 2003. « Pinatubo, diffuse light and the carbon cycle », *Science*, vol. 299, no. 5615, p. 1997–1998.

Feddema, J., K. Oleson, G. Bonan, L. Mearns, L. Buja, G. Meehl, et W. Washington. 2005. « The importance of land-cover change in simulating future climates », *Science*, vol. 310, no. 5754, p. 1674–1678.

Fellin, D. & J. Dewey. 1982. « Western spruce budworm », *Forest Insect and Disease Leaflet, USDA Forest Service*, vol. 53, p. 10.

Fichter, C., S. Marquart, R. Sausen, & D. Lee. 2005. « The impact of cruise altitude on contrails and related radiative forcing », *Meteorologische Zeitschrift*, vol. 14, no. 4, p. 563–572.

Foukal, P., C. Fröhlich, H. Spruit, & T. Wigley. 2006. « Variations in solar luminosity and their effect on the earth's climate », *Nature*, vol. 443, no. 7108, p. 161–166.

Franklin, J., T. Spies, R. Pelt, A. Carey, D. Thornburgh, D. Berg, D. Lindenmayer, M. Harmon, W. Keeton, D. Shaw, *et al.* 2002. « Disturbances and structural development of natural forest ecosystems with silvicultural implications, using Douglas-fir forests as an example », *Forest Ecology and Management*, vol. 155, no. 1-3, p. 399–423.

Frelich, L. 2002. *Forest dynamics and disturbance regimes : studies from temperate evergreen-deciduous forests.* Cambridge Univ Press. 266 pp.

Friedlingstein, P., L. Bopp, P. Ciais, J.-L. Dufresne, L. Fairhead, H. LeTreut, P. Monfray, & O. Aumont. 2001. « On the positive feedback between the climate system and the carbon cycle under the anthropogenic perturbation », *Geophysical Research Letters*, vol. 28, no. 8, p. 1543–1546.

Furniss, R. & V. Carolin. 1977. *Western forest insects.* T. 1339. Miscellaneous Publication, United States Department of Agriculture, Forest Service.

Galloway, J. & E. Cowling. 2002. « Reactive nitrogen and the world : 200 years of change », *Ambio*, vol. 31, no. 2, p. 64–71.

Garcia, C. & E. Yasukawa. 1983. « Mauna Loa sky conditions-Bench mark and present », *Astronomical Society of the Pacific, Publications*, vol. 95, p. 520–526.

Gea-Izquierdo, G., A. Mäkelä, H. Margolis, Y. Bergeron, T. Black, A. Dunn, J. Hadley, U. Kyaw Tha Paw, M. Falk, S. Wharton, R. Monson, D. Hollinger, T. Laurila, M. Aurela, H. McCaughey, C. Bourque, T. Vesala, et F. Berninger. 2010. « Modeling acclimation of photosynthesis to temperature in evergreen conifer forests », *New Phytologist*, vol. 188, no. 1, p. 175–186.

Gerber, H. & A. Deepak, éditeurs. 1984. *Aerosols and their climatic effects.* A. Deepak Publications. 297 pp.

Goudriaan, J. 1977. *Crop micrometeorology : a simulation study.* Centre for Agricultural Publishing and Documentation Wageningen, the Netherlands. 249 pp.

Grace, J. 1989. « Tree lines », *Philosophical Transactions of the Royal Society of London B*, vol. 324, p. 233–245.

Granger, C. 1969. « Investigating causal relations by econometric models and cross-spectral methods », *Econometrica*, vol. 37, no. 3, p. 424–438.

Graumlich, L. 1991. « Subalpine tree growth, climate, and increasing CO_2 : An assessment of recent growth trends », *Ecology*, vol. 72, no. 1, p. 1–11.

Gu, L., D. Baldocchi, S. Verma, T. Black, T. Vesala, E. Falge, & P. Dowty. 2002. « Advantages of diffuse radiation for terrestrial ecosystem productivity », *Journal of Geophysical Research*, vol. 107, no. 6, p. 4050–4072.

Gu, L., D. Baldocchi, S. Wofsy, J. Munger, J. Michalsky, S. Urbanski, & T. Boden. 2003. « Response of a Deciduous Forest to the Mount Pinatubo Eruption : Enhanced Photosynthesis », *Science*, vol. 299, no. 5615, p. 2035–2038.

Gurney, K., R. Law, A. Denning, P. Rayner, D. Baker, P. Bousquet, L. Bruhwiler, Y.-H. Chen, P. Ciais, S. Fan, & *et al.* 2002. « Towards robust regional estimates of co_2 sources and sinks using atmospheric transport models », *Nature*, vol. 415, no. 6872, p. 626–630.

Hagle, S., K. Gibson, & S. Tunnock. 2003. Field Guide to Diseases and Insect Pests of Northern and Central Rocky Mountain Conifers. Rapport, USDA Forest Service, State and Private Forestry.

Haigh, J. 1994. « The role of stratospheric ozone in modulating the solar radiative forcing of climate », *Nature*, vol. 370, no. 6490, p. 544–546.

———. 1996. « The impact of solar variability on climate », *Science*, vol. 272, no. 5264, p. 981–984.

———. 2001. « Climate variability and the influence of the sun », *Science*, vol. 294, no. 5549, p. 2109–2111.

Ham, F. & N. Faour. 1999. « Infrasound signal separation using independent component analysis ». In *Seismic Research Symposium : Technologies for Monitoring the Comprehensive Nuclear-Test-Ban Treaty*, Las Vegas, Nevada.

Hamback, P. & A. Beckerman. 2003. « Herbivory and plant resource competition : a review of two interacting interactions », *Oikos*, vol. 101, no. 1, p. 26–37.

Handler, P. 1984. « Possible association of stratospheric aerosols and El Niño type events », *Geophysical Research Letters*, vol. 11, no. 11, p. 1121–1124.

Hansen, J., A. Lacis, R. Ruedy, & M. Sato. 1992. « Potential climate impact of Mount Pinatubo eruption », *Geophysical Research Letters*, vol. 19, no. 2, p. 215–218.

Hansen, J., M. Sato, R. Ruedy, A. Lacis, & V. Oinas. 2000. « Global warming in the twenty-first century : An alternative scenario », *Proceedings of The National Academy of Sciences of The United States of America*, vol. 97, no. 18, p. 9875–9880.

Harrison, R. & M. Ambaum. 2008. « Enhancement of cloud formation by droplet charging », *Proceedings of the Royal Society A : Mathematical, Physical and Engineering Science*, vol. 464, no. 2098, p. 2561–2573.

Harrison, R. & K. Carslaw. 2003. « Ion-aerosol-cloud processes in the lower atmosphere », *Reviews of Geophysics*, vol. 41, no. 3, p. 1012–1037.

Himberg, J. & A. Hyvärinen. 2001. « Independent component analysis for binary data : An experimental study. ». In *Proc. Int. Workshop on Independent Component Analysis and Blind Signal Separation (ICA2001)*, p. 552–556, San Diego, California.

Hirono, M. 1988. « On the trigger of El Nino–Southern Oscillation by the forcing of early El Chichón volcanic aerosols », *Journal of Geophysical Research*, vol. 93, no. D5, p. 5365–5384.

Hobbie, S., J. Schimel, S. Trumbore, & J. Randerson. 2000. « Controls over carbon storage and turnover in high-latitude soils », *Global Change Biology*, vol. 6, no. s1, p. 196–210.

Hobbins, M., J. Ramírez, & T. Brown. 2004. « Trends in pan evaporation and actual evapotranspiration across the conterminous u.s. : Paradoxical or complementary ? », *Geophysical Research Letters*, vol. 31, no. 13, p. L13503.

Hoch, G. & C. Körner. 2003. « The carbon charging of pines at the climatic treeline : a global comparison. », *Oecologia*, vol. 135, no. 1, p. 10–21.

Holben, B., A. Smirnov, T. Eck, I. Slutsker, N. Abuhassan, W. Newcomb, J. Schafer, D. Tanre, B. Chatenet, & F. Lavenu. 2001. « An emerging ground-based aerosol

climatology- Aerosol optical depth from AERONET », *Journal of Geophysical Research*, vol. 106, no. D11, p. 12067–12097.

Hollinger, D. 1989. « Canopy organization and foliage photosynthetic capacity in a broad-leaved evergreen montane forest », *Functional Ecology*, vol. 3, no. 1, p. 53–62.

Hood, L. 1997. « The solar cycle variation of total ozone : Dynamical forcing in the lower stratosphere », *Journal of Geophysical Research*, vol. 102, no. D1, p. 1355–1370.

Hoover, W., E. Johnston, & F. Brackett. 1933. « CO2 assimilation in a higher plant », *Smithsonian Miscellaneous Collections*, vol. 87, p. 1–19.

Horton, P., A. Ruban, & R. Walters. 1996. « Regulation of light harvesting in green plants », *Annual Review of Plant Biology*, vol. 47, no. 1, p. 655–684.

Houghton, J., B. Callander, & S. Varney, éditeurs. 1992. *Climate Change 1992. The Supplementary Report to the IPCC Scientific Assessment.* Cambridge, UK : Cambridge University Press. 205 pp.

Houghton, J., L. Meira Filho, B. Lim, K. Treanton, I. Mamaty, Y. Bonduki, D. Griggs, & B. Callander. 1997. Revised 1996 Guidelines for National Greenhouse Gas Inventories : Reference Manual. Rapport, IPCC WGI Technical Support Unit.

Houghton, J., L. Meira Filho, B. Lim, K. Treanton, I. Mamaty, Y. Bonduki, D. Griggs, & B. Callender, éditeurs. 1996. *Revised 1996 IPCC Guidelines for National Greenhouse Gas Inventories.* UK Meteorological Office, Bracknell : IPCC/OECD/IEA.

Houghton, R. 2000. « Interannual variability in the global carbon cycle », *Journal of Geophysical Research*, vol. 105, no. D15, p. 20121–21130.

Houghton, R., E. Davidson, & G. Woodwell. 1998. « Missing sinks, feedbacks, and understanding the role of terrestrial ecosystems in the global carbon balance », *Global Biogeochemical Cycles*, vol. 12, p. 25–34.

Huang, J., Y. Bergeron, B. Denneler, F. Berninger, & J. Tardif. 2007. « Response of forest trees to increased atmospheric CO 2 », *Critical Reviews in Plant Sciences*, vol. 26, no. 5, p. 265–283.

Hulme, M. 1992. « A 1951–80 global land precipitation climatology for the evaluation of general circulation models », *Climate Dynamics*, vol. 7, no. 2, p. 57–72.

———. 1994. « Validation of large-scale precipitation fields in general circulation models », *Global Precipitation and Climate Change*, vol. 26, p. 387–405.

Hurtt, G. C., S. W. Pacala, P. R. Moorcroft, J. Caspersen, E. Shevliakova, R. A. Houghton, & I. Moore, B. 2002. « Projecting the future of the U.S. carbon sink », *Proceedings of The National Academy of Sciences of The United States of America*, vol. 99, no. 3, p. 1389–1394.

Hyvärinen, A., J. Karhunen, & E. Oja, éditeurs. 2001. *Independent Component Analysis*. Wiley Interscience. 504 pp.

Hyvärinen, A. & E. Oja. 2000. « Independent component analysis algorithms and applications », *Neural Networks*, vol. 13, no. 4-5, p. 411–430.

Jacoby, G. & R. D'Arrigo. 1997. « Tree rings, carbon dioxide, and climatic change », *Proceedings of The National Academy of Sciences of The United States of America*, vol. 94, no. 16, p. 8350–8353.

Jäger, H. 1992. « The Pinatubo eruption cloud observed by lidar at Garmisch-Partenkirchen », *Geophysical Research Letters*, vol. 19, no. 2, p. 191–194.

Jenkinson, D. & K. Coleman. 2008. « The turnover of organic carbon in subsoils. Part 2. Modelling carbon turnover », *European Journal of Soil Science*, vol. 59, no. 2, p. 400–413.

Jenkinson, D., K. Goulding, & D. Powlson. 1999. « Nitrogen deposition and carbon sequestration », *Nature*, vol. 400, no. 6745, p. 629.

Joos, F., I. Prentice, & J. House. 2002. « Growth enhancement due to global atmospheric change as predicted by terrestrial ecosystem models : consistent with us forest inventory data », *Global Change Biology*, vol. 8, no. 4, p. 299–303.

Jump, A., J. Hunt, & J. Penuelas. 2006. « Rapid climate change-related growth decline at the southern range edge of Fagus sylvatica », *Global Change Biology*, vol. 12, no. 11, p. 2163–2174.

Jung, T., S. Makeig, M. McKeown, A. Bell, T. Lee, & T. Sejnowski. 2001. « Imaging brain dynamics using independent component analysis », *Proceedings of the IEEE*, vol. 89, no. 7, p. 1107–1122.

Kalkstein, A. & R. Balling. 2004. « Impact of unusually clear weather on United States daily temperature range following 9/11/2001 », *Climate Research*, vol. 26, no. 1, p. 1–4.

Karnosky, D. 2003. « Impacts of elevated atmospheric CO2 on forest trees and forest ecosystems : knowledge gaps », *Environment International*, vol. 29, no. 2-3, p. 161–169.

Kaufmann, R. & D. Stern. 1997. « Evidence for human influence on climate from hemispheric temperature relations », *Nature*, vol. 388, no. 6637, p. 39–44.

Keyser, A., J. Kimball, R. Nemani, & S. Running. 2000. « Simulating the effects of climate change on the carbon balance of north american high-latitude forests », *Global Change Biology*, vol. 6, no. s1, p. 185–195.

Knutson, T., T. Delworth, K. Dixon, I. Held, J. Lu, V. Ramaswamy, M. Schwarzkopf, G. Stenchikov, & R. Stouffer. 2006. « Assessment of twentieth-century regional surface temperature trends using the GFDL CM2 coupled models », *Journal of Climate*, vol. 19, no. 9, p. 1624–1651.

Körner, C. 1999. *Alpine plant life : functional plant ecology of high mountain ecosystems.* Springer Verlag. 338 pp.

Körner, C. 2003a. *Alpine plant life.* Berlin : Springer, 2^d édition. 344 pp. + xi.

———. 2003b. « Ecological impacts of atmospheric co2 enrichment on terrestrial ecosystems », *Philosophical transactions : Mathematical, physical, and engineering sciences*, vol. 361, no. 1810, p. 2023–2041.

Körner, C., R. Asshoff, O. Bignucolo, S. Hättenschwiler, S. Keel, S. Peláez-Riedl, S. Pepin, R. Siegwolf, & G. Zotz. 2005. « Carbon flux and growth in mature deciduous forest trees exposed to elevated co_2 », *Science*, vol. 309, no. 5739, p. 1360–1362.

Krakauer, N. & J. Randerson. 2003. « Do volcanic eruptions enhance or diminish net primary production? Evidence from tree rings », *Global Biogeochemical Cycles*, vol. 17, no. 4, p. 1118–1129.

Kramer, P. 1981. « Carbon dioxide concentration, photosynthesis, and dry matter production », *BioScience*, vol. 31, no. 1, p. 29–33.

Kulmala, M., P. Hari, I. Riipinen, & V. Kerminen. 2009. « On the possible links between tree growth and galactic cosmic rays », *New Phytologist*, vol. 184, no. 3, p. 511–513.

Kulman, H. 1971a. « Effects of insect defoliation on growth and mortality of trees », *Annual Review of Entomology*, vol. 16, no. 1, p. 289–324.

———. 1971b. « Effects of insect defoliation on growth and mortality of trees », *Annual Review of Entomology*, vol. 16, no. 1, p. 289–324.

LaMarche, V., D. Graybill, H. Fritts, & M. Rose. 1984. « Increasing atmospheric carbon dioxide : tree ring evidence for growth enhancement in natural vegetation », *Science*, vol. 225, no. 4666, p. 1019–1021.

LaMarche, V. & K. Hirschboeck. 1984. « Frost rings in trees as records of major volcanic eruptions », *Nature*, vol. 307, no. 5947, p. 121–126.

Landscheidt, T. 2000. « Solar forcing of el niño and la niña », *ESA Special Publication*, vol. 463, p. 135–140.

Laut, P. 2003. « Solar activity and terrestrial climate : An analysis of some purported correlations », *Journal of Atmospheric and Solar-Terrestrial Physics*, vol. 65, no. 7, p. 801–812.

Lean, J. 1989. « Contribution of ultraviolet irradiance variations to changes in the sun's total irradiance », *Science*, vol. 244, no. 4901, p. 197–200.

Lee, T. & F. Bazzaz. 1980. « Effects of defoliation and competition on growth and reproduction in the annual plant Abutilon theophrasti », *The Journal of Ecology*, vol. 68, no. 3, p. 813–821.

Legendre, P. & L. Legendre. 1998. *Numerical ecology*. Elsevier Science BV, Amsterdam., 2 édition. 853 pp. + xv.

Lindenmayer, D. & J. Franklin. 2002. *Conserving forest biodiversity : a comprehensive multiscaled approach*. Island Press. 351 pp.

Linder, S. & J. Flower-Ellis. 1992. *Responses of Forest Ecosystems to Environmental Changes*, chapitre Environment and physiological constraints to forest yield, p. 149–164. New York : Elsevier Applied Sciences.

Lobato, I. & C. Velasco. 2004. « A simple test of normality for time series », *Econometric Theory*, vol. 20, no. 4, p. 671–689.

Long, S., S. Humphries, & P. Falkowski. 1994. « Photoinhibition of photosynthesis in nature », *Annual Review of Plant Biology*, vol. 45, no. 1, p. 633–662.

Lorimer, C. 1985. « Methodological considerations in the analysis of forest disturbance history », *Canadian Journal of Forest Research*, vol. 15, no. 1, p. 200–213.

Lorimer, C. & L. Frelich. 1989. « A methodology for estimating canopy disturbance frequency and intensity in dense temperate forests », *Canadian Journal of Forest Research*, vol. 19, no. 5, p. 651–663.

Magnani, F., M. Mencuccini, M. Borghetti, P. Berbigier, F. Berninger, S. Delzon, A. Grelle, P. Hari, P. Jarvis, P. Kolari, A. Kowalski, H. Lankreijer, B. Law, A. Lin-

droth, D. Loustau, G. Manca, J. Moncrieff, M. Rayment, V. Tedeschi, R. Valentini, & J. Grace. 2007. « The human footprint in the carbon cycle of temperate and boreal forests », *Nature*, vol. 447, no. 7146, p. 848–850.

Makela, A., P. Hari, F. Berninger, H. Hanninen, & E. Nikinmaa. 2004. « Acclimation of photosynthetic capacity in Scots pine to the annual cycle of temperature », *Tree Physiology*, vol. 24, no. 4, p. 369.

Mann, M., R. Bradley, & M. Hughes. 1998. « Global-scale temperature patterns and climate forcing over the past six centuries », *Nature*, vol. 392, no. 6678, p. 779–787.

Mannstein, H. & U. Schumann. 2005. « Aircraft induced contrail cirrus over Europe », *Meteorologische Zeitschrift*, vol. 14, no. 4, p. 549–554.

Marquart, S., M. Ponater, L. Strom, & K. Gierens. 2005. « An upgraded estimate of the radiative forcing of cryoplane contrails », *Meteorologische Zeitschrift*, vol. 14, no. 4, p. 573–582.

Marsh, N. & H. Svensmark. 2000. « Cosmic rays, clouds, and climate », *Space Science Reviews*, vol. 94, no. 1, p. 215–230.

McCullough, D., R. Werner, & D. Neumann. 1998. « Fire and insects in northern and boreal forest ecosystems of North America », *Annual Review of Entomology*, vol. 43, no. 1, p. 107–127.

McMurtrie, R., H. Gholz, S. Linder, & S. Gower. 1994. « Climatic factors controlling the productivity of pine stands : a modelbased analysis », *Ecological Bulletins*, vol. 43, p. 173–188.

Mercado, L., N. Bellouin, S. Sitch, O. Boucher, C. Huntingford, M. Wild, & P. Cox. 2009. « Impact of changes in diffuse radiation on the global land carbon sink », *Nature*, vol. 458, no. 7241, p. 1014–1017.

Millard, P., M. Sommerkorn, & G. Grelet. 2007. « Environmental change and carbon

limitation in trees : a biochemical, ecophysiological and ecosystem appraisal », *New Phytologist*, vol. 175, no. 1, p. 11–28.

Minnis, P., J. Ayers, R. Palikonda, & D. Phan. 2004. « Contrails, cirrus trends, and climate », *Journal of Climate*, vol. 17, no. 8, p. 1671–1685.

Mitchell, T. & P. Jones. 2005. « An improved method of constructing a database of monthly climate observations and associated high-resolution grids », *International Journal of Climatology*, vol. 25, no. 6, p. 693–712.

Moody, J. & Y. Howard. 1999. « Term structure of interactions of foreign exchange rates ». In Abu-Mostafa *et. al.*, éditeur, *Computational Finance, Proceedings of the sixth Int'l conference*, New York. MIT press.

Moody, J. & L. Wu. 1998. *Nonlinear Modeling of High Frequency Financial Times Series*, chapitre High frequency foreign exchange rates : price behaviour analysis and 'true price models, p. 23–47. Willey.

Morrow, P. & V. Lamarche. 1978. « Tree ring evidence for chronic insect suppression of productivity in subalpine Eucalyptus », *Science*, vol. 201, no. 4362, p. 1244–1246.

Murcray, W. 1970. « On the possibility of weather modification by aircraft contrails », *Monthly Weather Review*, vol. 98, no. 10, p. 745–748.

Muzika, R. & A. Liebhold. 1999. « Changes in radial increment of host and nonhost tree species with gypsy moth defoliation », *Canadian Journal of Forest Research*, vol. 29, no. 9, p. 1365–1373.

Nadelhoffer, K., B. Emmett, P. Gundersen, O. Kjø naas, C. Koopmans, P. Schleppi, A. Tietema, & R. Wright. 1999a. « Nitrogen deposition makes a minor contribution to carbon sequestration in temperate forests », *Nature*, vol. 398, no. 6723, p. 145–148.

Nadelhoffer, K., B. Emmett, P. Gundersen, C. Koopmans, P. Schleppi, A. Tietema, & R. Wright. 1999b. « Nitrogen deposition and carbon sequestration », *Nature*, vol. 400, no. 6745, p. 630.

Nakicenovic, N. & R. Swart, éditeurs. 2000. *Emissions Scenarios 2000. Special Report of the Intergovernmental Panel on Climate Change.* Cambridge, UK : Cambridge University Press. 570 pp.

Nash, T., H. Fritts, & M. Stokes. 1975. « A technique for examining non-climatic variation in widths of annual tree rings with special reference to air pollution », *Tree-Ring*, vol. 35, p. 15.

Newhall, C. & S. Self. 1982. « The volcanic explosivity index/VEI/- An estimate of explosive magnitude for historical volcanism », *Journal of Geophysical Research*, vol. 87, no. C2, p. 1231–1238.

Niinemets, U. & F. Valladares. 2004. « Photosynthetic acclimation to simultaneous and interacting environmental stresses along natural light gradients : optimality and constraints », *Plant Biology*, vol. 6, p. 254–268.

Niyogi, D., H. Chang, V. Saxena, T. Holt, K. Alapaty, F. Booker, F. Chen, K. Davis, B. Holben, T. Matsui, *et al.* 2004. « Direct observations of the effects of aerosol loading on net ecosystem CO_2 exchanges over different landscapes », *Geophysical Research Letters*, vol. 31, no. 20, p. L20506.

Niyogi, K. 1999. « Photoprotection revisited : genetic and molecular approaches », *Annual Review of Plant Biology*, vol. 50, no. 1, p. 333–359.

Nowacki, G. & M. Abrams. 1997. « Radial-growth averaging criteria for reconstructing disturbance histories from presettlement-origin oaks », *Ecological Monographs*, vol. 67, no. 2, p. 225–249.

Nozawa, T., T. Nagashima, H. Shiogama, & S. Crooks. 2005. « Detecting natural infl uence on surface air temperature change in the early twentieth century », *Geophysical Research Letters*, vol. 32, no. 20, p. L20719.

Oleksyn, J., J. Modrzỳnski, M. Tjoelker, R. Zytkowiak, P. Reich, et P. Karolewski. 1998. « Growth and physiology of Picea abies populations from elevational transects :

common garden evidence for altitudinal ecotypes and cold adaptation », *Functional Ecology*, vol. 12, no. 4, p. 573–590.

Oppenheimer, C. 2003. « Climatic, environmental and human consequences of the largest known historic eruption : Tambora volcano (Indonesia) 1815 », *Progress in Physical Geography*, vol. 27, no. 2, p. 230–259.

Pacala, S., G. Hurtt, D. Baker, P. Peylin, R. Houghton, R. Birdsey, L. Heath, E. Sundquist, R. Stallard, P. Ciais, P. Moorcroft, J. P. Caspersen, E. Shevliakova, B. Moore, G. Kohlmaier, E. Holland, M. Gloor, M. Harmon, S.-M. Fan, J. Sarmiento, C. Goodale, D. Schimel, & C. Field. 2001. « Consistent land- and atmosphere-based u.s. carbon sink estimates », *Science*, vol. 292, no. 5525, p. 2316–2320.

Pauling, A., J. Luterbacher, & C. Casty. 2006. « Five hundred years of gridded high-resolution precipitation reconstructions over europe and the connection to large-scale circulation », *Climate Dynamics*, vol. 26, no. 4, p. 387–405.

Payette, S., L. Filion, & A. Delwaide. 1990. « Disturbance regime of a cold temperate forest as deduced from tree-ring patterns : the Tantaré Ecological Reserve, Quebec », *Canadian Journal of Forest Research*, vol. 20, no. 8, p. 1228–1241.

Penner, J., D. Lister, D. Griggs, D. Dokken, & M. McFarland. 1999. *Aviation and the global atmosphere : a special report of IPCC Working Groups I and III in collaboration with the Scientific Assessment Panel to the Montreal Protocol on Substances that Deplete the Ozone Layer*. Cambridge University Press. 373 pp.

Penny, W., S. Roberts, & R. Everson. 2001. *Independent Component Analysis : Principles and Practice*, chapitre ICA : model order selection and dynamic source models, p. 299–314. Cambridge University Press.

Peterson, T., V. Golubev, & P. Groisman. 1995. « Evaporation losing its strength », *Nature*, vol. 377, p. 687–688.

Phillips, O., Y. Malhi, N. Higuchi, W. Laurance, P. Núñez, R. Vásquez, S. Laurance, L. Ferreira, M. Stern, S. Brown, & J. Grace. 1998. « Changes in the carbon balance

of tropical forests : Evidence from long-term plots », *Science*, vol. 282, no. 5388, p. 439–442.

Phillips, O., R. Vásquez Martínez, L. Arroyo, T. Baker, T. Killeen, S. Lewis, Y. Malhi, A. Monteagudo Mendoza, D. Neill, P. Núñez Vargas, M. Alexiades, C. Cerón, A. Di Fiore, T. Erwin, A. Jardim, W. Palacios, M. Saldias, & B. Vinceti. 2002. « Increasing dominance of large lianas in amazonian forests », *Nature*, vol. 418, no. 6899, p. 770–774.

Pielke, R. 2005. « Land use and climate change », *Science*, vol. 310, no. 5754, p. 1625–1626.

Pinker, R., B. Zhang, & E. Dutton. 2005. « Do Satellites Detect Trends in Surface Solar Radiation ? », *Science*, vol. 308, no. 5723, p. 850–854.

Quadfasel, D. 2005. « The atlantic heat conveyor slows », *Nature*, vol. 438, no. 7068, p. 565–566.

R Development Core Team. 2009. *R : A language and environment for statistical computing*. R Foundation for Statistical Computing, Vienna, Austria.

Rakonczay, Z. 2002. « Biome-specific forest definitions ». In *Second Expert Meeting on Harmonizing Forest Related Definitions for Use by Various Stakeholders. FAO, Rome, Italy.* available online at http ://www.fao.org/DOCREP/005/Y4171E/Y4171E52.htm.

Ramanathan, V., P. Crutzen, J. Kiehl, & D. Rosenfeld. 2001. « Aerosols, climate, and the hydrological cycle », *Science*, vol. 294, no. 5549, p. 2119–2124.

Rasmusson, E. & J. Wallace. 1983. « Meteorological aspects of the El Nino/southern oscillation », *Science*, vol. 222, no. 4629, p. 1195–1202.

Reich, P., S. Hobbie, T. Lee, D. Ellsworth, J. West, D. Tilman, J. Knops, S. Naeem, & J. Trost. 2006. « Nitrogen limitation constrains sustainability of ecosystem response to co2 », *Nature*, vol. 440, no. 7086, p. 922–925.

Reid, G. 2000. « Solar variability and the Earth's climate : Introduction and overview », *Space Science Reviews*, vol. 94, no. 1, p. 1–11.

Reiter, R., H. Jäger, W. Carnuth, & W. Funk. 1983. « The El Chichon cloud over central Europe, observed by Lidar at Garmisch-Partenkirchen during 1982 », *Geophysical Research Letters*, vol. 10, no. 11, p. 1001–1004.

Richey, J., J. Melack, A. Aufdenkampe, V. Ballester, & L. Hess. 2002. « Outgassing from amazonian rivers and wetlands as a large tropical source of atmospheric co_2 », *Nature*, vol. 416, no. 6881, p. 617–620.

Rigozo, N., D. Nordemann, H. da Silva, M. Pereira de Souza Echer, & E. Echer. 2007. « Solar and climate signal records in tree ring width from Chile (AD 1587–1994) », *Planetary and Space Science*, vol. 55, no. 1-2, p. 158–164.

Rigozo, N., L. Vieira, E. Echer, & D. Nordemann. 2003. « Wavelet analysis of solar-enso imprints in tree ring data from southern brazil in the last century », *Climatic Change*, vol. 60, no. 3, p. 329–340.

Ripley, B. 1996. *Pattern recognition and neural networks*. Cambridge University Press. 416 pp.

Robock, A. 1991. « The volcanic contribution to climate change of the past 100 years », *Developments in atmospheric science*, vol. 19, p. 429–443.

———. 2000. « Volcanic eruptions and climate », *Reviews of Geophysics*, vol. 38, no. 2, p. 191–219.

———. 2002. « Pinatubo eruption : The climatic aftermath », *Science*, vol. 295, no. 5558, p. 1242–1244.

———. 2005. « Cooling following large volcanic eruptions corrected for the effect of diffuse radiation on tree rings », *Geophysical Research Letters*, vol. 32, no. 6, p. L06702.

Robock, A. & J. Mao. 1995. « The volcanic signal in surface temperature observations », *Journal of Climate*, vol. 8, no. 5, p. 1086–1103.

Roderick, M. 2006. « The ever-flickering light », *Trends in Ecology & Evolution*, vol. 21, no. 1, p. 3–5.

Roderick, M. & G. Farquhar. 2002. « The Cause of Decreased Pan Evaporation over the Past 50 Years », *Science*, vol. 298, no. 5597, p. 1410–1411.

Roderick, M., G. Farquhar, S. Berry, & I. Noble. 2001. « On the direct effect of clouds and atmospheric particles on the productivity and structure of vegetation », *Oecologia*, vol. 129, no. 1, p. 21–30.

Romanou, A., B. Liepert, G. Schmidt, W. Rossow, R. Ruedy, & Y. Zhang. 2007. « 20th century changes in surface solar irradiance in simulations and observations », *Geophysical Research Letters*, vol. 34, no. 5, p. L05713.

Romme, W., D. Knight, & J. Yavitt. 1986. « Mountain pine beetle outbreaks in the Rocky Mountains : regulators of primary productivity ? », *American Naturalist*, vol. 127, no. 4, p. 484–494.

Rubino, D. & B. McCarthy. 2004. « Comparative analysis of dendroecological methods used to assess disturbance events », *Dendrochronologia*, vol. 21, no. 3, p. 97–115.

Ryerson, D., T. Swetnam, & A. Lynch. 2003. « A tree-ring reconstruction of western spruce budworm outbreaks in the San Juan Mountains, Colorado, USA », *Canadian Journal of Forest Research*, vol. 33, no. 6, p. 1010–1028.

Saleska, S., S. Miller, D. Matross, M. Goulden, S. Wofsy, H. da Rocha, P. de Camargo, P. Crill, B. Daube, H. de Freitas, L. Hutyra, M. Keller, V. Kirchhoff, M. Menton, J. Munger, E. Pyle, A. Rice, & H. Silva. 2003. « Carbon in amazon forests : unexpected seasonal fluxes and disturbance-induced losses », *Science*, vol. 302, no. 5650, p. 1554–1557.

Sarmiento, J., T. Hughes, R. Stouffer, & S. Manabe. 1998. « Simulated response of the ocean carbon cycle to anthropogenic climate warming », *Nature*, vol. 393, no. 6682, p. 245–249.

Schiermeier, Q. 2005. « A sea change », *Nature*, vol. 439, no. 7074, p. 256–260.

Schimel, D. 1995. « Terrestrial ecosystems and the carbon cycle », *Global Change Biology*, vol. 1, no. 1, p. 77–91.

———. 1998. « The carbon equation », *Nature*, vol. 393, no. 6682, p. 208–209.

Schimel, D., J. House, K. Hibbard, P. Bousquet, P. Ciais, P. Peylin, B. Braswell, M. Apps, D. Baker, A. Bondeau, J. Canadell, G. Churkina, W. Cramer, A. Denning, C. Field, P. Friedlingstein, C. Goodale, M. Heimann, R. Houghton, J. Melillo, B. Moore, D. Murdiyarso, I. Noble, S. Pacala, I. Prentice, M. R. Raupach, P. Rayner, R. Scholes, W. Steffen, & C. Wirth. 2001. « Recent patterns and mechanisms of carbon exchange by terrestrial ecosystems », *Nature*, vol. 414, no. 6860, p. 169–172.

Schindler, D. 1999. « Carbon cycling : The mysterious missing sink », *Nature*, vol. 398, no. 6723, p. 105–107.

Schumann, U. 2005. « Formation, properties and climatic effects of contrails », *Comptes rendus-Physique*, vol. 6, no. 4-5, p. 549–565.

Sellers, P., J. Berry, G. Collatz, C. Field, & E. Hall. 1992. « Canopy reflectance, photosynthesis, and transpiration. III. A reanalysis using improved leaf models and a new canopy integration scheme », *Remote Sensing of Environment*, vol. 42, p. 187–216.

Shindell, D., D. Rind, N. Balachandran, J. Lean, & P. Lonergan. 1999. « Solar cycle variability, ozone, and climate », *Science*, vol. 284, no. 5412, p. 305.

Siegenthaler, U. & J. Sarmiento. 1993. « Atmospheric carbon dioxide and the ocean », *Nature*, vol. 365, no. 6442, p. 119–125.

Sievering, H. 1999. « Nitrogen deposition and carbon sequestration », *Nature*, vol. 400, no. 6745, p. 629–630.

Simkin, T., L. Siebert, L. McClelland, D. Bridge, C. Newhall, & J. Latter. 1981. *Volcanoes of the world : a regional directory, gazetteer, and chronology of volcanism during the last 10,000 years.* US Hutchinson Ross Publishing. 368 pp.

Sinclair, T. 2006. « A Reminder of the Limitations in Using Beer's Law to Estimate Daily Radiation Interception by Vegetation », *Crop Science*, vol. 46, no. 6, p. 2343.

Sinclair, T., T. Shiraiwa, & G. Hammer. 1992. « Variation in crop radiation-use efficiency with increased diffuse-radiation », *Crop Science*, vol. 32, no. 5, p. 1281–1284.

Soden, B., R. Wetherald, G. Stenchikov, & A. Robock. 2002. « Global cooling after the eruption of Mount Pinatubo : A test of climate feedback by water vapor », *Science*, vol. 296, no. 5568, p. 727–730.

Solomon, S., D. Qin, M. Manning, Z. Chen, M. Marquis, K. Averyt, M. Tignor, et H. Miller, éditeurs. 2007. *Contribution of Working Group I to the Fourth Assessment Report of the Intergovernmental Panel on Climate Change*. Cambridge University Press, Cambridge, United Kingdom and New York, NY, USA. 996 pp.

Speer, J., T. Swetnam, B. Wickman, & A. Youngblood. 2001. « Changes in pandora moth outbreak dynamics during the past 622 years », *Ecology*, vol. 82, no. 3, p. 679-697.

Spracklen, D., K. Carslaw, M. Kulmala, V. Kerminen, S. Sihto, I. Riipinen, J. Merikanto, G. Mann, M. Chipperfield, A. Wiedensohler, *et al.* 2008. « Contribution of particle formation to global cloud condensation nuclei concentrations », *Geophysical Research Letters*, vol. 35, p. L06808.

Stanhill, G. & S. Cohen. 2001. « Global dimming : a review of the evidence for a widespread and significant reduction in global radiation with discussion of its probable causes and possible agricultural consequences », *Agricultural and Forest Meterology*, vol. 107, no. 4, p. 255–278.

Stone, J. 2004. *Independent Component Analysis : A Tutorial Introduction*. Coll. « Bradford Books ». Cambridge, MA : The MIT Press. 200 pp.

Stordal, F., G. Myhre, E. Stordal, W. Rossow, D. Lee, D. Arlander, et T. Svendby. 2005. « Is there a trend in cirrus cloud cover due to aircraft traffic », *Atmospheric Chemistry and Physics*, vol. 5, no. 8, p. 2155–2162.

Strong, A. 1984. « Monitoring El Chichón aerosol distribution using NOAA-7 satellite AVHRR sea surface temperature observations », *Geophysical Journal International*, vol. 23, p. 129–141.

Sturtevant, B., E. Gustafson, W. Li, & H. He. 2004. « Modeling biological disturbances in LANDIS : a module description and demonstration using spruce budworm », *Ecological Modelling*, vol. 180, no. 1, p. 153–174.

Sutton, R. & D. Hodson. 2005. « Atlantic ocean forcing of north american and european summer climate », *Science*, vol. 309, no. 5731, p. 115–118.

Svensmark, H., T. Bondo, & J. Svensmark. 2009. « Cosmic ray decreases affect atmospheric aerosols and clouds », *Geophysical Research Letters*, vol. 36, no. 15, p. L15101.

Svensmark, H. & N. Calder. 2007. *The chilling stars : A new theory of climate change.* Icon Books. 268 pp.

Swetnam, T., M. Thompson, & E. Sutherland. 1985. *Using dendrochronology to measure radial growth of defoliated trees.* T. 639. US Dept. of Agriculture, Forest Service, Cooperative State Research Service. 39 pp.

Swetnam, T., B. Wickman, H. Paul, & C. Baisan. 1995. Historical patterns of western spruce budworm and douglas-fir tussock moth outbreaks in the northern Blue Mountains, Oregon, since ad 1700. Forest Service research paper. Rapport, PB–96-158829/XAB, Forest Service, Portland, OR (United States). Pacific Northwest Research Station.

Takemura, T., T. Nozawa, S. Emori, T. Nakajima, & T. Nakajima. 2005. « Simulation of climate response to aerosol direct and indirect effects with aerosol transport-radiation model », *Journal of Geophysical Research*, vol. 110, no. D2, p. D02202.

Tamm, C. 1991. *Nitrogen in terrestrial ecosystems.* Berlin : Springer-Verlag. 115 pp.

Tans, P., I. Fung, & T. Takahashi. 1990. « Observational constraints on the global atmospheric carbon dioxide budget », *Science*, vol. 247, no. 4949, p. 1431–1438.

Ter Braak, C. 1986. « Canonical correspondence analysis : a new eigenvector technique for multivariate direct gradient analysis », *Ecology*, vol. 67, no. 5, p. 1167–1179.

Thomas, J. & G. Hill. 1949. *Photosynthesis in Plants*, chapitre Photo-synthesis under field conditions, p. 19–52. Iowa State College Press.

Tian, H., J. Melillo, D. Kicklighter, A. McGuire, J. Helfrich, B. Moore, et C. Vörösmarty. 1998. « Effect of interannual climate variability on carbon storage in amazonian ecosystems », *Nature*, vol. 396, no. 6712, p. 664–667.

Travis, D., A. Carleton, & R. Lauritsen. 2002. « Contrails reduce daily temperature range », *Nature*, vol. 418, no. 6898, p. 601.

———. 2004. « Regional variations in US diurnal temperature range for the 11–14 September 2001 aircraft groundings : Evidence of jet contrail influence on climate », *Journal of Climate*, vol. 17, no. 5, p. 1123–1134.

Triacca, U. 2001. « On the use of granger causality to investigate the human influence on climate », *Theoretical and Applied Climatology*, vol. 69, no. 3, p. 137–138.

Triacca, U. 2005. « Is granger causality analysis appropriate to investigate the relationship between atmospheric concentration of carbon dioxide and global surface air temperature ? », *Theoretical and Applied Climatology*, vol. 81, no. 3, p. 133–135.

United Nations. 1997. Kyoto protocol to the united nations framework convention on climate change. Kyoto, Japan. 23 pp.

Usoskin, I., N. Marsh, G. Kovaltsov, K. Mursula, & O. Gladysheva. 2004. « Latitudinal dependence of low cloud amount on cosmic ray induced ionization », *Geophysical Research Letters*, vol. 31, p. L16109.

Valladares, F. & R. Pearcy. 1998. « The functional ecology of shoot architecture in sun and shade plants of Heteromeles arbutifolia M. Roem., a Californian chaparral shrub », *Oecologia*, vol. 114, no. 1, p. 1–10.

Valladares, F. & R. Pearcy. 2002. « Drought can be more critical in the shade than in the sun : a field study of carbon gain and photo-inhibition in a Californian shrub during a dry El Nino year », *Plant, Cell and Environment*, vol. 25, no. 6, p. 749–759.

Van Den Wollenberg, A. 1977. « Redundancy analysis an alternative for canonical correlation analysis », *Psychometrika*, vol. 42, no. 2, p. 207–219.

Venable, W. & B. Ripley. 2002. *Modern applied statistics with S.* Springer, 4 édition. 495 pp. + xi.

Vigário, R., V. Jousmäki, M. Hämäläinen, & E. Hari, R. amd Oja. 1998. *Advances in Neural Information Processing Systems.* T. 10, chapitre Independent component analysis for identification of artifacts in magnetoencephalographic recordings, p. 229–235. MIT Press.

Vitousek, P. & R. Howarth. 1991. « Nitrogen limitation on land and in the sea : how can it occur ? », *Biogeochemistry*, vol. 13, no. 2, p. 87–115.

Walker, D. 2000. « Hierarchical subdivision of arctic tundra based on vegetation response to climate, parent material and topography », *Global Change Biology*, vol. 6, no. s1, p. 19–34.

Weaver, A. & C. Hillaire-Marcel. 2004. « Global warming and the next ice age », *Science*, vol. 304, no. 5669, p. 400–402.

Weber, U. & F. Schweingruber. 1995. « A dendroecological reconstruction of western spruce budworm outbreaks (*Choristoneura occidentalis*) in the Front Range, Colorado, from 1720 to 1986 », *Trees-Structure and Function*, vol. 9, no. 4, p. 204–213.

Wickman, B., R. Mason, & G. Trostle. 1981. « Douglas-fir tussock moth », *Forest Insect and Disease Leaflet, USDA Forest Service*, vol. 86, p. 10.

Wigley, T. 1993. « Balancing the carbon budget : Implications for projections of future carbon dioxide concentration changes », *Tellus Series B-Chemical And Physical Meteorology*, vol. 45, no. 5, p. 409–425.

Wild, M., H. Gilgen, A. Roesch, A. Ohmura, C. Long, E. Dutton, B. Forgan, A. Kallis, V. Russak, & A. Tsvetkov. 2005. « From dimming to brightening : decadal changes in solar radiation at earth's surface », *Science*, vol. 308, no. 5723, p. 847–850.

Wild, M., A. Ohmura, H. Gilgen, & D. Rosenfeld. 2004. « On the consistency of trends in radiation and temperature records and implications for the global hydrological cycle », *Geophysical Research Letters*, vol. 31, no. 11, p. L11201.

Wild, M., A. Ohmura, & K. Makowski. 2007. « Impact of global dimming and brightening on global warming », *Geophysical Research Letters*, vol. 34, no. 4, p. L04702.

Wittwer, S. 1979. « Future technological advances in agriculture and their impact on the regulatory environment », *BioScience*, vol. 29, no. 10, p. 603–610.

Wu, Z., N. E. Huang, S. R. Long, & C.-K. Peng. 2007. « On the trend, detrending, and variability of nonlinear and nonstationary time series », *Proceedings of The National Academy of Sciences of The United States of America*, vol. 104, no. 38, p. 14889–14894.

Yu, F. 2002. « Altitude variations of cosmic ray induced production of aerosols : Implications for global cloudiness and climate », *Journal of Geophysical Research*, vol. 107, no. A7, p. 1118.

Zerefos, C., K. Eleftheratos, D. Balis, P. Zanis, G. Tselioudis, & C. Meleti. 2003. « Evidence of impact of aviation on cirrus cloud formation », *Atmospheric Chemistry and Physics*, vol. 3, no. 3, p. 3335 3359.